TECHNICAL TRANSLATION ESRO TT-78

June 1974

CALCULATION OF THE PLANE SUPERSONIC FLOW THROUGH CASCADES USING THE METHOD OF ANALYTICAL CHARACTERISTICS

by

H.J. Lichtfuss

Deutsche Forschungs- und Versuchsanstalt für Luft- und Raumfahrt

Institut für Luftstrahlantriebe

Porz-Wahn, West Germany

(Report No. DLR-FB 73-34)

ORGANISATION EUROPEENNE DE RECHERCHES SPATIALES

EUROPEAN SPACE RESEARCH ORGANISATION

CALCULATION OF THE PLANE SUPERSONIC FLOW THROUGH CASCADES USING THE METHOD OF ANALYTICAL CHARACTERISTICS

H.-J. Lichtfuss

Translation of DLR-FB 73-34
"Berechnung der ebenen Überschallgitterströmung mit Hilfe des analytischen Charakteristikenverfahrens"

Deutsche Forschungs- und Versuchsanstalt für Luft- und Raumfahrt
Institut für Luftstrahlantriebe
Porz-Wahn

1973

743197

UDC (DK) 533.695.5.011
533.695.5.011.5
517.945

German Research-and-Testing-Establishment
for Aeronautics and Astronautics

INSTITUTE FOR JET PROPULSION
PORZ-WAHN, February 1973.

Director of the Institute:
Prof. H. Kühl

Author:
H.-J. Lichtfuss

The original report in German is published by the
Deutsche Forschungs- und Versuchsanstalt für Luft- und Raumfahrt E.V. (DFVLR)
Copies can be obtained from:
Abteilung Wissenschaftliches Berichtswesen der DFVLR
505 Porz-Wahn, Linder Höhe.

114 pages including
39 illustrations
7 tables
50 references

Price: DM 36.20.

Manuscript submitted on 16 February 1973.

Calculation of the Plane Supersonic Flow through Cascades using the Method of Analytical Characteristics*

ABSTRACT

The two-dimensional irrotational supersonic flow through straight blade cascades is calculated analytically. The flow fields found differ substantially depending on whether the axial components of the inlet flow and the outlet flow are subsonic or supersonic. Neutral inlet and outlet characteristics are determined as limits of the cascade shocks. Entropy changes due to the infinite number of cascade shocks are also given.

*This paper also appears as a thesis accepted by the Faculty of Mechanical Engineering of the Rheinisch-Westfälische Technische Hochschule of Aachen for the degree of "Doktor-Ingenieur".

(Technical University of the Rhineland and Westphalia at Aachen)

Contents

Foreword

This work was carried out at the Institute for Jet Propulsion of the German Research-and-Testing-Establishment for Aeronautics and Astronautics (DFVLR) in Porz-Wahn.

The Director of the Institute, Prof. Dr. -Ing. H. Kühl, assisted me with utmost generosity at all times. I owe thanks to Prof. Dr. -phil. A. Naumann for the valuable advice extended to me on a number of occasions.

The many discussions with Mr. H.H. Frühauf, Dr. -Ing. W. Heilmann, P. Schimming, Dr. -Ing. H. Starken and H. Weyer were equally helpful.

I wish to thank all those named above, and the staff who helped write the manuscript, together with those who prepared the diagrams and assisted me with the numerical calculations.

I extend my special thanks, however, to Prof. Dr. -phil. K. Oswatitsch, who encouraged me to carry out this work, and supported me in every respect.

List of symbols used

A	Parameter defined by equations (5.20) and (5.24)
$A^{(i)}(\eta)$	Abbreviation of equation (2.29), for initial values
A^*	Parameter defined by equation (2.22)
A^{**}	Parameter defined by equation (2.22)
$\bar{A}$	Parameter defined by equation (6.11)
B	Parameter defined by equations (5.20) and (5.24)
$B^{(i)}(\xi)$	Abbreviation of equation (2.28), for initial values
$\bar{B}$	Width of the cascade, normal to the plane of calculation
b	Length of arc along the shock in the x,y plane
b'	Length of arc along the shock in the ξ,η plane
C	Parameter defined by equations (5.20) and (5.24)
C^*_k	Parameter defined by equation (2.17)
C_j	Parameter defined by equation (2.16)
$\bar{C}$	Parameter defined by equation (6.11)
c	Speed of sound
c^*	Critical speed of sound
D	Parameter defined by equations (5.20) and (5.24)
D^*_k	Parameter defined by equation (2.17)
D_j	Parameter defined by equation (2.16)
$\bar{D}$	Parameter defined by equation (6.11)
E	Parameter defined by equation (5.13)
$E^{(i)}(\eta)$	Abbreviation of equation (2.28), for initial values
F	Parameter defined by equation (5.13)
$F^{(i)}(\xi)$	Abbreviation of equation (2.28), for initial values
$G^{(i)}(\eta)$	Integration limit of the inclination conditions
$g(\eta)$	Integration function of the inclination conditions (0th approximation)
$H^{(i)}(\xi)$	Integration limit of the inclination conditions

$h(\xi)$	Integration function of the conditions of inclination (0th approximation)
$I^{(i)}(\eta)$	Integration limit of the compatibility conditions
$J^{(i)}(\xi)$	Integration limit of the compatibility conditions
K_{ij}	Parameter defined by equation (3.7)
$\tilde{K}_{ij}$	Parameter defined by equation (3.7)
L_j	Parameter defined by equation (2.12)
l	Chord of cascade blade
M	Mach No.
M^*	Velocity related to the critical speed of sound, c^*
$\tilde{M}_j$	Parameter defined by equation (5.9)
m	Mass flow
$\tilde{N}_j$	Parameter defined by equation (5.9)
P_i	Abbreviation for equation (5.10)
p	Static pressure
Q_i	Abbreviation for equation (5.10)
R	Gas constant
S_i	Parameter defined by equation (2.32)
s	Specific entropy
T	Absolute temperature
t	Pitch of blade cascade
V_{ij}	Parameter defined by equation (6.8)
w	Velocity (normalized by equation (2.3)
x	Abscissa in Cartesian coordinates (normalized by equation (2.3)
y	Ordinate in Cartesian coordinates (normalized by equation (2.3)
Z1	Parameter defined by equation (5.29)
Z2	Parameter defined by equation (5.29)

Z3	Parameter defined by equation (5.29)
z	Variable introduced by equation (5.22)
α	Mach angle
β	Flow angle related to cascade face $\beta = 180^{\circ} + \theta + \theta_{\infty} - \Phi$
β_s	Stagger angle
γ	Shock angle
η	Coordinate of the right-handed characteristics (normalized by equation (2.3))
ϑ	Angle of the direction of flow related to the x-axis (normalized by equation (2.3))
κ	Ratio of specific heats
ν	Prandtl-Meyer function (defined by equation (2.9))
ξ	Coordinate of the left-handed characteristics (normalized by equation (2.3))
ρ	Density
Φ	Angle of cascade face to x-axis
ω	$= (p_{ges\ 1} - p_{ges})/(p_{ges\ 1} - p_1)$ Loss coefficient

Subscripts

Anf	Initial point
ax	Component normal to cascade face
Env	Envelope
ges	total condition
k	Boundary values along blade contour
N	Neutral Mach line of a single blade aerofoil
o	Tips of cascade blade aerofoils
p	Characteristics through the tip of the subsequent cascade aerofoil

s	Reference parameter for the development of the characteristic coordinates of the one sheet of the convolution in the characteristic coordinates of the other sheet
St	Shock
ψ	Streamlines
1	Inlet flow values of the double-infinite cascade
2	Outlet flow values of the double-infinite cascade
∞	Reference parameter (in chapter 5.2 constant inlet flow for the semi-infinite cascade)

Superscripts

(i)	Order of approximation and summation index
$\hat{}$	Values in the upstream sheet of a convolution
$\hat{\hat{}}$	Values in the sheet situated farthest downstream if two successive convulutions occur

1. Introduction

The object of this paper is the calculation of the steady two-dimensional supersonic flow through a straight blade cascade. For simplification let an irrotational flow and a thermally and calorifically ideal gas be assumed. The problem is solved by application of the method of analytical characteristics developed by Oswatitsch [1, 2], which also provides for the calculation of weak compression shocks and the centred Prandtl-Meyer expansions that occur.

The fundamental ideas of the method of analytical characteristics were already found by Lin [3], who also calculated the plane steady supersonic flow by an analytical method, whereas Fox [4, 5] used the same method to determine the one-dimensional non-steady flow. Fox was moreover able to determine in his work the position of the weak compression shocks.

The principle of this method consists in that, in addition to the variables of state, the position coordinates are also introduced as dependent variables into the calculation of a supersonic flow. The characteristic coordinates represent the independent variables. A perturbation formulation is then put for the new dependent position variables in which the individual perturbation quantities each differ by one order of magnitude. These formulae are introduced into the differential equations, and it is necessary that terms of the same order of magnitude satisfy them in each case.

For the special case of the two-dimensional flow investigated, closed solutions are obtained for the variables of state even without using the perturbation formulae, so that it would be possible to avoid them. But to obtain the simplest expressions possible, the closed solution is also subsequently developed in this work according to the perturbation variables.

The perturbation formulae for the previously independent position variables result in solutions being obtained in this way even if the conventional perturbation formulae fail in the dependent variables of state; see also Van Dyke [6]. The reason for the failure is, among

other things, that the Mach cone is defined by the undisturbed flow and that it does not change in approximations of a higher order. Outside the sphere of influence resulting from this Mach cone, no improvement in results can therefore be achieved; see Oswatitsch [7].

A perturbation formulation for the independent variables was introduced for the first time by Poincaré [8], Lighthill [9, 10] and Kuo [11, 12] (PLK method). Whitham [13] calculated the flow around bodies of revolution, by substituting in the equations of the acoustics theory a family of characteristics resulting from this theory as straight lines by their actual equation. With this method, which is valid even at a great distance from the body, he was able in [14] to calculate, approximately, shock fronts in the axisymmetrical case.

In the first part of this paper, chapters 2, 3 and 4, the equations of the steady supersonic flow are solved with given specific boundary values and initial values. These results are then used in part 2, chapter 5, specifically for the calculation of the supersonic flow though straight blade cascades. The analytical character of the method also makes it possible for the conditions, and above all the compression shocks, to be considered at infinity. Thus, with this method, the neutral entrance characteristics of a cascade with supersonic inlet flow can be determined, but with upstream effect, which had been found by Kantrowitz [15], Schwaar [16], Levine [17, 18], Yamaguchi [19] and lately also by Novak [20] and Starken [21] by other methods. The flow after the entry region in the channel of the cascade is calculated step by step. In this, the initial values of a new section are adopted from the solution of the preceding section. Lastly, with the aid of the method it is possible also to determine the supersonic outlet flow from the infinite cascade and the associated neutral cascade exit characteristics. The equations for the determination of the entropy change as a result of the compression shocks are given in chapter 6. These equations are then applied to the calculation of the losses due to the infinite number of cascade entry shocks.

Using the method by Oswatitsch, a number of problems have already been solved analytically in the last few years: Oswatitsch [22, 23], Schneider [24, 25], Rothmann [26, 27], Sun [28, 29], Leiter [30, 31], Leiter and Oswatitsch [32], Stuff [33, 34], Pokorny [35] and Sonn [36]. This thesis has much in common with the works by Lin, Schneider [24], Pokorny and Sonn.

2. Method of analytical characteristics

2.1. General equations

The method of analytical characteristics is used to calculate the flow through a straight blade cascade. The differential equations describing the flow must be hyperbolic to ensure the existence of true characteristic lines. For the further simplification of the subject, the flow must satisfy the following assumptions:

Let the flow be steady
Let the flow be two-dimensionally plane
Let the flow velocity be everywhere greater than the velocity of sound
Let no sources of mass be present in the flow
No action of external forces
No heat conduction
Let the flow be inviscid
Let no energy transfer take place
Let the flow be isoenergetic
Let the flow be irrotational

The flow medium shall satisfy the following conditions:

Let the gas be thermally and calorifically ideal
Let the specific heats of the fluid be constant

A further hypothesis of significance in the method, is the requirement that the approach flow shall be subject only to small changes from the steady condition (small perturbations). For steady flow, the requirement that supersonic velocity prevails everywhere is the

necessary and adequate condition for the system of differential equations, which being hyperbolic, characterize the flow. Under these hypotheses, the differential equations describing the flow are derived as follows (see Oswatitsch [37], equations (8.42) and (8.53):

$$\frac{\partial \eta}{\partial x} + \operatorname{tg}(\theta-\alpha)\,\frac{\partial \eta}{\partial y} = 0$$

(2.1)

$$\frac{\partial \xi}{\partial x} + \operatorname{tg}(\theta+\alpha)\,\frac{\partial \xi}{\partial y} = 0 \quad \text{as conditions of inclination}$$

and

$$\frac{\partial \theta}{\partial \xi} + \frac{\operatorname{ctg}\alpha}{w}\,\frac{\partial w}{\partial \xi} = 0$$

(2.2)

$$\frac{\partial \theta}{\partial \eta} - \frac{\operatorname{ctg}\alpha}{w}\,\frac{\partial w}{\partial \eta} = 0 \quad \text{as conditions of compatibility.}$$

x,y are the Cartesian position coordinates; w = the velocity; θ = the direction of flow, measured against the x-axis; ξ, η = the characteristic variables. α is the Mach angle which is a function only of the Mach Number. This in turn is a function of w, under the assumption made. This dependence is indicated in Table 1; also indicated in the table are further conversion formulae which are valid under the above assumptions. However, the normalization in equation (2.3) has already been used in the formulae given in the table.

By changing to the inverse form in equation (2.1) and introducing the non-dimensional quantities:

$$\tilde{x} = \frac{x}{l} \qquad \tilde{y} = \frac{y}{l} \qquad \tilde{\xi} = \frac{\xi}{l} \qquad \tilde{\eta} = \frac{\eta}{l}$$

(2.3)

$$\tilde{\theta} = \theta - \theta_\infty \qquad \tilde{w} = \frac{w}{w_\infty} - 1$$

the following system of equations is derived from equations (2.1) and (2.2); (the tilde symbol ~ will be omitted since in the subsequent discussions only these non-dimensional quantities will be used):

$$(2.4) \qquad \frac{\partial \theta}{\partial \xi} + \frac{ctg\alpha}{w+1} \frac{\partial w}{\partial \xi} = 0 \qquad\qquad \frac{\partial \theta}{\partial \eta} - \frac{ctg\alpha}{w+1} \frac{\partial w}{\partial \eta} = 0$$

$$(2.5) \qquad \frac{\partial y}{\partial \xi} - tg(\theta+\theta_\infty-\alpha) \frac{\partial x}{\partial \xi} = 0 \qquad\qquad \frac{\partial y}{\partial \eta} - tg(\theta+\theta_\infty+\alpha) \frac{\partial x}{\partial \eta} = 0$$

w_∞ and θ_∞ are reference quantities for which the incident flow quantities are normally selected. l is a random dimension of length of the object having the flow around it. The problem to be solved, i.e. to determine θ and w as functions of x and y is expressed in parametric form by the conditions of compatibility (2.4) and the conditions of inclination (2.5). The characteristic quantities ξ and η are the parameters which occur in the equations as independent variables, whereas θ, w and x,y are dependent variables.

Equations (2.4) and (2.5) are the initial equations of the method of analytical characteristics used here. Perturbation formulae are then written for the four dependent variables θ, w, and x, y; see Rothe, Szabo [39].

$$(2.6) \qquad \theta = \sum_{j=1}^{\infty} \theta^{(j)} \qquad\qquad w = \sum_{j=1}^{\infty} w^{(j)}$$

$$(2.7) \qquad x = \sum_{j=0}^{\infty} x^{(j)} \qquad\qquad y = \sum_{j=0}^{\infty} y^{(j)}$$

The successive terms in the progressions (2.6) and (2.7) must differ from each other by one order of magnitude. The j^{th} term of these progressions contains the j^{th} power of a perturbation parameter which is determined by the boundary conditions. The progressions for θ, w, where θ and w represent, as agreed, the quantities θ, w defined by equation (2.3), begin with the index 1 since in the undisturbed flow θ and w vanish, and therefore also the 0^{th} approximation in the

perturbation area. The terms of the progressions for x and y on the other hand begin with the order 0, since even in the undisturbed flow the dependence of the position coordinates on the characteristic quantities already exists.

The formulae (2.6) for the variables of state can be introduced into the closed solutions of the compatibility conditions which are obtained in the next chapter, whereas the formulae (2.7) for the position coordinates are inserted directly into the inclination conditions (2.5). The equations and differential equations are then written according to terms of equal order of magnitude, the requirement being that the terms of equal order of magnitude each by themselves satisfy the equations and differential equations. In this, the expressions of equal order of magnitude are in general the terms which also have the same sum index in the perturbation quantities.

2.2. Solution of the compatibility conditions

The compatibility conditions (2.4) can be processed as a line integral. The resulting solutions represent epicycloids in the hodographic plane. These are, see also Zierep [38].

$$\begin{aligned} &\theta + \nu = \text{const} \qquad \text{along } \eta = \text{const} \\ &\theta - \nu = \text{const} \qquad \text{along } \xi = \text{const} \end{aligned} \tag{2.8}$$

where ν as a Prandtl-Meyer function is defined as:

$$\nu = \sqrt{\frac{\kappa+1}{\kappa-1}}\,\operatorname{arctg}\sqrt{\frac{M^{*2}-1}{\frac{2}{\kappa-1}-(M^{*2}-1)}} - \operatorname{arctg}\sqrt{\frac{\kappa+1}{\kappa-1}\,\frac{M^{*2}-1}{\frac{2}{\kappa-1}-(M^{*2}-1)}} \tag{2.9}$$

where M^* is a non-dimensional velocity. The reference quantity is the speed of sound c^*, which occurs at the position where the speed just reaches sonic velocity. Under the assumptions made above, c^* is a constant in the whole flow field; see Table 1.

In order to simplify, at a later stage, the inclination conditions, we use in the further development of the calculations not the closed solution (2.8), but instead an approximate solution which is derived from equation (2.8) and which converges towards the exact solution as the

approximation progresses. In order to obtain the required approximation, the Prandtl-Meyer function is expanded to a series at the $w = 0$ position. This is possible because M^* depends only on w, and because on the other hand only small perturbations related to the incident flow are allowed in this work, i.e. w itself is to be of a small order of magnitude. Hence:

$$\nu(w) = \nu(0) + \sum_{k=1}^{\infty} \frac{1}{k!} \left[\left(\frac{d}{dw}\right)_{w=0} w \right]^k \nu(w) . \tag{2.10}$$

In applying the operator $(\frac{d}{dw} w)^k$ to ν, $w = 0$ is put in the differentiated expression of $\nu(w)$. This is indicated in the formula by the subscript $w = 0$. This expression is introduced into the equation (2.8) together with the perturbation formula (2.6). Arranging this then according to terms of equal magnitude and solving towards $\theta^{(i)}$, $\operatorname{ctg} \alpha_\infty \cdot w^{(i)}$ we obtain:

$$\theta^{(i)} = \frac{1}{2} \{ I^{(i)}(\eta) + J^{(i)}(\xi) \}$$

$$\operatorname{ctg}\alpha_\infty \, w^{(i)} = \sum_{j=1}^{i-1} L_j + \frac{1}{2} \{ I^{(i)}(\eta) - J^{(i)}(\xi) \} . \tag{2.11}$$

For abbreviation, the following was put:

$$L_j = - \frac{1}{(j+1)!} \left[\left(\frac{d}{dw}\right)_{w=0} \sum_{l=1}^{i} w^{(l)} \right]^{j+1} \nu(w) . \tag{2.12}$$

In doing this, it should be observed that on the right hand side of this equation only those terms may be taken into account which have the sum index i. $I^{(i)}(\eta)$ and $J^{(i)}(\xi)$ are arbitrary functions of the variables ξ, η. They will be defined further on by boundary values and initial values. The L_j expressions found on the right hand side under the sum index contain only $w^{(k)}$ terms with a k index which is smaller than i, i.e. $i-1$ maximum. For this reason, the right hand sides have already been calculated in the preceding approximations, being therefore given functions for the approximation of the i order. The value for first approximation of L_j is then:

$$(2.13) \qquad L_1 = -\frac{1}{2} \cdot \frac{1 + \frac{\kappa-1}{2} M_\infty^4}{ctg\alpha_\infty} \left(\sum_{1=1}^{i} w^{(1)} \right)^2 .$$

In the squared expression only those terms may be taken into account in this case which have the sum index i.

2.3. Solution of the inclination conditions

Before integrating the inclination conditions (2.5), the coefficients $tg\,(\theta + \theta_\infty + \alpha)$ and $tg\,(\theta + \theta_\infty - \alpha)$ occurring in it are expanded in a Taylor series. The Mach Number M and consequently also the Mach angle α are here only functions of the velocity w. It is therefore possible to express the two coefficients as functions of θ and w and since these two quantities of state are, according to the assumption, to be of a small order of magnitude, both expressions can be expanded in a series at the positions $w = 0$ and $\theta = 0$; this is (see also Rothe [40]):

(2.14)

$$tg\left(\theta+\theta_\infty \mp \alpha(w)\right) = tg\left(0+\theta_\infty \mp \alpha(0)\right) + \sum_{k=1}^{\infty} \frac{1}{k!} \left[\left(\frac{\partial}{\partial\theta}\right)_{\substack{\theta=0 \\ w=0}} \theta + \left(\frac{\partial}{\partial w}\right)_{\substack{\theta=0 \\ w=0}} w \right]^k \times$$

$$\times\; tg\left(\theta+\theta_\infty \mp \alpha(w)\right) .$$

By inserting in these equations the perturbation formulae (2.6) and introducing the equations thus obtained together with the perturbation formulae (2.7) into the inclination conditions, there is obtained for terms of the same order of magnitude:

(2.15)

$$\frac{\partial y^{(i)}}{\partial \xi} - tg(\theta_\infty - \alpha_\infty) \frac{\partial x^{(i)}}{\partial \xi} = \sum_{j=1}^{i} C_j \frac{\partial x^{(i-j)}}{\partial \xi} \qquad \text{along } \eta = \text{const}$$

$$\frac{\partial y^{(i)}}{\partial \eta} - tg(\theta_\infty + \alpha_\infty) \frac{\partial x^{(i)}}{\partial \eta} = \sum_{j=1}^{i} D_j \frac{\partial x^{(i-j)}}{\partial \eta} \qquad \text{along } \xi = \text{const}$$

To abbreviate this, we put:

$$(2.16) \qquad C_j = \sum_{k=1}^{j} C_k^* \qquad\qquad D_j = \sum_{k=1}^{j} D_k^*$$

where

$$(2.17) \qquad \begin{matrix} C_k^* \\ D_k^* \end{matrix} = \frac{1}{k!} \left[\left(\frac{\partial}{\partial\theta}\right)_{\substack{w=0 \\ \theta=0}} \sum_{l=1}^{j} \theta^{(l)} + \left(\frac{\partial}{\partial w}\right)_{\substack{w=0 \\ \theta=0}} \sum_{l=1}^{j} w^{(l)} \right]^k \times$$

$$\times \operatorname{tg}\left(\theta + \theta_\infty \mp \alpha(w)\right) .$$

The upper sign denotes the quantities C_k^* whereas the lower sign denotes D_k^*. The subscript expressions $w = 0$, $\theta = 0$ for the partial derivative symbols $(\frac{\partial}{\partial\theta})$ and $(\frac{\partial}{\partial w})$ indicate that $w = 0$ and $\theta = 0$ will be put in the differentiated expressions of $\operatorname{tg}\ (\theta + \theta_\infty \pm \alpha)$.

In the expressions on the right hand sides, only those terms may be taken into account where the sum index is j.

The equations (2.15) are linear partial differential equations for the position coordinates $x^{(i)}$, $y^{(i)}$ of the order i. The right hand sides of these equations are perturbation functions of the linear differential equations which are already known from the preceding approximations, because they contain the variables of state θ, w only up to the terms of the order of i, and the position coordinates only up to the order of $i-1$.

The first two approximations for the coefficients C_k^*, D_k^* result in:

$$(2.18) \qquad \begin{matrix} C_1^* \\ D_1^* \end{matrix} = \left[1 + \operatorname{tg}^2\left(\theta_\infty \mp \alpha_\infty\right)\right] \sum_{l=1}^{j} \theta^{(l)} \pm \operatorname{tg}\alpha_\infty \left[1 + \frac{\kappa-1}{2} M_\infty^2\right] \times$$

$$\times \left[1 + \operatorname{tg}^2\left(\theta_\infty \mp \alpha_\infty\right)\right] \sum_{l=1}^{j} w^{(l)}$$

(2.18)
$$\begin{matrix} C_2^* \\ D_2^* \end{matrix} = \frac{1}{2}\{2\,\mathrm{tg}(\theta_\infty \mp \alpha_\infty)\left[1+\mathrm{tg}^2(\theta_\infty \mp \alpha_\infty)\right]\left(\sum_{l=1}^{j}\theta^{(l)}\right)^2 \pm$$

$$\pm \quad 2\,\mathrm{tg}(\theta_\infty \mp \alpha_\infty)\left[1+\mathrm{tg}^2(\theta_\infty \mp \alpha_\infty)\right]\,\mathrm{tg}\alpha_\infty\left[1+\frac{\kappa-1}{2}M_\infty^2\right] \times$$

$$\times \left(\sum_{l=1}^{j}\theta^{(l)}\right)\cdot\left(\sum_{l=1}^{j}w^{(l)}\right)+\mathrm{tg}^2\alpha_\infty\left[1+\frac{\kappa-1}{2}M_\infty^2\right] \times$$

$$\times \left[1+\mathrm{tg}^2(\theta_\infty \mp \alpha_\infty)\right]\cdot\left[\pm\mathrm{tg}\alpha_\infty\left(1+\frac{\kappa-1}{2}M_\infty^4-(\kappa+1)M_\infty^2\right)-\right.$$

$$\left.-\,2\left[1+\frac{\kappa-1}{2}M_\infty^2\right]\mathrm{tg}(\theta_\infty \mp \alpha_\infty)\right]\cdot\left(\sum_{l=1}^{j}w^{(l)}\right)^2\}\,.$$

where α_∞ stands for $\alpha(o)$.

In these equations, once again only those terms may be considered where the sum index is j. The integration of the differential equations (2.15) gives, solving also for $x^{(i)}$, $y^{(i)}$, the solution of the inclination conditions which is to be found:

(2.19)
$$x^{(i)}(\xi,\eta) = \frac{1}{\mathrm{tg}(\theta_\infty+\alpha_\infty)-\mathrm{tg}(\theta_\infty-\alpha_\infty)}\left[\sum_{j=1}^{i}\int_{G^{(i)}(\eta)}^{\xi} C_j\frac{\partial x^{(i-j)}}{\partial\xi}\,d\xi - \right.$$

$$\left. -\sum_{j=1}^{i}\int_{H^{(i)}(\xi)}^{\eta} D_j\frac{\partial x^{(i-j)}}{\partial\eta}\,d\eta\right]$$

(2.19)

$$y^{(i)}(\xi,\eta) = \frac{1}{tg(\theta_\infty+\alpha_\infty) - tg(\theta_\infty-\alpha_\infty)} \left[tg(\theta_\infty+\alpha_\infty) \sum_{j=1}^{i} \int_{G^{(i)}(\eta)}^{\xi} C_j \frac{\partial x^{(i-j)}}{\partial \xi} \, d\xi - \right.$$

$$\left. - tg(\theta_\infty-\alpha_\infty) \sum_{j=1}^{i} \int_{H^{(i)}(\xi)}^{\eta} D_j \frac{\partial x^{(i-j)}}{\partial \eta} \, d\eta \right] .$$

The lower limits of the integrals $G^{(i)}(\eta)$ and $H^{(i)}(\xi)$ are arbitrary functions of ξ and η. They can be eliminated using the initial and boundary values which are to be prescribed (see Section 2.4). From the equations, the solution of the 0^{th} order is obtained as:

(2.20)

$$x^{(0)} = \frac{1}{tg(\theta_\infty+\alpha_\infty) - tg(\theta_\infty-\alpha_\infty)} \{g(\eta) - h(\xi)\}$$

$$y^{(0)} = \frac{1}{tg(\theta_\infty+\alpha_\infty) - tg(\theta_\infty-\alpha_\infty)} \{tg(\theta_\infty+\alpha_\infty)\, g(\eta) - tg(\theta_\infty-\alpha_\infty)\, h(\xi)\} .$$

The two functions that occur, $g(\eta)$ and $h(\xi)$ can be chosen arbitrarily; they cannot be specified by initial and boundary values. To determine them, a linear formula is expressed incorporating two constants A^* and A^{**}:

$$h(\xi) = - \left[tg(\theta_\infty+\alpha_\infty) - tg(\theta_\infty-\alpha_\infty) \right] A^{**} \xi$$

$$g(\eta) = + \left[tg(\theta_\infty+\alpha_\infty) - tg(\theta_\infty-\alpha_\infty) \right] A^{*} \eta .$$

These expressions substituted in equation (2.20) then provide the position coordinates in the 0^{th} approximation:

(2.21)

$$x^{(0)} = A^{*}\eta + A^{**}\xi$$

$$y^{(0)} = tg(\theta_\infty+\alpha_\infty)\, A^{*} \eta + tg(\theta_\infty-\alpha_\infty)\, A^{**}\xi .$$

If in the solutions $\theta^{(i)}$, $w^{(i)}$ of the compatibility conditions only terms of the 1^{st} order are taken into account, and in the solutions $x^{(i)}$, $y^{(i)}$ of the inclination conditions only terms of the 0^{th} order, then the results obtained are the same as those in the theory of acoustics. In the latter, conventionally (see Oswatitsch [37])

$$(2.22a) \qquad A^* = \frac{1}{2} \qquad A^{**} = \frac{1}{2}$$

are selected.

Another selection is:

$$(2.22b) \qquad A^* = \cos(\theta_\infty + \alpha_\infty) \qquad A^{**} = \cos(\theta_\infty - \alpha_\infty)$$

Here, ξ, η correspond exactly to the curved length of the characteristic lines (which are straight lines in this case) in the $x^{(0)}$, $y^{(0)}$ plane.

The values chosen for the constants A*, A** are of no consequence, they merely alter the numbering of the characteristic lines.

2.4. Boundary conditions and initial values

The boundary values of the problem to be solved are normally given in the physical plane, i.e. in the x, y plane. In the case considered here, let the contour of the body be given as

$$y = y_k(x).$$

The subscript k indicates that for the quantities concerned the values at the boundary are used. For a given body contour, the distribution of angles along the boundary of the body is specified at the same time, for which the following is valid:

$$(2.23a) \qquad \theta_k = -\theta_\infty + \operatorname{arctg} \frac{dy_k}{dx}$$

where θ_∞ is the reference angle and θ_k the contour angle (see also equation (2.3)). To be solved, however, is the problem of the flow around a body in the characteristic ξ, η plane. It is therefore

necessary that the boundary conditions given in the physical plane be transferred to the characteristic plane. The equation for the blade contour in the characteristic coordinates is required to be found either as $\eta = \eta_k(\xi)$ or as $\xi = \xi_k(\eta)$. It will be seen that the first form is required if in addition to the blade boundary conditions, initial values along a left-handed Mach line ξ_A are given (see Fig. 1), whereas the second form is necessary if initial values along a right-handed line η_A are given (see Fig. 2).

We limit ourselves here to the case where the initial values given run along the left-handed characteristic ξ_A. Corresponding expressions can also be derived for the case where the initial values given run along a right-handed line η_A. The equation for the wall contour in characteristic coordinates is required in terms of $\eta = \eta_k(\xi)$.

In the x, y coordinates, the equation applicable to the contour is then written as:

$$y = y_k\left(\xi, \eta_k(\xi)\right) ; \qquad x = x_k\left(\xi, \eta_k(\xi)\right) .$$

The angle θ_k of the body boundary is then:

$$\theta = \theta_k\left(\xi, \eta_k(\xi)\right) .$$

If the formula (2.7) is substituted in the equation for the blade contour, we obtain:

$$y_k = y_k^{(0)} + y_k^{(1)} + y_k^{(2)} + \ldots$$

Using the approximation of the zeroth order for the coordinates x, y, equation (2.21) then gives:

$$y_k = \mathrm{tg}(\theta_\infty + \alpha_\infty) A^* \eta_k(\xi) + \mathrm{tg}(\theta_\infty - \alpha_\infty)\ A^{**}\xi + y_k^{(1)} + y_k^{(2)} + \ldots$$

Solving the equation for $\eta = \eta_k(\xi)$ then provides the required relationship for the body contour in the characteristic coordinates.

(2.24)

$$\eta_k(\xi) = \frac{1}{tg(\theta_\infty+\alpha_\infty)\ A^{**}} \left\{-tg(\theta_\infty-\alpha_\infty)\ A^{**}\xi+y_k(x_k)-\left[y_k^{(1)}+y_k^{(2)}+\ldots\right]\right\} .$$

As the argument for y_k, $x = x_k\ (\xi,\ \eta_k\ (\xi)) = x_k^{(0)} + x_k^{(1)} = \ldots$ is to be put on the right side of this equation. The equation can, however, be solved only by iteration, since the relationship $\eta_k(\xi)$, which is to be found, is also contained on the right side in the relationships for $x_k\ (\xi,\ \eta_k\ (\xi))$ and $y_k\ (\xi,\ \eta_k\ (\xi))$. The order of the terms $x_k^{(i)}$ and $y_k^{(i)}$, which are considered in equation (2.24), determine the order of the approximation for $\eta_k(\xi)$. This means that for a zeroth order approximation, only the $x_k^{(0)}$ term need be considered and for a 1st order approximation only the terms $x_k^{(0)}$, $x_k^{(1)}$ and $y_k^{(1)}$.

If the iteration is to be avoided, then the next lower approximation can be put for η_k in the equations of the right hand side. This would of course result in reduced accuracy. For the zeroth approximation, a separate consideration will then be necessary because no previous approximation exists for the right side. In this case, the approximation

$$y_k - tg\theta_\infty\ x_k \approx 0$$

is used. This relationship can be considered as the most extreme approximation for the condition that the extension of the body contour in a direction at right angles to the incident flow is to be small, i.e. precisely 0. Hence, with equation (2.21) this yields

(2.25)* $$\eta_k^{(00)} = -\left(\frac{tg(\theta_\infty-\alpha_\infty) - tg(\theta_\infty)}{tg(\theta_\infty+\alpha_\infty) - tg(\theta_\infty)} \cdot \frac{A^{**}}{A^{*}} \cdot \xi\right) .$$

The contour angle θ_k as a function of the characteristic coordinates results from equation (2.23a), where, however, x is not independent, but where $x = x_k\ (\xi,\ \eta_k\ (\xi))$ along the contour is a function of the characteristic quantities. Therefore:

(2.23)* $$\theta_k(x_k) = -\theta_\infty + arctg\left(\frac{dy_k}{dx}\right)_{x=x_k} .$$

[* Translator's note: These numbers are as per original]

In this equation, the accuracy of the expression is given by the order of the terms which are taken into account on the right side for $x_k = x_k^{(0)} + x_k^{(1)} + \ldots$

Having shown the interrelationship of the boundary values in the physical and characteristic planes, the integration limits $I^{(i)}(\eta)$, $J^{(i)}(\xi)$ for equation (2.11) and $G^{(i)}(\eta)$, $H^{(i)}(\xi)$ for equation (2.19) must be determined from the boundary and initial values. There occur the characteristic initial value problems, and characteristic mixed boundary and initial value problems, in solving the differential equations established in this work. In the case of the pure initial value problems, the initial values along left-handed initial characteristics and right-handed initial characteristics are given (see Fig. 3). Both initial characteristics limit the range of certainty of the solution. In the case of the boundary/initial value problems, initial values along the initial characteristics ξ_A or η_A and boundary values along the non-characteristic boundary line $\eta_k(\xi)$ or $\xi_k(\eta)$ are given (see Figs. 1 and 2). In this case, the initial characteristics and the boundary line of the range of certainty determine the solution. The variables of state θ, w and the coordinates x, y cannot be freely selected along the initial characteristics. They must satisfy the differential equations (2.4) and (2.5) which are valid along the characteristic line in question. Details of the characteristic initial value problem and the mixed boundary and initial value problem were found by Sauer [41]. Let us now first consider the case of the mixed characteristic boundary/initial value problem. Thus, the initial values are given along the initial characteristics $\xi = \xi_A = \text{const.}$, and the boundary values along the blade contour which are represented as $\eta = \eta_k(\xi)$. Along ξ_A:

$$\theta^{(i)} = \theta^{(i)}(\xi_A, \eta) \qquad w^{(i)} = w^{(i)}(\xi_A, \eta) \qquad x^{(i)} = x^{(i)}(\xi_A, \eta)$$

$$y^{(i)} = y^{(i)}(\xi_A, \eta)$$

If the initial values are written into the equations (2.11), then $J^{(i)}(\xi)$ can be eliminated and solved for $I^{(i)}(\eta)$:

$$I^{(i)}(\eta) = \theta^{(i)}(\xi_A,\eta) + ctg\alpha_\infty\, w^{(i)}(\xi_A,\eta) - \sum_{j=1}^{i-1} (L_j)_{\xi_A,\eta} .$$

Substituting this expression in the 1st equation (2.11) and considering the equation along the boundary curve obtained, $\eta = \eta_k(\xi)$, the second integration limit $J^{(i)}(\xi)$ can be determined as:

$$J^{(i)}(\xi) = 2\theta_k^{(i)}(\xi,\eta_k(\xi)) - \left[\theta^{(i)}(\xi_A,\eta_k(\xi)) + ctg\alpha_\infty\, w^{(i)}(\xi_A,\eta_k(\xi))\right] + \sum_{j=1}^{i-1} (L_j)_{\xi_A,\eta_k(\xi)} .$$

Writing the quantities $I^{(i)}(\eta)$ and $J^{(i)}(\xi)$ thus established into equation (2.11) finally gives

(2.26)

$$\theta^{(i)}(\xi,\eta) = \theta_k^{(i)}(\xi,\eta_k(\xi)) + \frac{1}{2}\left\{\left[\theta^{(i)}(\xi_A,\eta) + ctg\alpha_\infty\, w^{(i)}(\xi_A,\eta)\right] - \left[\theta^{(i)}(\xi_A,\eta_k(\xi)) + ctg\alpha_\infty\, w^{(i)}(\xi_A,\eta_k(\xi))\right] + \sum_{j=1}^{i-1} (L_j)_{\xi_A,\eta_k(\xi)} - \sum_{j=1}^{i-1} (L_j)_{\xi_A,\eta}\right\}$$

$$ctg\alpha_\infty\, w^{(i)}(\xi,\eta) = -\theta_k^{(i)}(\xi,\eta_k(\xi)) + \sum_{j=1}^{i-1} (L_j)_{\xi,\eta} + \frac{1}{2}\left\{\left[\theta^{(i)}(\xi_A,\eta) + ctg\alpha_\infty\, w^{(i)}(\xi_A,\eta)\right] + \left[\theta^{(i)}(\xi_A,\eta_k(\xi)) + ctg\alpha_\infty\, w^{(i)}(\xi_A,\eta_k(\xi))\right] - \sum_{j=1}^{i-1} (L_j)_{\xi_A,\eta} - \sum_{j=1}^{i-1} (L_j)_{\xi_A,\eta_k(\xi)}\right\} .$$

This is now the definitive solution of the compatibility conditions including the given boundary and initial values.

For the determination of the integration limits $G^{(i)}(\eta)$ of the inclination conditions it is necessary to consider the equations (2.19) for the initial characteristics $\xi = \xi_A$. This gives:

$$y^{(i)}(\xi_A,\eta) - tg(\Theta_\infty-\alpha_\infty)\, x^{(i)}(\xi_A,\eta) = \int_{G^{(i)}(\eta)}^{\xi_A} \sum_{j=1}^{i} C_j \frac{\partial x^{(i-j)}}{\partial \xi}\, d\xi \,.$$

The right hand side integral is split into two sub-integrals:

$$\int_{G^{(i)}(\eta)}^{\xi_A} \ldots = \int_{G^{(i)}(\eta)}^{\xi} \ldots + \int_{\xi}^{\xi_A} \ldots = \int_{G^{(i)}(\eta)}^{\xi} \ldots - \int_{\xi_A}^{\xi} .$$

Hence, the integral $\int_{G^{(i)}(\eta)}^{\xi} \ldots$ can be substituted by the initial values along ξ_A and by an integral having the fixed lower limit ξ_A.

$$\int_{G^{(i)}(\eta)}^{\xi} \ldots = \int_{G^{(i)}(\eta)}^{\xi_A} \ldots + \int_{\xi_A}^{\xi} \ldots = y^{(i)}(\xi_A,\eta) - tg(\Theta_\infty-\alpha_\infty)\, x^{(i)}(\xi_A,\eta) + \int_{\xi_A}^{\xi} \ldots$$

If this expression is written into the equation (2.19) of the coordinates, then this leaves only the integration limit $H^{(i)}(\xi)$ still to be determined. To establish the function $H^{(i)}(\xi)$, a value can be freely selected along the boundary curve $\eta = \eta_k(\xi)$. We take, as Schneider [24]:

$$y^{(i)}(\xi,\eta_k(\xi)) = y_k^{(i)}(\xi,\eta_k(\xi)) = y_k^{(i)}(\xi_A,\eta_k(\xi_A)) = \text{const},$$

i.e. the y values for the first and all subsequent approximations are regarded as constants. Following the establishment of $G^{(i)}(\eta)$ and the selection of $y^{(i)}(\xi, \eta_k(\xi))$ it is possible to eliminate from the equations (2.19) the quantity $H^{(i)}(\xi)$, and the solution of the inclination conditions including the boundary and initial values is obtained as:

(2.27)

$$x^{(i)}(\xi,\eta) = \frac{y_k^{(i)}(\xi_A,\eta_k(\xi_A))}{tg(\theta_\infty-\alpha_\infty)} + \frac{1}{tg(\theta_\infty+\alpha_\infty)-tg(\theta_\infty-\alpha_\infty)} \times$$

$$\times\Big\{\sum_{j=1}^{i}\int_{\xi_A}^{\xi} C_j\frac{\partial x^{(i-j)}}{\partial\xi}\,d\xi - \frac{tg(\theta_\infty+\alpha_\infty)}{tg(\theta_\infty-\alpha_\infty)}\sum_{j=1}^{i}\Big(\int_{\xi_A}^{\xi} C_j\frac{\partial x^{(i-j)}}{\partial\xi}\,d\xi\Big)_{\eta_k(\xi)} -$$

$$-\sum_{j=1}^{i}\int_{\eta_k(\xi)}^{\eta} D_j\frac{\partial x^{(i-j)}}{\partial\eta}\,d\eta + \Big[y^{(i)}(\xi_A,\eta)-tg(\theta_\infty-\alpha_\infty)\,x^{(i)}(\xi_A,\eta)\Big] -$$

$$-\frac{tg(\theta_\infty+\alpha_\infty)}{tg(\theta_\infty-\alpha_\infty)}\Big[y^{(i)}(\xi_A,\eta_k(\xi))-tg(\theta_\infty-\alpha_\infty)\,x^{(i)}(\xi_A,\eta_k(\xi))\Big]\Big\}$$

(2.27)

$$y^{(i)}(\xi,\eta) = y_k^{(i)}(\xi_A,\eta_k(\xi_A)) + \frac{1}{tg(\theta_\infty+\alpha_\infty)-tg(\theta_\infty-\alpha_\infty)} \{tg(\theta_\infty+\alpha_\infty) \times$$

$$\times\left[\sum_{j=1}^{i}\int_{\xi_A}^{\xi} C_j \frac{\partial x^{(i-j)}}{\partial\xi}\,d\xi - \sum_{j=1}^{i}\left(\int_{\xi_A}^{\xi} C_j \frac{\partial x^{(i-j)}}{\partial\xi}\,d\xi\right)_{\eta_k(\xi)}\right] -$$

$$- tg(\theta_\infty-\alpha_\infty)\sum_{j=1}^{i}\int_{\eta_k(\xi)}^{\eta} D_j \frac{\partial x^{(i-j)}}{\partial\eta}\,d\eta + tg(\theta_\infty+\alpha_\infty) \times$$

$$\times\Big\{\left[y^{(i)}(\xi_A,\eta)-tg(\theta_\infty-\alpha_\infty)\, x^{(i)}(\xi_A,\eta)\right] -$$

$$- \left[y^{(i)}(\xi_A,\eta_k(\xi))-tg(\theta_\infty-\alpha_\infty)\, x^{(i)}(\xi_A,\eta_k(\xi))\right]\Big\}\,.$$

If the initial values along a right-handed characteristic line are given, or if the pure initial value problem is concerned, then the expressions equivalent to the equations (2.26) and (2.27) are obtained. These are given in Table 2, the following being put as an abbreviation:

(2.28)

$$A^{(i)}(\eta) = \theta^{(i)}(\xi_A,\eta) + ctg\alpha_\infty w^{(i)}(\xi_A,\eta) - \sum_{j=1}^{i-1}(L_j)_{\xi_A,\eta}$$

$$B^{(i)}(\xi) = \theta^{(i)}(\xi,\eta_A) - ctg\alpha_\infty w^{(i)}(\xi,\eta_A) + \sum_{j=1}^{i-1}(L_j)_{\xi,\eta_A}$$

$$E^{(i)}(\eta) = y^{(i)}(\xi_A,\eta) - tg(\theta_\infty-\alpha_\infty)\, x^{(i)}(\xi_A,\eta)$$

$$F^{(i)}(\xi) = y^{(i)}(\xi,\eta_A) - tg(\theta_\infty+\alpha_\infty)\, x^{(i)}(\xi,\eta_A)$$

2.5. Streamline equations

The differential equation of the streamline is written in Cartesian coordinates, observing the normalization conditions (2.3) as:

$$\left[\frac{dy}{dx}\right]_{\Psi} = tg\,(\theta + \theta_{\infty})\ . \tag{2.29}$$

The subscript Ψ indicates that streamlines are concerned. By transition to the characteristic coordinates we obtain from equation (2.29), using also the equations (2.5), the streamline equation in the ξ, η plane as:

$$\left(\frac{d\eta}{d\xi}\right)_{\psi} = \frac{\frac{\partial x}{\partial \xi}}{\frac{\partial x}{\partial \eta}} \cdot \frac{\cos(\theta + \theta_{\infty}+\alpha)}{\cos(\theta + \theta_{\infty}-\alpha)}\ . \tag{2.30}$$

Substituting the series (2.6) and (2.7) for θ, w and x,y then enables the streamline to be calculated by integration of the differential equation (2.30) as $\eta_{\Psi} = \eta_{\Psi}(\xi)$ if an initial point (ξ_{Anf}, η_{Anf}) is also given. The accuracy of this streamline is governed by the order of the terms taken into account on the right side of equation (2.30).

In some cases, a simplification can be achieved by a series expansion of the right side of equation (2.30). Expanding the second factor at the position $w = 0$, $\theta = 0$, we then obtain:

(2.31)

$$\left(\frac{d\eta}{d\xi}\right)_{\psi} = \frac{\frac{\partial x}{\partial \xi}}{\frac{\partial x}{\partial \eta}} \cdot \left[S_1 + S_2\theta + S_3\, w + S_4\,\frac{\theta^2}{2} + S_5\,\frac{w^2}{2} + S_6\theta \cdot w + \ldots\right]$$

where

(2.32)

$$S_1 = \frac{\cos(\theta_\infty+\alpha_\infty)}{\cos(\theta_\infty-\alpha_\infty)} \qquad S_2 = -\frac{\sin(2\,\alpha_\infty)}{\cos^2(\theta_\infty-\alpha_\infty)}$$

$$S_3 = \frac{\sin(2\,\theta_\infty)}{\cos^2(\theta_\infty-\alpha_\infty)} \cdot \frac{1+\frac{\kappa-1}{2} M_\infty^2}{\sqrt{M_\infty^2-1}} \qquad S_4 = -2 \cdot \frac{\sin(\theta_\infty-\alpha_\infty)\,\sin(2\,\alpha_\infty)}{\cos^3(\theta_\infty-\alpha_\infty)}$$

$$S_5 = 2\,\frac{\sin(\theta_\infty-\alpha_\infty)\,\sin(2\,\theta_\infty)}{\cos^3(\theta_\infty-\alpha_\infty)} \cdot \frac{(1+\frac{\kappa-1}{2} M_\infty^2)^2}{M_\infty^2-1} +$$

$$+ \frac{\sin(2\,\theta_\infty)}{\cos^2(\theta_\infty-\alpha_\infty)} \frac{1+\frac{\kappa-1}{2} M_\infty^2}{(M_\infty^2-1)^{3/2}} \left[\frac{\kappa-1}{2} M_\infty^4 - (\kappa+1) M_\infty^2 + 1\right]$$

$$S_6 = 2\,\frac{\cos(\theta_\infty+\alpha_\infty)}{\cos^3(\theta_\infty-\alpha_\infty)} \frac{1+\frac{\kappa-1}{2} M_\infty^2}{\sqrt{M^2-1}}$$

.
.
.

3. Weak compression shocks as a convolution of the characteristics

3.1. General shock equations

Using the equations established in Chapter 2 it is possible to calculate the flow conditions θ, w at every x, y position provided the required initial and boundary values are given. In this Chapter, an equation is to be developed which makes the calculation of the form of the shock possible, when an oblique compression shock configuration occurs in the flow field considered. For the derivation of this equation it is assumed here that the conditions at a certain distance upstream and downstream of the shock are known, whereas the position of the shock itself is yet to be determined.

In the supersonic flow around bodies there may be areas in the physical x, y plane in which characteristics of the same family (e.g. left-handed

characteristics) intersect. This occurs in flows around aerofoils whose contours have a concave shape (see Fig. 4) or have a concave break (see Fig. 5). In the case shown in Fig. 4 the characteristics generate an envelope, see Courant, Friedrichs [42]. The area between the two branches of the envelope is triply covered by Mach lines of the same kind. If there is no concave shaped contour but rather a concave break, then no envelope formation will occur. In that case, the two characteristics, which run through the break point, occur instead of the envelope. The area between the two Mach lines is doubly covered by characteristics of the same kind. There are therefore points in the physical x, y plane which are correlated to three or two points respectively in the characteristic ξ, η plane. Since each point in the characteristic plane is also associated with a specific value of the variables of state θ, w, the qualitative configurations shown in Figs. 6 and 7 are obtained by plotting the surface of state for θ or w over the x, y plane. It is seen in Fig. 6 that three different variables of state are obtained for one paired value of x, y coordinates in the area bordered by the envelope. For the case shown in Fig. 7, the calculation gives two different conditions for a point in the flow field if this is situated within the two characteristics running through the break point.

Physically, of course, to have two or three different conditions at one position is nonsensical. These doubly or triply covered zones are called convolutions of the flow field. The choice of the name convolution becomes apparent in Fig. 6, where the surface of state θ or w, plotted above the physical plane, folds over exactly in that area. A condition of instability, i.e. a compression shock, occurs in the convolution area. Upstream of this shock front, the solution shown by the lower (upper) sheet of the convolution applies whilst downstream the condition given by the upper (lower) sheet applies. The middle sheet, which possibly occurs in the case of the concave shaped wall, has no physical significance, and the flow values given by the position of this sheet will not be taken

into consideration in what follows. The shock front which separates the two different areas of the surface of state is a priori unknown. It originates in the cusp of the envelope at zero value and runs between the two branches of the envelope. The cusp of the envelope, i.e. the initial point of the shock is also an unknown priori. This must be determined by a separate consideration. This is undertaken in Chapter 3.2.

In the case where the shock occurs as a result of a concave break, Fig. 5, it begins at this break position with a finite strength and runs between the two Mach lines passing through this point.

To calculate the shock front, we have the shock equations. They are valid under the hypothesis mentioned in Chapter 2; they do, however, still apply even if the conditions of isoenergy and irrotation are abandoned. Likewise, the supersonic approach flow, $M_\infty > 1$ need not be found, but instead only the supersonic flow ahead of the shock is required. The shock equations are found, e.g. by Oswatitsch [37]. Introducing polar coordinates θ, w into his equations, observing equation (2.3), and following some transformations, the slope of the shock front is then derived as:

$$(3.1) \qquad tg\gamma = \left(\frac{dy}{dx}\right)_{St} = \frac{\hat{M}^* \cos(\hat{\theta}+\theta_\infty) - M^* \cos(\theta+\theta_\infty)}{M^* \sin(\theta+\theta_\infty) - \hat{M}^* \sin(\hat{\theta}+\theta_\infty)}$$

and the shock equation (shock polars) as:

$$(3.2)$$

$$\hat{M}^{*3} + \hat{M}^{*2}\left\{-2M^* \cos(\hat{\theta}-\theta) - \frac{2}{\kappa+1} M^* tg(\hat{\theta}-\theta) \sin(\hat{\theta}-\theta) - \frac{1}{M^* \cos(\hat{\theta}-\theta)}\right\} +$$

$$+ \hat{M}^*\{M^{*2} + 2\} + \left\{\frac{-M^*}{\cos(\hat{\theta}-\theta)}\right\} = 0 .$$

The quantities provided with the symbol ^ identify the conditions directly after the shock, whilst the quantities not marked express the state directly ahead of the shock. The shock polars are derived from a relation-

ship between the four quantities θ, w, $\hat{\theta}$, $\hat{w}$. Being a cubic equation in $\hat{M}^*$, it yields three different solutions for one value of θ. This is shown qualitatively in Fig. 8. In this illustration, point 1 identifies the solution of the weak shock, and point 2 the solution of the severe shock whilst the 3rd possible solution at point 3 has no physical significance. In this work only the weak solution is used. It is apparent in equations (3.1) and (3.2) that the state after the shock can be calculated by the two equations, if the shock inclination and the state ahead of the shock are given. Here, further on, the reverse is pursued, namely the inclination angle is calculated from the conditions ahead of and following the shock. The shock is therefore arranged in the flow field in such a way that the shock equations (3.1) and (3.2) are compatible with the flow field ahead of, and after the shock.

In order to obtain the differential equation for the shock front, equation (3.1) is used for the inclination of the shock front and the differential $(\frac{dy}{dx})_{St}$ is written instead of $tg\gamma$, and characteristic coordinates are introduced into this differential. The result is:

$$(3.3) \qquad tg\gamma = \left(\frac{dy}{dx}\right)_{St} = \frac{\frac{\partial y}{\partial \xi}\left(\frac{d\xi}{d\eta}\right)_{St} + \frac{\partial y}{\partial \eta}}{\frac{\partial x}{\partial \xi}\left(\frac{d\xi}{d\eta}\right)_{St} + \frac{\partial x}{\partial \eta}} .$$

Substituting the relationships (2.5) for $\frac{\partial y}{\partial \xi}$ and $\frac{\partial y}{\partial \eta}$, we obtain in solving for $(\frac{d\xi}{d\eta})_{St}$:

$$(3.4) \qquad \left(\frac{d\xi}{d\eta}\right)_{St} = -\frac{\frac{\partial x}{\partial \eta}}{\frac{\partial x}{\partial \xi}} \cdot \frac{1 - ctg\gamma\ tg(\theta+\theta_\infty+\alpha)}{1 - ctg\gamma\ tg(\theta+\theta_\infty-\alpha)} .$$

with equation (3.1) and after some transformations it follows that:

(3.5)

$$\left(\frac{d\xi}{d\eta}\right)_{St} = -\frac{\frac{\partial x}{\partial \eta}}{\frac{\partial x}{\partial \xi}}\left[\frac{1+tg(\theta+\theta_\infty)tg\alpha}{1-tg(\theta+\theta_\infty)tg\alpha}\cdot\left[\hat{M}^*\cos(\hat{\theta}+\theta_\infty) - M^*\cos(\theta+\theta_\infty) - \right.\right.$$

$$- M^*\sin(\theta+\theta_\infty)tg(\theta+\theta_\infty) + \hat{M}^*\sin(\hat{\theta}+\theta_\infty)tg(\theta+\theta_\infty) -$$

$$\left.- \hat{M}^*tg\alpha\{\cos(\hat{\theta}+\theta_\infty)tg(\theta+\theta_\infty) - \sin(\hat{\theta}+\theta_\infty)\}\right] \Big/ \left[\hat{M}^*\cos(\hat{\theta}+\theta_\infty) -\right.$$

$$- M^*\cos(\theta+\theta_\infty) - M^*\sin(\theta+\theta_\infty)tg(\theta+\theta_\infty) +$$

$$+ \hat{M}^*\sin(\hat{\theta}+\theta_\infty)tg(\theta+\theta_\infty) + \hat{M}^*tg\alpha\{\cos(\hat{\theta}+\theta_\infty)tg(\theta+\theta_\infty) -$$

$$\left.\left.- \sin(\hat{\theta}+\theta_\infty)\}\right]\right] .$$

The expression in squared brackets is a function of the four quantities w, θ, $\hat{w}$, $\hat{\theta}$. Taking the shock equations (3.2) into account, $\hat{w}$ can be considered as a function of the remaining quantities. The expansion of the bracketed expression at positions $\hat{w} = w$, $\hat{\theta} = \theta$, and the subsequent series expansion of the coefficients occurring at positions $w = 0$ and $\theta = 0$ gives:

(3.6)

$$\left(\frac{d\xi}{d\eta}\right)_{St} = -\frac{\frac{\partial x}{\partial \eta}}{\frac{\partial x}{\partial \xi}}\left[\left\{K_{11} + K_{12}w + K_{13}\theta + K_{14}\frac{w^2}{2} + K_{15}w\theta + K_{16}\frac{\theta^2}{2} + \ldots\right\}\times\right.$$

$$\left.\times(\hat{\theta}-\theta) + \{K_{21} + \ldots\}\frac{(\hat{\theta}-\theta)^2}{2} + \ldots\right]$$

for left-handed shocks.

The equation for right-handed shocks follows by exchanging ξ for η and substituting K_{ij} by $\tilde{K}_{ij}$.

Indexing the quantities in the downstream sheet with the symbol $\hat{}$, the differential shock equation in the coordinates of the downstream sheet of the convolution is obtained from equation (3.6) by substituting the quantities $\hat{x}$, $\hat{\xi}$, $\hat{\eta}$, $\hat{w}$, of the 2nd sheet for x, ξ, η and w and replacing by $\hat{\theta}$.

The coefficients K_{ij} and $\tilde{K}_{ij}$ for approximations up to the 2nd order follow as:

(3.7)

$$\frac{K_{11}}{\tilde{K}_{11}} = \pm \frac{1 \pm tg\theta_\infty \, tg\alpha_\infty}{1 \mp tg\theta_\infty \, tg\alpha_\infty} \cdot \frac{\kappa+1}{8} \cdot \frac{M_\infty^4}{(M_\infty^2-1)^{3/2}}$$

$$\frac{K_{12}}{\tilde{K}_{12}} = \frac{\kappa+1}{8} \cdot \frac{M_\infty^4}{(M_\infty^2-1)^{5/2}} \cdot \frac{1+\frac{\kappa-1}{2} M_\infty^2}{[1 \mp tg\theta_\infty \, tg\alpha_\infty]^2} \times$$

$$\times \{\pm [M_\infty^2-4] - tg\theta_\infty \, tg\alpha_\infty [2 M_\infty^2 \pm tg\theta_\infty \, tg\alpha_\infty (M_\infty^2-4)]\}$$

$$\frac{K_{13}}{\tilde{K}_{13}} = \frac{\kappa+1}{4} \cdot \frac{M_\infty^4}{(M_\infty^2-1)^2} \cdot \frac{1+tg^2\,\theta_\infty}{[1 \mp tg\theta_\infty \, tg\alpha_\infty]^2}$$

$$\frac{K_{21}}{\tilde{K}_{21}} = \frac{1 \pm tg\theta_\infty \, tg\alpha_\infty}{1 \mp tg\theta_\infty \, tg\alpha_\infty} \cdot \frac{\kappa+1}{8} \cdot \frac{M_\infty^4}{(M_\infty^2-1)^3} \{M_\infty^2(\kappa-1)+2\} .$$

One further quantity, namely $\hat{\theta}(\hat{\xi}, \hat{\eta})$ must be expressed in the coordinates of the other sheet in the differential equation (3.6). The required relationship

(3.8) $\qquad \hat{\xi} = \hat{\xi}(\xi,\eta) \qquad \hat{\eta} = \hat{\eta}(\xi,\eta)$

is obtained in the implicit form if it is observed that

(3.9) $\qquad x(\xi,\eta) = \hat{x}(\hat{\xi},\hat{\eta}) \quad y(\xi,\eta) = \hat{y}(\hat{\xi},\hat{\eta})$

is valid for the convolution range.

This equation expresses the fact that in the convolution region two (real) pairs of value ξ, η and $\hat{\xi}$, $\hat{\eta}$ of the characteristic coordinates are associated with one point in the physical x, y plane. It is seldom possible to solve this problem analytically. It is simpler to expand the equations (3.9) at one position $\hat{\xi} = \hat{\xi}_s(\xi, \eta)$, $\hat{\eta} = \hat{\eta}_s(\xi, \eta)$ and then to solve for $\hat{\xi}$ and $\hat{\eta}$. This can be implemented explicitly up to terms of the 2nd order; it leads to biquadratic equations. Considering only terms up to the 1st order, we obtain:

(3.10)

$$\hat{\xi} = \hat{\xi}_s + \frac{\left(\frac{\partial \hat{y}}{\partial \hat{\eta}}\right)_{\hat{\xi}_s,\hat{\eta}_s}\left[x(\xi,\eta)-\hat{x}(\hat{\xi}_s,\hat{\eta}_s)\right]-\left(\frac{\partial \hat{x}}{\partial \hat{\eta}}\right)_{\hat{\xi}_s,\hat{\eta}_s}\left[y(\xi,\eta)-\hat{y}(\hat{\xi}_s,\hat{\eta}_s)\right]}{\left(\frac{\partial \hat{x}}{\partial \hat{\xi}}\right)_{\hat{\xi}_s,\hat{\eta}_s}\left(\frac{\partial \hat{y}}{\partial \hat{\eta}}\right)_{\hat{\xi}_s,\hat{\eta}_s}-\left(\frac{\partial \hat{y}}{\partial \hat{\eta}}\right)_{\hat{\xi}_s,\hat{\eta}_s}\left(\frac{\partial \hat{x}}{\partial \hat{\eta}}\right)_{\hat{\xi}_s,\hat{\eta}_s}} + \ldots$$

$$\hat{\eta} = \hat{\eta}_s + \frac{\left(\frac{\partial \hat{y}}{\partial \hat{\xi}}\right)_{\hat{\xi}_s,\hat{\eta}_s}\left[x(\xi,\eta)-\hat{x}(\hat{\xi}_s,\hat{\eta}_s)\right]-\left(\frac{\partial \hat{x}}{\partial \hat{\xi}}\right)_{\hat{\xi}_s,\hat{\eta}_s}\left[y(\xi,\eta)-\hat{y}(\hat{\xi}_s,\hat{\eta}_s)\right]}{\left(\frac{\partial \hat{x}}{\partial \hat{\eta}}\right)_{\hat{\xi}_s,\hat{\eta}_s}\left(\frac{\partial \hat{y}}{\partial \hat{\xi}}\right)_{\hat{\xi}_s,\hat{\eta}_s}-\left(\frac{\partial \hat{y}}{\partial \hat{\eta}}\right)_{\hat{\xi}_s,\hat{\eta}_s}\left(\frac{\partial \hat{x}}{\partial \hat{\xi}}\right)_{\hat{\xi}_s,\hat{\eta}_s}} + \ldots$$

$\hat{\theta}$, $(\hat{\xi}, \hat{\eta})$ can also be expanded in series. To a first order of accuracy, it is:

$$(3.11) \qquad \hat{\theta}(\hat{\xi},\hat{\eta}) = \hat{\theta}(\hat{\xi}_s,\hat{\eta}_s)+\left(\frac{\partial \hat{\theta}}{\partial \hat{\xi}}\right)_{\hat{\xi}_s,\hat{\eta}_s}(\hat{\xi}-\hat{\xi}_s)+\left(\frac{\partial \hat{\theta}}{\partial \hat{\eta}}\right)_{\hat{\xi}_s,\hat{\eta}_s}(\hat{\eta}-\hat{\eta}_s) + \ldots$$

Substituting in equation (3.11) the above relationships (3.10) for the variables $\hat{\xi}$ and $\hat{\eta}$ and introducing the resulting expression for $\hat{\theta}$ into equation (3.6), then the differential equation for the shock front is derived in the form: $\left(\frac{d\xi}{d\eta}\right)_{St} = f(\xi, \eta)$. The solution of the resulting ordinary differential equation of the 1st order will in most cases have to be carried out numerically. Choosing the quantities $\hat{\eta}_s$ and $\hat{\xi}_s$, for left-handed shocks we have: $\hat{\xi}_s = \xi_{Anf}$, $\hat{\eta}_s = \eta$; and correspondingly for right-handed shocks: $\hat{\eta}_s = \eta_{Anf}$, $\hat{\xi}_s = \xi$. ξ_{Anf} and η_{Anf} are the values in the initial point of the shock. A further

improvement in accuracy can be achieved if those ξ, η values are adopted which belong to the compression shock point calculated last, instead of the values ξ_{Anf}, η_{Anf} in the initial point of the shock.

Equations (3.10) and (3.11) are valid for the case where the quantities of the downstream sheet are taken as a function of the quantities of the upstream sheet. Substituting in equations (3.10) and (3.11) for the quantities of the one sheet the corresponding quantities of the other sheet, then the variables of state ahead of the shock are obtained as a function of the values after the shock front.

3.2. Determination of the initial shock points in the flow around concave curved walls

It has been shown in Chapter 3.1. that in the flow along a concave curved contour, there occur interesections of Mach lines of the same family. This area in the physical x, y plane in which there is a triple cover is bounded by an envelope which is formed by these Mach lines (Fig. 4).

In calculating the envelope, we consider the characteristic ξ, η lines of the x, y plane as families of curves given in the parameter form $x = x(\xi, \eta)$, and $y = y(\xi, \eta)$ having the two family parameters ξ, η. The equation of an envelope whose generating element is given in parametric form is given by

$$\frac{\partial x}{\partial \xi}\,\frac{\partial y}{\partial \eta} - \frac{\partial x}{\partial \eta}\,\frac{\partial y}{\partial \xi} = f(\xi, \eta) = 0 \tag{3.12}$$

see Ostrowski [43]. Using equation (2.5), (3.12) can be further simplified to

$$\frac{\partial x}{\partial \xi}\,\frac{\partial x}{\partial \eta}\left[\operatorname{tg}(\theta+\theta_{\infty}+\alpha) - \operatorname{tg}(\theta+\theta_{\infty}-\alpha)\right] = 0.$$

Since the bracketed expression is generally unlike 0, it follows that

$$\frac{\partial x}{\partial \xi}\,\frac{\partial x}{\partial \eta} = 0. \tag{3.13}$$

Since a product is zero if one of the factors is zero, we then have

(3.14) $$\frac{\partial x}{\partial \xi} = 0 \quad \text{or} \quad \frac{\partial x}{\partial \eta} = 0 .$$

These equations yield in the implicit form the equation $\eta_{Env} = \eta_{Env}(\xi)$ which is to be found if the envelope concerned applies to left-handed characteristics.

The cusp of the envelope which is to be found and which is the initial point of the shock is then yielded as the minimum of the curve, i.e. the coordinates of the cusp are obtained from $\frac{d\eta}{d\xi}\,\text{Env} = 0$.

In the case of the envelope of the left-handed Mach lines, equation (3.14) and

(3.15) $$\frac{\partial^2 x}{\partial \xi^2} = 0 \quad \text{or} \quad \frac{\partial^2 x}{\partial \eta\, \partial \xi} = 0 .$$

then yield the coordinates of the cusp.

The accuracy with which the envelope and also its cusp are calculated of course depends once again on the order of the terms $x^{(i)}, y^{(i)}$ used in (3.14) and (3.15).

In the intersection of the right-handed Mach lines, by the corresponding treatment, equations (3.14) give the envelope equation as: $\xi_{Env} = \xi_{Env}(\eta)$ whereas the coordinates of the envelope cusp can be calculated again from equations (3.15) by interchanging ξ and η.

4. Centered Prandtl-Meyer expansions

In a flow around a convex corner, a centered Prandtl-Meyer expansion forms in the flow (Fig. 9). The expansion fan is limited upstream by the Mach line ξ_A and downstream by ξ_E. The whole region between these two characteristics is shown in Fig. 10 projected on one single Mach line in the $x^{(0)}, y^{(0)}$ plane in the zeroth approximation (acoustics theory).

This means in the equations for the calculation of the $x^{(0)}, y^{(0)}$ coordinates that retaining η a like value for $x^{(0)}, y^{(0)}$ must be allocated for two different values ξ_A and ξ_E and even for all in-between values of

the characteristic coordinate ξ. This can be realised, according to Schneider [24] by dropping the dependence of ξ, i.e. by putting $A^{**}= 0$ in equation (2.21) in the domain of a centred Prandtl-Meyer expansion.

An arbitrary function can be selected in ξ as boundary values to be given for the flow direction θ in the cusp A - E which represents for $\xi = \xi_A$ the direction of the flow $(\theta_K)_A$ at the wall ahead of the corner and for $\xi = \xi_E$ the direction of the wall $(\theta_K)_E$ after the corner. A linear relationship is assumed here as the simplest function:

$$\theta_k = (\theta_k)_A + \left[(\theta_K)_E - (\theta_k)_A\right] \cdot \frac{\xi - \xi_A}{\xi_E - \xi_A} \tag{4.1.}$$

The numerical value $\xi_E - \xi_A$ is an arbitrarily given value which, like the selection of the function, varies only the numbering of the Mach line. All the other equations for the calculation of $x^{(i)}$, $y^{(i)}$, $\theta^{(i)}$ and $w^{(i)}$ retain their validity observing $A^{**}= 0$.

The disadvantage of the agreement $A^{**}= 0$ is that as a result the universal validity of equation (2.21) is no longer true. For $\xi > \xi_E$ values,

$$x^{(0)} = A^{*}\eta + A^{**}\left[\xi - (\xi_E - \xi_A)\right]$$

$$y^{(0)} = \operatorname{tg}(\Theta_\infty+\alpha_\infty)\, A^{*}\eta + \operatorname{tg}(\Theta_\infty-\alpha_\infty)\, A^{**}\left[\xi - (\xi_E - \xi_A)\right]. \tag{4.2}$$

is then valid instead of (2.21).

Equation (2.21) and (4.2) must be appropriately expanded if several centered Prandtl-Meyer expansions occur. If instead of left-handed Mach lines, centering of the right-handed characteristics occurs, then $A^{*} = 0$ must be put in the centred Prandtl-Meyer expansion domain. ξ is then to be substituted by η in equation (4.1), and in (4.2) the η coordinate is to be supplemented appropriately instead of ξ.

5. Flow through plane, straight blade cascades

5.1. General

A double infinite plane, straight blade cascade can be imagined as generated by applying a co-axial section through a spatial, axial rotor or stator of a compressor or turbine stage which is then projected into the plane and extended at both ends to infinity. The section of this type of cascade is shown in Fig. 11 together with the most important notations.

In the supersonic approach flow to a double infinite cascade, a distinction must be made between two flow configurations which are significantly different from each other. With the one flow form, perturbations run, in spite of the flow being supersonic, from the blade suction sides upstream ahead of the cascade inlet front (Fig. 12). In this case, the axial component $M_1 \cdot \sin\beta_1$ of the approach flow lies in the subsonic range, and an effect on the approach flow due to the cascade occurs. The special peculiarities resulting from this flow condition are described in detail in Chapter 5.2. If, on the other hand, the axial component of the approach flow lies in the supersonic range (Fig. 13), then there is no such effect on the approach flow by the cascade because all the disturbances originating in the aerofoils run into the cascade passage and not upstream ahead of the cascade front.

In order to represent the conditions in a cascade wind tunnel better, a semi-infinite blade row is considered here instead of a double infinite one. For an axial subsonic approach flow, the flow image of a semi-infinite cascade (Figs. 14, 15, 16) is different from that of a double infinite cascade (Fig. 12). It will be seen, however, that for the irrotational supersonic flow the calculation of the semi-infinite flow field also determines the double infinite flow field. For the axial supersonic approach flow, Fig. 13 and Fig. 17, this differentiation in respect of the incident flow between the single and the double infinite cascade is not necessary. Borderline cases do occur if a shock configuration passes exactly through the cusp of the next blade (Fig. 18)

or if a Mach line of the centered Prandtl-Meyer expansion falls exactly in the cascade front, (Fig. 19). In the first case, for a double infinite cascade, a reduction in the incident flow flow Mach No. gives a sudden transition to an approach flow with an axial subsonic incident flow component, whereas in the second case the axial component of the double infinite cascade is exactly 1.

To calculate the flow through the blade cascade, the whole flow field is sub-divided into several zones which require different treatment. Such an area, for example, is given where a family of characteristics comes from a zone of constant state. In the case of the entrance region which will be investigated in the next chapter, a Mach line family comes for example always from a constant state region.

5.2. Entrance region

5.2.1. Equations of flow in the entrance region

The entrance region is the front part of the cascade in which there is a family of characteristic lines running from a constant state zone. In a semi-infinite cascade, this constant state prevails in front of the first Mach line issuing from the lowest blade.

For the calculation of the flow in the entrance region, this constant state is selected in this chapter to serve at the same time as the reference quantity in equation (2.3); it is therefore identified by the ∞ symbol. The state of the incident flow in the semi-infinite cascade (index ∞) should be carefully distinguished from the incident flow state for the double infinite cascade (index 1). In Fig. 20, the entrance region of the cascade illustrated is characterized by the right-handed lines η = constant coming from the area of the incident flow. This area is limited upstream by the left-handed Mach line which passes through the point of the bottom aerofoil, or through the left-handed shock front if a compression shock occurs. The other demarcations form the right-handed Mach lines which pass through the aerofoil tips if right-handed shocks are formed there.

The flow configuration shown in Fig. 21 produces two entrance regions which differ from one another: a lower region denoted I and an upper region denoted II. Right-handed characteristics once again run from the constant approach region in area I and the left-handed characteristics run into area II. The downstream characteristics and the appropriate compression shocks through the aerofoil tips limit the areas I and II. The right-handed lines limit area II upstream and area I downstream whilst the left-handed ones limit area I upstream and area II downstream. The same conditions as those in the entrance region of a blade cascade are also obtained in the flow around a single aerofoil if its approach flow has a constant Mach Number (Fig. 22). In the range above the aerofoil, the right-handed Mach lines are coming from the constant region whereas the left-handed Mach lines below the body are coming from the incident flow area. For this reason, all the equations valid in the entrance range are also valid for the single aerofoil. In order to obtain the equations for the flow states θ, w and the coordinates x, y in these particular flow ranges, we restrict ourselves initially to the case where the right-handed Mach lines come from the undisturbed incident flow region (Fig. 20, and Fig. 21 for region I). The equations applicable to the case where the left-handed characteristics come from the constant region, are derived similarly.

The state $\theta^{(i)} = 0$, $w^{(i)} = 0$ prevails everywhere in the constant region upstream of the cascade. This then gives by equation (2.11) a relationship valid along right-handed characteristics:

$$(5.1) \qquad \theta^{(i)}(\xi,\eta) + \operatorname{ctg}\alpha_\infty w^{(i)}(\xi,\eta) - \sum_{j=1}^{i-1} (L_j)_{\xi,\eta} = I^{(i)}(\eta) = 0 .$$

This is the linearised form of the equation $\theta + \nu$ = constant along η = constant which, because of the irrotational flow required, is also valid for left-handed shocks. By equation (5.1) a relationship between the flow direction θ and the velocity w is given which is valid for the whole entrance region considered. This relationship (5.1) is of course

also valid along the initial line ξ_A so that by its application the initial values occurring in equation (2.26) can be immediately eliminated.

Hence for the initial values of the coordinates in equation (2.27), since in the undisturbed approach flow $x = x^{(0)}$, $y = y^{(0)}$ is valid (i.e. $x^{(i)} = 0$, $y^{(i)} = 0$ for $i \geq 1$):

$$y^{(i)}(\xi_A,\eta) - tg(\vartheta_\infty-\alpha_\infty)\, x^{(i)}(\xi_A,\eta) = 0 .$$

With the initial conditions thus established, the required variables of state and the position variables result from equations (2.26) and (2.27). Because of the periodicity of the boundary conditions and the irrotationality, it is possible to transform the equations so that the consideration can be limited to one single blade.

The characteristics through the blade tips are denoted by ξ_0, η_0. If a compression shock occurs at the aerofoil tips, then ξ_0 represents the characteristic in the downstream sheet of the convolution. If a centered Prandtl-Meyer expansion occurs, then ξ_0 is the characteristic, farthest downstream, through the blade tip. The coordinates are correspondingly called $x_0^{(i)}$, $y_0^{(i)}$. The variables of state $\vartheta^{(i)}$ and $w^{(i)}$ are then, because of the periodicity, a function only of the quantities $\xi - \xi_0$ and $\eta - \eta_0$. Hence, from equation (2.26) it follows, with (5.1), that:

$$\vartheta^{(i)}(\xi-\xi_0,\eta-\eta_0) = \vartheta_k^{(i)}(\xi-\xi_0,(\eta-\eta_0)_k)$$

(5.2)

$$ctg\alpha_\infty w^{(i)}(\xi-\xi_0,\eta-\eta_0) = - \vartheta_k^{(i)}(\xi-\xi_0,(\eta-\eta_0)_k) + \sum_{j=1}^{i-1} (L_j)_{\substack{\xi-\xi_0 \\ \eta-\eta_0}} .$$

The quantity $(\eta - \eta_0)_k$, which is to be formed along the aerofoil boundary, represents a function only of $\xi - \xi_0$. The first of the equations (5.2) reveals immediately that the direction of flow $\vartheta^{(i)}$ depends also on $\xi - \xi_0$ alone. In the second equation, the first item on the right side is also a function only of $\xi - \xi_0$. In the calculation of the velocity term $w^{(i)}$ of the order i, the second item contains the preceding

approximations $w^{(k)}$. Since the index is $k \leq i-1$ and the first approximation gives $w^{(1)} = w^{(1)}(\xi - \xi_0)$, the second summand is also a function only of $\xi - \xi_0$. The direction of flow as well as the velocity are therefore a function only of a characteristic coordinate (the simple wave, see e.g. Zierep [38]). The coordinates are derived from equation (2.27) if it is observed that the quantities C_j and D_j are functions of $w^{(k)}$, $\theta^{(k)}$ which depend only on $\xi - \xi_0$ due to equation (5.2), so that the integration can be carried out for η as follows:

(5.3)

$$x^{(i)} - x_0^{(i)} = \frac{1}{tg(\theta_\infty+\alpha_\infty) - tg(\theta_\infty-\alpha_\infty)} \left\{ \sum_{j=1}^{i} \left[\int_0^{\xi-\xi_0} C_j \frac{\partial (x-x_0)^{(i-j)}}{\partial(\xi-\xi_0)}\, d(\xi-\xi_0) - \right.\right.$$

$$- \frac{tg(\theta_\infty+\alpha_\infty)}{tg(\theta_\infty-\alpha_\infty)} \left(\int_0^{\xi-\xi_0} C_j \frac{\partial (x-x_0)^{(i-j)}}{\partial(\xi-\xi_0)}\, d(\xi-\xi_0) \right)_{(\eta-\eta_0)_k} -$$

$$\left.\left. - D_j (x-x_k)^{(i-j)} \right] \right\}$$

$$y^{(i)} - y_0^{(i)} = \frac{1}{tg(\theta_\infty+\alpha_\infty) - tg(\theta_\infty-\alpha_\infty)} \left\{ \sum_{j=1}^{i} \left(tg(\theta_\infty+\alpha_\infty) \times \right.\right.$$

$$\times \left[\int_0^{\xi-\xi_0} C_j \frac{\partial (x-x_0)^{(i-j)}}{\partial(\xi-\xi_0)}\, d(\xi-\xi_0) - \right.$$

$$\left. - \left(\int_0^{\xi-\xi_0} C_j \frac{\partial (x-x_0)^{(i-j)}}{\partial(\xi-\xi_0)}\, d(\xi-\xi_0) \right)_{(\eta-\eta_0)_k} \right] -$$

$$\left.\left. - tg(\theta_\infty-\alpha_\infty)\, D_j (x-x_k)^{(i-j)} \right) \right\} .$$

For the zeroth approximation, equation (2.21) yields:

$$x^{(0)}-x_0^{(0)} = A^*(\eta-\eta_0) + A^{**}(\xi-\xi_0)$$

(5.4)

$$y^{(0)}-y_0^{(0)} = tg(\theta_\infty+\alpha_\infty)\, A^*(\eta-\eta_0) + tg(\theta_\infty-\alpha_\infty)\, A^{**}(\xi-\xi_0)\,.$$

The equation of the aerofoil contour $(y - y_0)_k$ is a given function of $(x - x_0)_k$. This yields for the angle θ_k along the wall contour:

(5.5) $$\theta_k = -\theta_\infty + \operatorname{arctg}\left[\frac{d(y-y_0)_k}{d(x-x_0)_k}\right]_{(x-x_0)_k}$$

Equation (2.24) then gives the boundary contour $(\eta - \eta_0)_k$ in characteristic coordinates:

(5.6)

$$(\eta-\eta_0)_k = \frac{1}{A^*tg(\theta_\infty+\alpha_\infty)}\left\{- tg(\theta_\infty-\alpha_\infty)\, A^{**}(\xi-\xi_0) + \left[(y-y_0)_k\right]_{(x-x_0)_k}\right\}.$$

It should be observed that $(y - y_0)_k^{(i)} = 0$ was selected for $i \geq 1$. The equations of the variables of state of the first order are then:

$$\theta^{(1)}(\xi-\xi_0,\eta-\eta_0) = \theta^{(1)}(\xi-\xi_0,(\eta-\eta_0)_k) = \theta_k^{(1)}(\xi-\xi_0)$$

(5.7)

$$ctg\alpha_\infty w^{(1)}(\xi-\xi_0,\eta-\eta_0) = -\theta_k^{(1)}(\xi-\xi_0)$$

where

$$\frac{\partial(x-x_0)^{(0)}}{\partial(\xi-\xi_0)} = A^{**} \qquad \frac{\partial(x-x_0)^{(0)}}{\partial(\eta-\eta_0)} = A^*$$

The equations of the 1st order of the coordinates are obtained:

(5.8)

$$(x-x_0)^{(1)} = A^{**}M_1 \int_0^{\xi-\xi_0} \theta_k^{(1)}(\xi-\xi_0)\, d(\xi-\xi_0) + A^*N_1\theta_k^{(1)}(\xi-\xi_0)\cdot[\eta-\eta_k]$$

$$(y-y_0)^{(1)} = A^*tg(\theta_\infty-\alpha_\infty)\, N_1\theta_k^{(1)}(\xi-\xi_0)\cdot[\eta-\eta_k]\,.$$

In this:

$$\tilde{M}_1 = - \frac{P_1 \cdot Q_1}{tg(\theta_\infty - \alpha_\infty)}$$

(5.9)

$$\tilde{N}_1 = - \frac{P_2 \cdot Q_2}{tg(\theta_\infty + \alpha_\infty) - tg(\theta_\infty - \alpha_\infty)}$$

in which

$$P_1 = 1 + tg^2(\theta_\infty - \alpha_\infty)$$

$$P_2 = 1 + tg^2(\theta_\infty + \alpha_\infty)$$

(5.10)

$$Q_1 = 1 - tg^2\alpha_\infty(1 + \frac{\kappa-1}{2} M_\infty^2)$$

$$Q_2 = 1 + tg^2\alpha_\infty(1 + \frac{\kappa-1}{2} M_\infty^2)$$

In the derivation of the equation (5.8) it was observed that the direction coordinate $\theta_k = \theta_k (\xi - \xi_0)$ acting as the integrand is only a function of $\xi - \xi_0$, so that

$$\int_0^{\xi-\xi_0} \theta_k \, d(\xi-\xi_0) = \left(\int_0^{\xi-\xi_0} \theta_k \, d(\xi-\xi_0) \right)_{(\eta-\eta_0)_k}$$

is valid.

Interchanging in equations (5.6), (5.7), (5.8) and (5.9) the quantities ξ, η and A*, A** and P_1, P_2 and substituting $-\alpha_\infty$ for α_∞, yields the equations for the case where the left-handed Mach line comes from the constant approach flow region.

For the calculation of the streamlines to the 1st approximation, the series of formulae for the variables of state and the coordinates are inserted in

the differential equation (2.31). Taking only the first terms into account, this gives:

$$(5.11)\qquad \left(\frac{d\eta}{d\xi}\right)_{\psi} = \left[S_1 + S_2\,\theta^{(1)} + S_3\,w^{(1)}\right]\frac{\frac{\partial x^{(0)}}{\partial \xi}}{\frac{\partial x^{(0)}}{\partial \eta}} + S_1\frac{\frac{\partial x^{(1)}}{\partial \xi}\frac{\partial x^{(0)}}{\partial \eta} - \frac{\partial x^{(0)}}{\partial \xi}\frac{\partial x^{(1)}}{\partial \eta}}{\left(\frac{\partial x^{(0)}}{\partial \eta}\right)^2}\,.$$

One obtains from this for the entrance region of the cascade by substitution of the equations (5.4), (5.7) and (5.8):

$$(5.12)\qquad \left(\frac{d(\eta-\eta_0)}{d(\xi-\xi_0)}\right)_{\psi} = E\cdot(\eta-\eta_0) + F$$

in which

(5.13)

$$E = S_1\cdot\tilde{N}_1\cdot\frac{\partial\theta_k^{(1)}}{\partial(\xi-\xi_0)}$$

$$F = (1/A^*)\cdot\left\{S_1\cdot\left[A^{**} + A^*\tilde{M}_1\theta_k^{(1)} - A^*\tilde{N}_1\frac{\partial\theta_k^{(1)}}{\partial(\xi-\xi_0)}\cdot(\eta-\eta_0)_k - A^*\theta_k^{(1)}\frac{\partial(\eta-\eta_0)_k}{\partial(\xi-\xi_0)} - A^{**}\tilde{N}_1\theta_k^{(1)}\right] + A^{**}\left[S_2 - tg\alpha_\infty S_3\right]\theta_k^{(1)}\right\}.$$

E and F are only functions of $(\xi - \xi_0)$, and equation (5.12) is therefore a normal differential equation whose closed integration is possible except for a remaining quadrature. The equation of the streamline in characteristic coordinates is then:

(5.14)

$$(\eta-\eta_0)_\psi = e^{\int_{(\xi-\xi_0)_{Anf}}^{\xi-\xi_0} E\cdot d(\xi-\xi_0)'} \left[(\eta-\eta_0)_p + \int_{(\xi-\xi_0)_{Anf}}^{\xi-\xi_0} F\cdot e^{-\int_{(\xi-\xi_0)_{Anf}}^{(\xi-\xi_0)'} E\cdot d(\xi-\xi_0)''} d(\xi-\xi_0)'\right].$$

$(\xi - \xi_0)_{Anf}$ and $(\eta - \eta_0)_{Anf}$ are initial values of the considered streamline which are to be pre-assigned.

By the above transpositions, the equations are obtained for the second boundary initial value problem. If within the entrance region of the cascade there is a flow around a concave contour, then the equation of the envelope which arises, being the envelope of the characteristics of the same family, is calculated from equation (3.14). With the aid of equation (5.8) it is apparent that in this case only $\frac{\partial x}{\partial \xi} = 0$ can yield the solution. This is for a 1st order approximation:

$$(5.15)\qquad \frac{\partial x^{(0)}}{\partial \xi} + \frac{\partial x^{(1)}}{\partial \xi} = A^{**} + A^{**}\tilde{M}_1\theta_k^{(1)} + A^{*}\tilde{N}_1\left[\frac{\partial \theta_k^{(1)}}{\partial(\xi-\xi_0)}(\eta-\eta_k) - \theta_k^{(1)}\frac{\partial(\eta-\eta_0)_k}{\partial(\xi-\xi_0)}\right] = 0 .$$

From this, the equation of the envelope can be given in the explicit form

$$(5.16)\qquad \eta_{Env} - \eta_k = \left(1/\frac{\partial \theta_k^{(1)}}{\partial(\xi-\xi_0)}\right)\left\{\theta_k^{(1)}\frac{\partial(\eta-\eta_0)_k}{\partial(\xi-\xi_0)} - \left[A^{**}/(A^{*}\tilde{N}_1)\right]\cdot\left[1 + \tilde{M}_1\theta_k^{(1)}\right]\right\} .$$

From $d(\eta_{Env} - \eta_0)/d(\xi - \xi_0) = 0$ the coordinates of the cusp of the envelope being the initial point of the shock are then obtained in the implicit form as:

(5.17)

$$\frac{\partial\theta_k^{(1)}}{\partial(\xi-\xi_0)}\left\{\theta_k^{(1)}\,\frac{\partial^2(\eta-\eta_0)_k}{\partial(\xi-\xi_0)^2}+\frac{\partial\theta_k^{(1)}}{\partial(\xi-\xi_0)}\left[2\,\frac{\partial(\eta-\eta_0)_k}{\partial(\xi-\xi_0)}-\frac{A^{**}\tilde{M}_1}{A^{*}\tilde{N}_1}\right]\right\}+$$

$$+\frac{\partial^2\theta_k^{(1)}}{\partial(\xi-\xi_0)^2}\left\{\frac{A^{**}}{A^{*}\tilde{N}_1}\left[1+\tilde{M}_1\theta_k^{(1)}\right]-\theta_k^{(1)}\,\frac{\partial(\eta-\eta_0)_k}{\partial(\xi-\xi_0)}\right\}=0\,.$$

The iterative calculation yields $(\xi_{Env})_{Anf}$, and substitution in equation (5.16) yields $(\eta_{Env})_{Anf}$.

The formulae for the flow domain corresponding to equations (5.16) and (5.17), in which the left-handed Mach lines come from a constant state domain, are once again obtained by the transpositions given above.

5.2.2. Equations of the shocks in the entrance region

The differential equation of the left-handed shocks in characteristic coordinates is derived from equation (3.6):

$$\left(\frac{d(\hat{\xi}-\hat{\xi}_0)}{d(\hat{\eta}-\hat{\eta}_0)}\right)_{St}=-\frac{\dfrac{\partial(\hat{x}-\hat{x}_0)}{\partial(\hat{\eta}-\hat{\eta}_0)}}{\dfrac{\partial(\hat{x}-\hat{x}_0)}{\partial(\hat{\xi}-\hat{\xi}_0)}}\left\{\left[K_{11}+K_{12}\hat{w}+K_{13}\hat{\theta}+\ldots\right]\cdot(\theta-\hat{\theta})+\right.$$

$$\left.+K_{21}\,\frac{(\theta-\hat{\theta})^2}{2}+\ldots\right\}.$$

The quantities having a ^ symbol are the states and coordinates prevailing in the sheet of the convolution which lies downstream of the shock, whereas the non-identified quantity θ is to be formed in the sheet of the convolution which lies upstream of the shock.

If only an approximation of the 1st order is considered and if it is observed that in forming $\partial(x - x_0)/\partial(\xi - \xi_0)$ that part of the 1st order approximation

is to be taken into account which contains $\eta - \eta_k$ as a factor since this becomes large in relation to $\theta^{(1)} - \hat{\theta}^{(1)}$ for large $\eta - \eta_k$ values, then we have:

$$\left(\frac{d(\hat{\xi}-\hat{\xi}_0)}{d(\hat{\eta}-\hat{\eta}_0)}\right)_{St} = \frac{A^*K_{11}\,(\hat{\theta}^{(1)} - \theta^{(1)})}{A^{**} + \tilde{N}_1 A^* \dfrac{\partial\hat{\theta}_k}{\partial(\hat{\xi}-\hat{\xi}_0)}\,(\hat{\eta}-\hat{\eta}_k)} \cdot$$

If a domain of constant state exists upstream of the shock, then $\theta^{(1)}$ = constant, and the equation can be integrated immediately, at least numerically. In the other case, $\theta^{(1)}$ must be expressed with the aid of equations (3.10) and (3.11) as a function of $\hat{\xi}$, $\hat{\eta}$ to make an integration possible. Observing the relationship $\partial\theta^{(1)}/\partial\eta = 0$, which is valid here, we obtain from equation (3.11):

$$\hat{\theta}^{(1)} - \theta^{(1)} = \hat{\theta}^{(1)} - (\theta^{(1)})_s - \left(\frac{\partial\theta^{(1)}}{\partial(\xi-\xi_0)}\right)_s \times$$

$$\times\left[\left(\frac{\partial(y-y_0)}{\partial(\eta-\eta_0)}\right)_s \{(\hat{x}-\hat{x}_0) - (x-x_0)_s + (\hat{x}_0-x_0)\} -\right.$$

$$\left. - \left(\frac{\partial(x-x_0)}{\partial(\eta-\eta_0)}\right)_s \{(\hat{y}-\hat{y}_0) - (y-y_0)_s + (\hat{y}_0-y_0)\}\right] \times$$

$$\times 1/\left\{\frac{\partial(x-x_0)}{\partial(\xi-\xi_0)}\,\frac{\partial(y-y_0)}{\partial(\eta-\eta_0)} - \frac{\partial(x-x_0)}{\partial(\eta-\eta_0)}\,\frac{\partial(y-y_0)}{\partial(\xi-\xi_0)}\right\}_s \cdot$$

The subscript s signifies that the quantities are to be formed at the position $(\xi - \xi_0)_s$. For the selection of $(\xi - \xi_0)_s$ and $(\eta - \eta_0)_s$, please refer to Chapter 3.1. The magnitudes of the numerator in large brackets are of the 1st order, and for this reason only terms of the zeroth order and those of the 1st order which become large in relation to the corresponding 1st order terms of the variables of state are taken into account in the expressions

$$\frac{\partial(x-x_0)}{\partial(\xi-\xi_0)}\,,\quad \frac{\partial(x-x_0)}{\partial(\eta-\eta_0)}\,,\quad \frac{\partial(y-y_0)}{\partial(\xi-\xi_0)} \quad \text{and} \quad \frac{\partial(y-y_0)}{\partial(\eta-\eta_0)}$$

$$\hat{\theta}^{(1)}-\theta^{(1)} = \{\left[tg(\theta_\infty+\alpha_\infty)-tg(\theta_\infty-\alpha_\infty)\right]\cdot\{A^{**}\left[\hat{\theta}^{(1)}-(\theta^{(1)})_s\right] +$$

$$+ A^{*}\tilde{N}_1\hat{\theta}^{(1)}\left(\frac{\partial\theta^{(1)}}{\partial(\xi-\xi_0)}\right)_s\cdot\left[(\eta_s-\hat{\eta})+(\hat{\eta}_k-\hat{\eta}_0)-(\eta_k-\eta_0)_s+(\hat{\eta}_0-\eta_0)\right] +$$

$$+ A^{**}\left(\frac{\partial(\theta^{(1)})}{\partial(\xi-\xi_0)}\right)_s\cdot\left[(\xi-\xi_0)_s-(\hat{\xi}-\hat{\xi}_0)\right]\} +$$

$$+ A^{**}\tilde{M}_1 tg(\theta_\infty+\alpha_\infty)\left(\frac{\partial\theta^{(1)}}{\partial(\xi-\xi_0)}\right)_s\cdot\left[\int_0^{(\xi-\xi_0)_s}\theta^{(1)}d(\xi-\xi_0) -\right.$$

$$\left. - \int_0^{\hat{\xi}-\hat{\xi}_0}\hat{\theta}^{(1)}d(\hat{\xi}-\hat{\xi}_0)\right] +\left(\frac{\partial\theta^{(1)}}{\partial(\xi-\xi_0)}\right)_s\left[(\hat{y}_0-y_0)-tg(\theta_\infty+\alpha_\infty)(\hat{x}_0-x_0)\right]\}\times$$

$$\times 1/\{\left[tg(\theta_\infty+\alpha_\infty)-tg(\theta_\infty-\alpha_\infty)\right]\cdot\left[A^{**}+A^{*}\tilde{N}_1\left(\frac{\partial\theta^{(1)}}{\partial(\xi-\xi_0)}\right)_s(\eta-\eta_k)_s\right]\} .$$

By selecting $\eta_s = \hat{\eta}$ and taking into account in the above equation only terms of the lst order, it follows that:

(5.18)

$$\hat{\theta}^{(1)}-\theta^{(1)} = \left[tg(\theta_\infty+\alpha_\infty)-tg(\theta_\infty-\alpha_\infty)\right]\cdot\left[A^{**}(\hat{\theta}^{(1)}-\theta_s^{(1)})+\left(\frac{\partial\theta^{(1)}}{\partial(\xi-\xi_0)}\right)_s \times\right.$$

$$\times\ \{A^{**}\left[(\xi-\xi_0)_s-(\hat{\xi}-\hat{\xi}_0)\right]+\hat{\theta}^{(1)}A^{*}\tilde{N}_1\left[(\hat{\eta}_k-\hat{\eta}_0)-(\eta_k-\eta_0)_s+\right.$$

$$\left.+(\hat{\eta}_0-\eta_0)\right]+tg(\theta_\infty+\alpha_\infty)\left[(x_k^{(1)}-x_0^{(1)})_s-(\hat{x}_k^{(1)}-\hat{x}_0^{(1)})\right]+$$

$$\left.+\left[(\hat{y}_0-y_0)-tg(\theta_\infty+\alpha_\infty)(\hat{x}_0-x_0)\right]\}\right]\Big/\{\left[tg(\theta_\infty+\alpha_\infty)-tg(\theta_\infty-\alpha_\infty)\right]\times$$

$$\times\ \{A^{**}+A^{*}\tilde{N}_1\left(\frac{\partial\theta^{(1)}}{\partial(\xi-\xi_0)}\right)_s\cdot\left[(\hat{\eta}-\hat{\eta}_0)-(\eta_k-\eta_0)_s+(\hat{\eta}_0-\eta_0)\right]\}\}.$$

This then gives the Riccati equation as the shock equation

$$(5.19)\qquad \left(\frac{d(\hat{\xi}-\hat{\xi}_0)}{d(\hat{\eta}-\hat{\eta}_0)}\right)_{St} = \frac{A}{B(\hat{\eta}-\hat{\eta}_0)^2+C(\hat{\eta}-\hat{\eta}_0)+D}\ .$$

The quantities A, B, C, D are functions only of $\hat{\xi}-\hat{\xi}_0$ and $(\xi-\xi_0)_s$ and give:

(5.20)

$$A = A^{*}K_{11}\left[A^{**}(\hat{\theta}^{(1)}-\theta_s^{(1)})+\left(\frac{\partial\theta^{(1)}}{\partial(\xi-\xi_0)}\right)_s\cdot\{A^{**}\left[(\xi-\xi_0)_s-(\hat{\xi}-\hat{\xi}_0)\right]+\right.$$

$$+\hat{\theta}^{(1)}A^{*}\tilde{N}_1\left[(\hat{\eta}_k-\hat{\eta}_0)-(\eta_k-\eta_0)_s+(\hat{\eta}_0-\eta_0)\right]+$$

$$+\left[tg(\theta_\infty+\alpha_\infty)\left[(x_k^{(1)}-x_0^{(1)})_s-(\hat{x}_k^{(1)}-\hat{x}_0^{(1)})\right]+\left[(\hat{y}_0-y_0)-tg(\theta_\infty+\alpha_\infty)\times\right.\right.$$

$$\left.\left.\times(\hat{x}_0-x_0)\right]\right]\Big/\left[tg(\theta_\infty+\alpha_\infty)-tg(\theta_\infty-\alpha_\infty)\right]\}\Big]$$

$$B = (A^{*}\tilde{N}_1)^2\ \frac{\partial\hat{\theta}^{(1)}}{\partial(\hat{\xi}-\hat{\xi}_0)}\cdot\left(\frac{\partial\theta^{(1)}}{\partial(\xi-\xi_0)}\right)_s\ .$$

(5.20)

$$C = A^{*}A^{**}\tilde{N}_1\left[\frac{\partial\hat{\theta}^{(1)}}{\partial(\hat{\xi}-\hat{\xi}_0)}+\left(\frac{\partial\theta^{(1)}}{\partial(\xi-\xi_0)}\right)_s\right]+(A^{*}\tilde{N}_1)^2\,\frac{\partial\hat{\theta}^{(1)}}{\partial(\hat{\xi}-\hat{\xi}_0)}\cdot\left(\frac{\partial\theta^{(1)}}{\partial(\xi-\xi_0)}\right)_s \times$$

$$\times\left[(\hat{\eta}_0-\eta_0)-(\hat{\eta}_k-\hat{\eta}_0)-(\eta_k-\eta_0)_s\right]$$

$$D = A^{**}A^{***}+A^{**}A^{*}\tilde{N}_1\left\{\left(\frac{\partial\theta^{(1)}}{(\xi-\xi_0)}\right)_s\left[(\hat{\eta}_0-\eta_0)-(\eta_k-\eta_0)_s\right]-\frac{\partial\hat{\theta}^{(1)}}{\partial(\hat{\xi}-\hat{\xi}_0)}\,(\hat{\eta}_k-\hat{\eta}_0)\right\}-$$

$$-A^{*2}\tilde{N}_1^2\,\frac{\partial\hat{\theta}^{(1)}}{\partial(\hat{\xi}-\hat{\xi}_0)}\cdot\left(\frac{\partial\theta^{(1)}}{\partial(\xi-\xi_0)}\right)_s\cdot\left[\hat{\eta}_k-\hat{\eta}_0\right]\cdot\left[(\hat{\eta}_0-\eta_0)-(\eta_k-\eta_0)_s\right]\ .$$

From equation (5.19) it follows that:

$$(5.21)\qquad (\hat{\xi}-\hat{\xi}_0)_{St}-(\hat{\xi}-\hat{\xi}_0)_{Anf}=\int_{(\hat{\eta}-\hat{\eta}_0)_{Anf}}^{\hat{\eta}-\hat{\eta}_0}\frac{A}{B(\hat{\eta}-\hat{\eta}_0)^2+C(\hat{\eta}-\hat{\eta}_0)+D}\,d(\hat{\eta}-\hat{\eta}_0)\ .$$

In this equation, the upper integration limit can converge towards ∞. The right hand integral then becomes an improper integral. In numerical integration it is therefore appropriate to carry out a transformation of variables which transforms the improper to the proper; see F.A. Willers [44]:

$$(5.22)\qquad \hat{\eta}-\hat{\eta}_0=\frac{1}{z}+(\hat{\eta}-\hat{\eta}_0)_{Anf}-1\ .$$

Hence, equation (5.21) is written:

(5.23)

$$(\hat{\xi}-\hat{\xi}_0)_{St}-(\hat{\xi}-\xi_0)_{Anf}=\int_z^1 A\,dz\Big/\left(z^2\left\{B\left[(\hat{\eta}-\hat{\eta}_0)_{Anf}-1\right]^2+C\left[(\hat{\eta}-\hat{\eta}_0)-1\right]+D\right\}+\right.$$

$$\left.+\,z\left\{2B\left[(\hat{\eta}-\hat{\eta}_0)_{Anf}-1\right]+C\right\}+B\right)$$

where $0 \le z \le 1$ for

$$\infty \geq (\hat{\eta}-\hat{\eta}_0) \geq (\hat{\eta}-\hat{\eta}_0)_{Anf}.$$

The special case of a compression shock, where a constant state prevails upstream of the shock front, is contained in equation (5.21) if it is considered that $\theta^{(1)}$ = constant and $\partial\theta^{(1)}/\partial(\xi - \xi_0) = 0$. The quantities A, B, C and D are then simplified to

$$A = A^{*}A^{**}K_{11}(\hat{\theta}^{(1)}-\theta^{(1)})$$

$$B = 0$$

(5.24)

$$C = A^{*}A^{**}\tilde{N}_1 \frac{\partial\hat{\theta}^{(1)}}{\partial(\hat{\xi}-\hat{\xi}_0)}$$

$$D = A^{**2}-A^{*}A^{**}\tilde{N}_1 \frac{\partial\hat{\theta}^{(1)}}{\partial(\hat{\xi}-\hat{\xi}_0)}\cdot(\hat{\eta}-\hat{\eta}_0)_k .$$

The character of the differential equation changes considerably because of B = 0. The Riccati differential equation (5.19) transforms to a linear differential equation of the 1st order, and the integration can be reduced to a quadrature; see Kuipers, Timman [45]. However, the shock is in that case presented in the inverse form $(\hat{\eta} - \hat{\eta}_0)_{st} = f(\xi - \xi_0)$. It will generally be necessary to carry out the quadrature numerically. Hence:

$$(\hat{\eta}-\hat{\eta}_0)_{St} = e^{\int_{(\hat{\xi}-\hat{\xi}_0)_{Anf}}^{\hat{\xi}-\hat{\xi}_0} \frac{C}{A}\, d(\hat{\xi}-\hat{\xi}_0)} \{(\hat{\eta}-\hat{\eta}_0)_{Anf} + \int_{(\hat{\xi}-\hat{\xi}_0)_{Anf}}^{\hat{\xi}-\hat{\xi}_0} \frac{D}{A} e^{-\int_{(\hat{\xi}-\hat{\xi}_0)_{Anf}}^{\hat{\xi}-\hat{\xi}_0} \frac{C}{A}\, d(\hat{\xi}-\hat{\xi}_0)''} d(\hat{\xi}-\hat{\xi}_0)'\} . \tag{5.25}$$

The similarly derived formulae for right-handed shocks in an entrance region where the left-handed characteristics come from the approach flow region are obtained here once again by the interchanging of ξ, η and A^*, A^{**} and P_1, P_2 and substituting $-\alpha_\infty$ for α_∞.

5.2.3. Calculation of the flow and of the shocks in the entrance region

With the aid of the equations derived in Chapters 5.2.1. and 5.2.2. it is now possible to calculate the flow state for the entire entrance range. It is useful to interpret the flow configurations obtaining for the cascade aerofoils separately for a convex and a concave aerofoil suction side. Let us consider first the blades with convex shaped aerofoils.

The bottom blade is subject to a convolution or a centered Prandtl-Meyer expansion, depending on whether the direction of the approach flow is flatter or steeper than the tangent of the blade suction side contour at the blade tip; see Figs. 14, 15, 16. The illustrations show only the left-handed characteristics and shocks and the one right-handed shock which defines the entrance area, or the appropriate Mach line. To explain the definitions used, Fig. 23 shows the two bottom blades of a semi-infinite cascade and some continuous left-handed Mach lines.

ξ_∞ is the characteristic of the undisturbed incident flow through the first blade tip. ξ_0 is the characteristic passing through the blade tip which characterises the state of the flow disturbed by the aerofoil. The numerical value for ξ_0 and ξ_∞ has been chosen to be identical in the case of the convolution as illustrated in the picture. In the case of the centered Prandtl-Meyer expansion, Fig. 16, the difference ξ_0 and ξ_∞ is an arbitrary constant value (see Chaper 4). Downstream of the line ξ_0 there occurs, due to the convex curvature of the aerofoil, an acceleration of the flow resulting in a lesser slope of the Mach lines. If an expansion takes place at the blade tip, then the velocity along the characteristic ξ_0 is already greater than the velocity of the incident flow. Downstream of ξ_0 it will continue to increase for

as long as the curvature of the aerofoil is convex. If a convolution occurs at the blade tip, then the velocity along ξ_0 is lower than the velocity of the incident flow. As a result of the expansion downstream of ξ_0, there will be a line ξ_N along which the velocity and, because of the irrotationality, also the direction, agree with the values of the incident flow. This characteristic is at the same time the limiting position of the shock forming in the convoluted area of the bottom blade; because if the shock assumes the direction of this characteristic, then the states in front of and after the shock coincide and the characteristic is now the limiting position of the compression shock.

Let the characteristic which passes through the tip of the second blade be defined as ξ_p; the velocity along this characteristic is higher and the flow direction is flatter (small θ) than along the characteristic ξ_0. On the other hand, the flow states between ξ_0 and ξ_p, are identical on the second blade because of the periodicity already established above. The characteristic $\hat{\xi}_0$ is therefore only a parallel displacement of the characteristic ξ_0 and the state along ξ_0 and $\hat{\xi}_0$ is identical. Since the flow direction along ξ_p is flatter than along ξ_0, there occurs a convolution of the flow field at the second blade and consequently the formation of a compression shock independent of whether at the first blade a convolution occurs or a centered Prandtl-Meyer expansion. The shock which occurs here has the effect that the expansion existing at the first blade is revoked for the second blade, precisely due to this compression shock. After this shock front, the same expansion takes place again, and exactly the same flow conditions prevail as those at the first blade. The characteristics originating in the lower aerofoil, which run into the shock originating in the upper aerofoil, are limited upstream by the characteristic ξ_1. The characteristics of the upper aerofoil, which also run into this shock, are limited downstream by the line $\hat{\xi}_1$. Since the flow relationships are the same on all blades, exactly the same shock formations as at the second blade occur also on the 3rd and all subsequent blades. For this reason, the lines ξ_1 and $\hat{\xi}_1$ must also be in complete agreement, i.e.

these lines are also displaced parallel by one pitch. This line ξ_1, which is an unknown priori and which is not so easy to calculate as the position of line ξ_N, has the property of being the boundary characteristic of the shock of the second blade and of all shocks originating in the subsequent blades, after a displacement parallel to the cascade front by always one pitch. Since the cascade shocks originating in the blade tips, with the exception of a shock which might be present at the very bottom blade, are perfectly identical, they consequently correspond to the shock configurations occurring on a double infinite cascade. The Mach lines ξ_1, $\hat{\xi}_1$, $\hat{\hat{\xi}}_1$ etc., which are completely homologous, characterize these shocks to infinity. The flow state on these characteristic lines is therefore exactly the state which represents the state of the incident flow to a double infinite cascade; Kantrowitz [15], Ferri [46].

Since the constant state of the incident flow prevails ahead of a compression shock which might arise at the very bottom blade, this first shock is different from the subsequent shocks, no constant state prevailing upstream in front of them. The first shock can now be infinitely steeper, Fig. 14, or flatter, Fig. 15, than the cascade shocks. This is decided by whether ξ_N lies upstream or downstream of ξ_1. In the first case the first shock is cancelled out atinfinity because it has blended with a characteristic line, namely ξ_N, and no interaction with the subsequent shock occurs. It the second case, where ξ_N lies downstream of ξ_1, the first shock is flatter than the remaining cascade shocks and will impinge on the second shock. The shock originating after this interesection of the two can be calculated exactly in the same way as the first shock, the point of intersection being the initial point of the shock calculation. Upstream of this shock, the constant incident flow condition again prevails and behind it the flow state of the second aerofoil which is, however, identical to that of the first aerofoil. The other form of this shock front compared with the shock front of the first blade up to the point of interesection with the cascade shock emerges only through the other initial point of this shock. What is important is that the characteristic $\hat{\xi}_N$

which is identical to ξ_N apart from a one pitch displacement, is the limiting line of this shock which is also the reason why the latter must strike the 3rd shock, which of course has a Mach line corresponding to ξ_1 as its limiting line. It is for this reason that the first shock in this case also strikes all the subsequent shocks of the cascade. At infinity, a finite shock strength is maintained which corresponds to the difference in the flow states on the characteristic lines ξ_N and ξ_1.

If the aerofoils in the blade cascade have a concave shaped suction side in the entrance region, then the following results are obtained:
If the lowest blade is subject to an incident flow arriving at an angle which is flatter than the contour angle of the aerofoil tip, then an oblique compression shock is formed in the tips, Fig. 24. Since the contour has a concave curvature, all the characteristics downstream of the initial Mach line ξ_∞ are inclined more acutely than ξ_0. Let the characteristic passing through the next blade tip again be called ξ_p. Since the same image of characteristics appears again along each blade, which means that the characteristics of the first aerofoil need all be displaced only by integral multiples of the pitch, it is immediately apparent that a centered Prandtl-Meyer expansion occurs at the tip of the second aerofoil and consequently also at all the other aerofoil tips. On the other hand, due to the concave boundary contours and subsequent to the expansion there occurs a compression which leads to a convolution with the formation of an envelope.

The shock resulting from this is intersected in the surrounding of its initial point at both sides by ξ = constant characteristics, which emanate from the concave aerofoil contour of the second blade. Starting at the position where the shock intersects the Mach line $\hat{\xi}_0$, upstream of the shock the centered Prandtl-Meyer expansion Mach lines run into the shock and downstream the characteristics emanating from the blade contour run into the shock. If the shock intersects the characteristic $\hat{\xi}_p$, then upstream the characteristics of the Prandtl-Meyer expansion of the second blade, and downstream the characteristics of the Prandtl-Meyer expansion of the 3rd blade, run into this shock. At infinity, the shock will blend into a characteristic $\hat{\xi}_1$, as boundary. This means that all

characteristics downstream of $\hat{\xi}_1$ and all characteristics upstream of $\hat{\hat{\xi}}_1$ run into this shock. The line ξ_1 which is parallel to $\hat{\xi}_1$, $\hat{\hat{\xi}}_1$ is once again the boundary of the shock configuration forming at a double infinite cascade. The value of ξ_1 is obtained by letting η go to ∞ in the shock equations (5.21).

If the flow conditions lead to the formation of a shock in the tip of the first aerofoil, as in Fig. 24, then this shock has as its boundary line the approach flow characteristic ξ_∞ which passes through the tip. Since on the other hand all the characteristics downstream of this first shock are more acutely inclined than ξ_∞ it will not be able to take this boundary position. $\hat{\xi}_1$ is steeper than ξ_∞ and the first shock will consequently run into the shock of the second aerofoil and further into each of the following shocks originating in the subsequent blades. At infinity there remains a finite shock strength which corresponds with the difference in the states along ξ_∞ and ξ_1. However, if the incident flow to the first aerofoil is such that a centered Prandtl-Meyer expansion occurs there as well, then the shock which now occurs at the first blade will be equal, at least at the starting portion, to the shocks arising at the other blades. A criterion as to whether this first shock runs into the subsequent ones is the position of ξ_∞ in relation to ξ_1. If ξ_∞ is steeper or if it has the same slope as ξ_1, then the shocks are equal at all blades and no interaction between them takes place.

The subsequent illustrations show the results of some calculated examples for the different flow and cascade configurations. Figs. 12 and 25 show the shock formations and the left-handed Mach lines in the entrance region of a double infinite cascade: in the first picture for a cascade with convex suction side contour, and in the second case for a cascade with a concave suction side aerofoil contour in the cascade entrance region. Figs. 14, 15 and 26 show a semi-infinite cascade where a compression shock occurs at the tip of the first blade. In the first two cases the blade upper sides are again convex shaped whereas in the 3rd case they are concave. Figs. 16 and 27 show the appropriate cascade for the case where a centered Prandtl-Meyer expansion occurs at the bottom aerofoil.

As a result of the periodicity of the flow in the entrance region, and because of the constant approach flow values at infinity ahead of the cascade, a coupling of incident flow direction and incident flow Mach Number exists for double infinite cascades if the approach flow velocities have axial components which are smaller than the speed of sound. This functional dependence $\beta_1 = f(M_1)$ is plotted in Fig. 28 for a cascade having convex aerofoil suction sides. The left hand branch of the curve is limited by the circumstance that sonic speed is reached for the first time at the aerofoil tip after the shock and that the calculation method used here fails for still smaller incident flow Mach Numbers. Towards the right, the coupling is valid until the axial component of the approach flow just reaches the speed of sound. Above this right hand limiting point A, the line $M_1 \cdot \sin \beta_1 = 1$ which represents just axial sonic speed acts as the limiting curve. The flow which corresponds to a point on this curve has qualitatively the appearance shown in Fig. 19. On the right of this limiting curve, the direction as well as the Mach Number can be selected independently, and the flow image corresponds to that shown in Fig. 17. Beneath point A there emerges a limiting curve which is given by flow conditions as shown in Fig. 18. Here, the cascade entrance shocks pass exactly through the aerofil tips of the subsequent blades. At the right of this boundary, β_1 and M_1 are again independently selectable and the flow which emerges is that shown in Fig. 13. For the calculation of these flow configurations with shocks at the cascade entrance and axial components which are in the supersonic range, the method of the 1^{st} order used here very soon yields inaccurate values, and for deflections by the cascade entrance shock of more than 10°, even higher approximations are to no purpose in view of the high incident flow Mach Numbers if entropy changes are not also taken into account in the calculation of the flow field. This boundary curve is therefore plotted in Fig. 28 only for a small change in the angle of incidence.

Fig. 29 shows how the interrelationship of $\beta_1 = f(M_1)$ changes for three different pitch ratios t/l if the stagger angle β_s is maintained constant. Conversely, Fig. 30 shows the effect of the stagger angle on the angle of incidence for a constant pitch ratio.

5.3. Channel region

The flow region of a blade cascade to which the characteristics of the steady flow area do not extend is called the blade channel. In this region, none of the flow states along the Mach lines are constant, and these are consequently no longer straight lines. To calculate the flow fields, it is therefore necessary to use the complete equations (2.26) and (2.27). The considerations once again extend only to the case where initial values along a left-handed characteristic ξ_A and boundary values along a non-characteristic boundary $\eta_k(\xi)$ are given. The equations for the other two characteristic initial and boundary initial value problems are comprised in Table 3.

Once again we shall linit ourselves in what follows to terms of the first magnitude. From equations (2.26) we obtain for the quantities of state:

(5.26)

$$\theta^{(1)}(\xi,\eta) = \theta_k^{(1)}(\xi,\eta_k(\xi)) + \frac{1}{2}\left[A^{(1)}(\eta) - A^{(1)}(\eta_k(\xi))\right]$$

$$\mathrm{ctg}\alpha_\infty w^{(1)}(\xi,\eta) = -\theta_k^{(1)}(\xi,\eta_k(\xi)) + \frac{1}{2}\left[A^{(1)}(\eta) + A^{(1)}(\eta_k(\xi))\right],$$

whilst

(5.27)

$$x_k^{(1)}(\xi,\eta_k(\xi)) = \frac{1}{\mathrm{tg}(\theta_\infty-\alpha_\infty)}\{y_k^{(1)}(\xi_A,\eta_k(\xi_A)) - A^{**}P_1\,Q_1 \times$$

$$\times \int_{\xi_A}^{\xi}\left[\theta_k^{(1)}(\xi,\eta_k(\xi)) - \frac{1}{2}A^{(1)}(\eta_k(\xi))\right]d\xi -$$

$$- A^{**}P_1\,Q_2\left[\xi-\xi_A\right]\frac{1}{2}A^{(1)}(\eta_k(\xi)) - E^{(1)}(\eta_k(\xi))\}$$

(5.27)

$$x^{(1)}(\xi,\eta)-x_k^{(1)}(\xi,\eta_k(\xi)) = \frac{1}{tg(\theta_\infty+\alpha_\infty)-tg(\theta_\infty-\alpha_\infty)} \{-\left[A^*P_2\ Q_2 \times\right.$$

$$\times\left[\theta_k^{(1)}(\xi,\eta_k(\xi))-\frac{1}{2}A^{(1)}(\eta_k(\xi))\right] \times$$

$$\left.\times\left[\eta-\eta_k(\xi)\right]+A^*P_2\ Q_1\ \frac{1}{2}\int_{\eta_k(\xi)}^{\eta} A^{(1)}(\eta)d\eta\right] +$$

$$+\left[A^{**}P_1\ Q_2\left[\xi-\xi_A\right]\ \frac{1}{2}\left[A^{(1)}(\eta)-A^{(1)}(\eta_k(\xi))\right]+\right.$$

$$\left.+\ E^{(1)}(\eta)-E^{(1)}(\eta_k(\xi))\right]\}$$

$$y^{(1)}(\xi,\eta) = y_k^{(1)}(\xi_A,\eta_k(\xi_A)) + \frac{1}{tg(\theta_\infty+\alpha_\infty)-tg(\theta_\infty-\alpha_\infty)} \{-tg(\theta_\infty-\alpha_\infty) \times$$

$$\times\left[A^*P_2\ Q_2\left[\theta_k^{(1)}(\xi,\eta_k(\xi))-\frac{1}{2}A^{(1)}(\eta_k(\xi))\right]\left[\eta-\eta_k(\xi)\right]+\right.$$

$$\left.+A^*P_2\ Q_1\ \frac{1}{2}\int_{\eta_k(\xi)}^{\eta} A^{(1)}(\eta)d\eta\right]+tg(\theta_\infty+\alpha_\infty)\left[A^{**}P_1\ Q_2\left[\xi-\xi_A\right]\times\right.$$

$$\left.\times\ \frac{1}{2}\left[A^{(1)}(\eta)-A^{(1)}(\eta_k(\xi))\right]+E^{(1)}(\eta)-E^{(1)}(\eta_k(\xi))\right]\}\ .$$

is yielded for the position coordinates from equations (2.27).

The quantities P_i, Q_i are the constant values given by equation (5.10). $A^{(1)}(\eta)$ and $E^{(1)}(\eta)$ are abbreviations for the initial values pre-assigned along ξ_A; these are in full:

$$
\begin{aligned}
A^{(1)}(\eta) &= \theta^{(1)}(\xi_A,\eta) + \operatorname{ctg}\alpha_\infty w^{(1)}(\xi_A,\eta) \\
B^{(1)}(\xi) &= \theta^{(1)}(\xi,\eta_A) - \operatorname{ctg}\alpha_\infty w^{(1)}(\xi,\eta_A) \\
E^{(1)}(\eta) &= y^{(1)}(\xi_A,\eta) - \operatorname{tg}(\theta_\infty-\alpha_\infty)\, x^{(1)}(\xi_A,\eta) \\
F^{(1)}(\xi) &= y^{(1)}(\xi,\eta_A) - \operatorname{tg}(\theta_\infty+\alpha_\infty)\, x^{(1)}(\xi,\eta_A) .
\end{aligned}
\tag{5.28}
$$

$B^{(1)}(\xi)$ and $F^{(1)}(\xi)$ are the initial values along the right-handed characteristic η_A. They are required for the equations comprised in Table 3 when the problems concerned are the pure initial value problems or when the inital values along η_A are pre-assigned in addition to the boundary values.

The total flow field of a double infinite cascade is shown in Fig. 31. The incident flow along an axial component which is smaller than the speed of sound and an upstream effect is therefore achieved. The resulting neutral cascade entrance characteristic is shown as a broken line. The entrance region of the flow represented in the illustration is limited upstream by the aerofoil suction side, the right-handed shock through the aerofoil tip and the right-handed shock through the aerofoil trailing edge. Since the two right-handed shocks do not intersect until downstream of the cascade exit face, the entrance region extends in this example even as far as behind the cascade exit face. The entire remaining flow field between the blades and behind the cascade here corresponds to flow through a channel. In the area between the blades it is evident that one family of Mach lines originate in the suction side and the other family in the pressure side and that consequently they do not come from a constant domain. With respect to the zone behind the cascade it is seen that the left-handed shock through the aerofoil trailing edge in the example considered runs downstream behind the cascade exit face. For this reason, left-handed Mach lines issuing from the aerofoil suction side also get behind the cascade exit face. Since the aerofoils now continue periodically in both directions and to infinity, it is realised that the total flow field downstream of the cascade exit face is covered by these left-handed characteristics which

issue from the aerofoil suction side. On the other hand, all the right-handed charactersitics come from the aerofoil pressure sides, at least after the intersection point of the two right-handed shocks (not shown in the picture). Consequently, in this area, the conditions of a flow through a channel are also satisfied. It should also be remembered that the total flow state in the cascade is clearly established following the selection of the incident flow, and that the outlet flow cannot be affected from the rearward position. The axial outlet flow component is greater in this example than sonic speed which physically explains that a reaction from downstream is not possible.

For the calculation of the outlet flow occurring at an infinite distance behind the cascade it would be necessary to calculate to infinity the right-handed as well as the left-handed shock issuing from the trailing edge. There, both shocks pass over into the Mach lines, and the state thus characterized is precisely the outlet flow quantity which is to be found. Since with the exception of the two characteristics running asymptotically into the shocks all Mach lines have been cancelled out in infinity by the left and right-handed shocks, these two remaining characteristics can be defined as neutral cascade exit characteristics. However, the two Mach lines are not straight lines, nor is the flow condition along them constant so that no significant gain of information is related to their determination. They are therefore not included in the illustration. The calculation of the cascade exit shocks has proved considerably more difficult than than of the cascade entrance shocks specifically because of the right-handed and left-handed shocks intersecting an infinite number of times. Another method is therefore applied here to the calculation of the outlet flow which is to be found. The calculation of the flow field is discontinued for any position behind the cascade, and the calculation further downstream abandoned. However, the entirely indispensable constant state at an infinite distance behind the cascade is calculated based on the flow data in the cascade exit face according to a method given by Scholz [47] and applied to the supersonic outlet flow for the first time by Amecke [48]. This method is based on the application of the four conservation theories (continuity equation,

momentum theory tangential to the cascade face, and momentum theory normal to the cascade face, energy theory) to the flow region between the cascade exit face and the constant outlet flow behind the cascade. The energy theory is a priori satisfied in the calculation method used here because T_{ges} = constant and need not be taken into account in what follows. Since the flow values in the cascade exit face are known, it is possible to calculate with the other three conservation theories the unknown quantities w_2, θ_2 and also, beyond the procedure used so far, the total pressure p_{ges2} and as a result the shock losses between the cascade exit face and constant outlet flow. The conservation theories are given in equations (5.29):

$$(5.29a)\quad Z1 = \frac{1}{t}\int_0^t \frac{p_{ges}}{p_{ges\infty}} \cdot \left[\frac{\kappa+1}{\kappa-1} - M^{*2}\right]^{\frac{1}{\kappa-1}} \cdot M^* \cdot \sin\beta \, dt =$$

$$= \frac{p_{ges2}}{p_{ges\infty}} \cdot \left[\frac{\kappa+1}{\kappa-1} - M_2^{*2}\right]^{\frac{1}{\kappa-1}} \cdot M_2^* \cdot \sin\beta_2$$

$$(5.29b)\quad Z2 = \frac{1}{2}\,\frac{\kappa-1}{\kappa}\,\frac{1}{t}\int_0^t \frac{p_{ges}}{p_{ges\infty}} \cdot \left[\frac{\kappa+1}{\kappa-1} - M^{*2}\right]^{\frac{\kappa}{\kappa-1}} dt +$$

$$+ \frac{1}{t}\int_0^t \frac{p_{ges}}{p_{ges\infty}} \cdot \left[\frac{\kappa+1}{\kappa-1} - M^{*2}\right]^{\frac{1}{\kappa-1}} \cdot M^{*2} \cdot \sin^2\beta \, dt =$$

$$= \frac{1}{2} \cdot \frac{\kappa-1}{\kappa} \cdot \frac{p_{ges2}}{p_{ges\infty}} \cdot \left[\frac{\kappa+1}{\kappa-1} - M_2^{*2}\right]^{\frac{\kappa}{\kappa-1}} +$$

$$+ \frac{p_{ges2}}{p_{ges\infty}} \cdot \left[\frac{\kappa+1}{\kappa-1} - M_2^{*2}\right]^{\frac{1}{\kappa-1}} \cdot M_2^{*2} \cdot \sin^2\beta_2$$

$$(5.29c)\quad Z3 = \frac{1}{t}\int_0^t \frac{p_{ges}}{p_{ges\infty}} \cdot \left[\frac{\kappa+1}{\kappa-1} - M^{*2}\right]^{\frac{1}{\kappa-1}} \cdot M^{*2} \cdot \sin\beta \cdot \cos\beta \, dt =$$

$$= \frac{p_{ges2}}{p_{ges\infty}} \cdot \left[\frac{\kappa+1}{\kappa-1} - M_2^{*2}\right]^{\frac{1}{\kappa-1}} \cdot M_2^{*2} \cdot \sin\beta_2 \cdot \cos\beta_2 \,.$$

The resulting solution is:

(5.30)

$$(M_2^{*2})_{1,2} = \frac{2\kappa}{\kappa+1} \cdot \left\{ \left(\frac{Z3}{Z1}\right)^2 + \frac{\kappa}{\kappa+1} \left(\frac{Z2}{Z1}\right)^2 - \frac{\kappa+1}{2\kappa} \pm \right.$$

$$\left. \pm \sqrt{\left(\frac{\kappa}{\kappa+1}\right)^2 \left(\frac{Z2}{Z1}\right)^4 + \frac{\kappa-1}{\kappa+1}\left(\frac{Z3 \cdot Z2}{Z1 \cdot Z1}\right)^2 - \left(\frac{Z2}{Z1}\right)^2} \right\}$$

$$\cos \beta_2 = \left(\frac{Z3}{Z1}\right) \cdot \frac{1}{M_2^*}$$

$$\frac{p_{ges2}}{p_{ges\infty}} = Z1 \Big/ \left\{ \left[\frac{\kappa+1}{\kappa-1} - M_2^{*2}\right]^{\frac{1}{\kappa-1}} \cdot M_2^* \cdot \sin \beta_2 \right.$$

The loss coefficient ω which incorporates the shock losses from the cascade outlet face up to the balanced flow in the infinitely distant plane 2 is therefore:

$$\omega = \frac{p_{ges1} - p_{ges}}{p_{ges1} - p_1} = \frac{1 - (p_{ges} / p_{ges1})}{1 - \left[1 + \frac{\kappa-1}{2} M_1^2\right]^{-\frac{\kappa}{\kappa-1}}} =$$

$$= \frac{1 - (p_{ges} / p_{ges1})}{1 - \left(\frac{\kappa+1}{\kappa-1}\right)^{-\frac{\kappa}{\kappa-1}} \left[\frac{\kappa+1}{\kappa-1} - M_1^{*2}\right]^{\frac{\kappa}{\kappa-1}}} .$$

5.4. Outlet flow region

In Fig. 31, the outlet flow takes place via a supersonic axial component. As has been shown in the previous chapter, the whole flow behind the cascade is fixed by the selection of a specific incident flow. The back pressure consequently also having been established cannot be continuously

varied by throttling. Due to subsonic areas present in wakes, as a result of side wall boundary layers, compression shocks and non-periodic non-steady processes, it is possible, however, to get from the outlet flow previously considered to the flow shown in Fig. 32 discontinuously by throttling. The blade aerofoil, cascade geometry and the incident flow are in this instance identical to those in Fig. 31. Only that section of the flow which lies downstream of the left-handed shock through the aerofoil trailing edge is different from the flow image considered first. The axial outlet flow component in the flow considered last is smaller than sonic velocity and there are no left-handed characteristics running from the aerofoil suction side to behind the cascade exit face. The left-handed Mach lines which are situated behind the left-handed shock through the aerofoil trailing edge now stem from the region at an infinite distance behind the cascade. Since there again a constant outlet flow is supposed to exist, the flow prevailing downstream of the last left-handed shock is again a simple wave flow. This area, which occupies the whole region behind the cascade is defined as the outlet region in a similar way to the entrance region. The right-handed Mach lines here are straight lines, the state along them being constant. Once an outlet flow, which is again perfectly periodic, exists, it can be varied continuously by changing the back pressure without causing a variation in the incident flow. In this case, the back pressure is a new independent parameter. This reaction is physically explained by the axial subsonic component of the outlet flow. The minimum back pressure is achieved when the left-handed trailing edge shock runs through the next adjacent blade tip. A further progressive reduction in pressure is not possible. A sudden jump into the flow state shown in Fig. 31 then occurs, with an axial supersonic outlet flow component. The maximum possible throttling is reached when the incident flow is still just not affected by the outlet flow. However, since the calculation method applied here pre-supposes a supersonic flow, the calculation must be discontinued even before reaching this maximum back pressure, namely at the time when the speed of sound occurs in the flow field for the first time.

The infinite axial subsonic outlet flow can be calculated in principle by the same method as the infinite incident flow in the entrance region. The only difference is that in one part of the outlet flow zone a purely characteristic initial value problem is concerned. Here once again, there exists a neutral outlet flow characteristic which, because of the simple wave flow, represents a constant state, i.e. that of the outlet flow. At infinity, the right-handed shock passes over asymptotically into this straight Mach line. It is shown in Fig. 32 as a dotted line. In calculating the different states of throttling it is appropriate to pre-assign the flow angle at the blade trailing edge instead of the back pressure and to calculate the pressure from the resulting outlet flow quantities θ_2, w_2.

For the flow shown in Figs. 31 and 32, the axial outlet flow component lies in the unthrottled case in the supersonic range. Under other approach flow conditions or for other cascase configurations, flow conditions can occur, however, where in the unthrottled state all the left-handed Mach lines issuing from the aerofoil suction side still run into the cascade.

If with this type of flow configuration the flow direction at the blade trailing edge coincides with that of the aerofoil suction side at the trailing edge, then we speak of a matched flow condition. For more throttling, a left-handed shock, which runs into the cascade, forms at the trailing edge. The flow diagram then agrees qualitatively with that shown in Fig. 32. If on the other hand, the back pressure is further reduced beyond the matched condition, a centered expansion occurs at the blade trailing edge, whose left-handed Mach lines, however, must still run into the cascade. The minimum back pressure is achieved when the last of the left-handed Mach lines of the fan just meets the next blade trailing edge. The axial outlet flow component just reaches the speed of sound in this case. A further pressure reduction is not possible because of the necessary periodicity. In this type of flow condition, the axial outlet flow is therefore always subsonic and can reach at a maximum sonic speed.

5.5. Cascade flow with reaction of the outlet flow on the approach flow

In the flow conditions so far considered, the approach flow was freely selectable within certain limits (axially supersonic), or there was a coupling of the direction and the speed (axially subsonic) which is fixed by the suction side contour of the blade aerofoils. The approach flow, however, was in any case independent of the outflow from the cascade. However, as a result of very high pitch ratios or big stagger angles, flow configurations can emerge where all left-handed characteristics issuing from the aerofoil suction sides run upstream in front of the subsequent blade aerofoils, Fig. 33. In that type of flow, the axial component of the approach flow as well as the outlet flow is below sonic speed and a simple wave flow exists in the whole flow field. The left-handed Mach lines issuing from the suction sides are straight lines because all the right-handed characteristics in the area covered by them come from the constant approach flow region. Likewise, the right-handed Mach lines issuing from the aerofoil pressure sides are straight, because all the left-handed characteristics there come from the constant outlet flow region. In the flow field which is limited by the shocks issuing from the trailing edge and the shocks issuing from the leading edge of the adjacent blade, a constant flow condition does in fact prevail since there the right-handed Mach lines come from the incident flow and the left-handed ones come from the outlet flow.

Because of the simple wave flow, the formulae given in Chapter 5.2 for the calculation of the entrance region can be used for the calculation of the flow field. To calculate the approach flow to the infinite cascade, it is necessary to calculate the left-handed shocks issuing from the trailing edge and the next blade leading edge, up to their intersection point. The calculation of the one shock which results after the intersection must then be continued to infinity. The incident flow state characterized by this limit is plotted as a broken line in the diagram

as a neutral left-handed cascade entrance characteristic. The application of the same calculation method to the appropriate right-handed shocks then yields the outlet flow at infinity behind the cascade once again as the limiting position of the shock. The right-handed neutral cascade exit characteristic is also shown as a broken line in the diagram.

For the convex aerofoil geometries considered, a centered Prandtl-Meyer expansion can also occur for variable flow and cascade configurations instead of the one of the two parallel shocks. This, however, does not principally change anything in the behaviour of the flow under consideration.

Two flow magnitudes can be freely selected for the calculation of this cascade flow. If, for example, the inlet flow is fixed by β_1, M_1, then the entire remaining flow field is clearly defined, including particularly the outlet flow β_2, M_2. If, on the other hand, the outlet flow is pre-assigned, then the complete flow including the approach flow, is fixed.

For practical purposes, neither the approach flow nor the outlet flow is pre-assigned in what follows, but the constant state β_E, M_E between the cascade blades. As a result of the state along the A - B straight line being constant, Fig. 34, connecting the aerofoil trailing edge with the adjacent aerofoil leading edge, and of the pre-assignment of the flow β_E, M_E prevailing there, the rate of flow through a cascade pitch can be readily calculated. This rate of flow must now be equal to the flow through a pitch t formed with the approach flow magnitudes and also the flow formed with the outlet flow magnitudes, Fig. 34. This yields, following some intermediate calculations:

$$\left[\frac{\kappa+1}{\kappa-1} - M^*_E{}^2\right]^{\frac{1}{\kappa-1}} M_E^* \left[\sin \beta_E + \frac{1}{t} \cdot \sin(\beta_E - \beta_S)\right] =$$

$$= \left[\frac{\kappa+1}{\kappa-1} - M_1{}^{*2}\right]^{\frac{1}{\kappa-1}} M_1^* \sin \beta_1$$

(5.31)

$$\left[\frac{\kappa+1}{\kappa-1} - M_E{}^{*2}\right]^{\frac{1}{\kappa-1}} M_E^* \left[\sin \beta_E + \frac{1}{t} \cdot \sin(\beta_E - \beta_S)\right] =$$

$$= \left[\frac{\kappa+1}{\kappa-1} - M_2{}^{*2}\right]^{\frac{1}{\kappa-1}} M_2^* \sin \beta_2 \,.$$

Because of the simple wave flow, the relationship (5.1) must be valid between the quantities of the incident flow and those in the E area. A corresponding equation with a negative sign is then valid between the outlet flow and E. Hence, for 1st order terms following an intermediate calculation:

$$\beta_E + \frac{\mathrm{ctg}\alpha_\infty}{M^*_\infty} M^*_E = \beta_1 + \frac{\mathrm{ctg}\alpha_\infty}{M^*_\infty} M^*_1$$

(5.32)

$$\beta_E - \frac{\mathrm{ctg}\alpha_\infty}{M^*_\infty} M_E^* = \beta_2 - \frac{\mathrm{ctg}\alpha_\infty}{M^*_\infty} M_2^* \,.$$

The equations (5.31) and (5.32) thus represent an equation system for the four unknown quantities β_1, M_1 and β_2, M_2 that can be solved by iteration.

It is apparent from the equations with the interrelationship between incident flow, outlet flow and state in the E region depend entirely on the cascade geometry t/l and β_s, and not on the aerofoil contour. This statement is still valid if instead of the two equations (5.32) which constitute the 1st approximation, the exact solutions of the compatability conditions

$$\beta_E + \nu_E = \beta_1 + \nu_1$$
$$\beta_E - \nu_E = \beta_2 - \nu_2 \qquad (5.33)$$

are used. The equation of the aerofoil contour enters the relationship between approach and outlet flow only if the loss effect due to shock on the flow quantities is taken into account.

The reaction of the outlet flow on the incident flow was established for the first time by Strauss (described by Oswatitsch [37]) for an infinitely thin plate cascade.

6. Calculation of the entropy losses in oblique shocks

6.1. Calculation of the entropy losses along an oblique compression shock

Let the oblique compression shock be given in the x, y plane as $y_{St} = y_{St}(x)$, Fig. 35. Let the length of the curve along this shock be b. The total entropy loss $\overline{\Delta s}$ from a selected initial point b_A to a random point b is then:

$$\overline{\Delta s} = \frac{\int_{m(b_A)}^{m(b)} (\hat{s}-s)\,dm}{m} \qquad (6.1)$$

with s the specific entropy before the shock and $\hat{s}$ after the shock, and m the mass flow through a pitch. Hence for dm :

$$dm = \bar{B}\cdot\rho\cdot w_\infty(w+1)\cdot\sin(\gamma-\theta-\theta_\infty)\cdot db \; . \qquad (6.2)$$

$\bar{B}$ is the constant side extension of the flow configuration under consideration, at rightangles to the diagram plane. ρ is the density of the flow medium, which because of the irrotationality is a function only of the flow velocity.

For the transition from the curve length to the Cartesian coordinates

$$db = dx/\cos\gamma, \quad \text{where} \quad tg\,\gamma = tg\,\gamma(x) = (dy/dx)_{St}$$

is valid as the shock angle in relation to the x-axis. Equation (6.2) then yields:

$$(6.3) \qquad dm = \bar{B}\cdot w_\infty \rho (w+1)\left[tg\gamma\cdot\cos(\theta+\theta_\infty)-\sin(\theta+\theta_\infty)\right]dx\ .$$

When considering the shock in the ξ, η plane, a left-handed shock is plotted as $\xi_{St} = \xi_{St}(\eta)$, Fig. 36. The entropy loss from b'_A to b' is then:

$$(6.4) \qquad \overline{\Delta s} = \frac{\int_{m(b'_A)}^{m(b')} (\hat{s}-s)\,dm}{m}\ .$$

b' is the curve length along the shock in the ξ, η plane. Substituting then the characteristic coordinates into the equation (6.3) yields, following some transformations:

(6.5)

$$dm = \bar{B} w_\infty \rho (w+1)\,\frac{\partial x}{\partial \eta}\left\{\cos(\theta+\theta_\infty)\left[tg(\theta+\theta_\infty-\alpha)\,\frac{\frac{\partial x}{\partial \xi}}{\frac{\partial x}{\partial \eta}}\left(\frac{d\xi}{d\eta}\right)_{St}+tg(\theta+\theta_\infty+\alpha)\right]-\right.$$
$$\left.-\sin(\theta+\theta_\infty)\left[\frac{\frac{\partial x}{\partial \xi}}{\frac{\partial x}{\partial \eta}}\left(\frac{d\xi}{d\eta}\right)_{St}+1\right]\right\}d\eta\ .$$

Here, $\frac{\partial x/\partial \xi}{\partial x/\partial \eta}\cdot\left(\frac{d\xi}{d\eta}\right)_{St}$ can be substituted by equation (3.6). The relevant equation for right-handed shocks results from equation (6.5) by interchanging ξ and η. The quantity $\hat{s} - s$ in equation (6.4) is obtained as (see Sauer [49]) :

$$(6.6)\qquad -\left(\frac{\hat{s}-s}{R}\right) = \ln\frac{p_{g\hat{e}s}}{p_{ges}} = \frac{\kappa}{\kappa-1}\ln\left[\frac{(\kappa+1)M^2\sin^2(\gamma-(\theta+\theta_\infty))}{2+(\kappa-1)M^2\sin^2(\gamma-(\theta+\theta_\infty))}\right] -$$

$$- \frac{1}{\kappa-1}\ln\left[\frac{2\kappa M^2\sin^2(\gamma-(\theta+\theta_\infty))-(\kappa-1)}{(\kappa+1)}\right] .$$

Here, $M = M(w)$ and $\gamma = \gamma(w, \theta, \hat{\theta})$; see equations (3.1) and (3.2). The expansion into a series at the position $\hat{\theta} = \theta$ then gives, following a further expansion into a series of the coefficients at the position $w = 0$:

(6.7)

$$-\left(\frac{\hat{s}-s}{R}\right) = \{V_{10} + V_{11}w + \ldots\}\frac{(\hat{\theta}-\theta)^3}{6} + \{V_{20} + \ldots\}\frac{(\hat{\theta}-\theta)^4}{24} + \ldots$$

For the first V_{ij} coefficients one obtains:

$$V_{10} = \mp\,\kappa\frac{(\kappa+1)}{2}\,\frac{M_\infty^6}{(M_\infty^2-1)^{3/2}}$$

$$(6.8)\qquad V_{11} = \mp\,\frac{3}{4}\,\kappa(\kappa+1)\,\frac{M_\infty^6}{(M_\infty^2-1)^{5/2}}\,\{(\kappa-1)\,M_\infty^4+2(2-\kappa)\,M_\infty^2-4\}$$

$$\vdots$$

$$V_{20} = \frac{3}{2}\,\kappa(\kappa+1)\,\frac{M_\infty^6}{(M_\infty^2-1)^3}\,\{(\kappa-1)\,M_\infty^4+2(2-\kappa)\,M_\infty^2-4\}$$

$$\vdots$$

The top sign relates to the left-handed and the bottom one to right-handed shocks. It is seen from equation (6.7) that the first approximation, which differs from zero, is for $-(s - \hat{s})/R$ a quantity of the 3rd order in $(\hat{\theta} - \theta)$.

6.2. Calculation of the shock losses in the entrance region of the double infinite cascade with upstream effect

For a double infinite cascade with upstream effect, there emerges the shock configuration of which Fig. 37 is an example. This diagram shows the shocks as well as the dynamic streamlines which impinge on the tips of the individual cascade aerofoils. The diagram shows that each streamline has to cross an infinity of shocks before reaching the cascade. In calculating the total shock losses between two adjacent dynamic streamlines it is necessary to add up the losses along an infinity of partial shocks which intersect the two streamlines. In the example in Fig. 37, the losses are composed of losses which are the result of integration along the partial shocks 1-2, 2-3, 3-4 etc. However, due to the periodicity of the flow in front of the cascade, all the shocks and streamlines are identical when they are displaced parallel to the cascade face by complete pitch multiples. For this reason, the partial shock 2-3 is identical to the partial shock 2'-3" and likewise 3-4 to 3"-4"' etc. The shock losses arising upstream of the cascade between two dynamic streamlines can therefore be calculated by integrating one cascade shock from the initial point of the shock to infinity (see Klapproth [50]). This consideration is not restricted to conditions with attached shocks because it is based only on the hypothesis of periodicity of the flow.

For the entropy change of the flow through a blade passage due to the infinity of cascade entrance shocks we obtain, following some calculations, to the 1st approximation:

$$(6.9)\qquad -\left(\frac{\overline{\hat{s}-s_1}}{R}\right) = \ln\left(\frac{\overline{\hat{p}_{ges}}}{p_{ges_1}}\right) = \frac{1}{t}\cdot\frac{A^*}{6}\,\frac{\cos\vartheta_\infty}{\sin\beta_\infty}\times$$

$$\times\left\{tg(\vartheta_\infty+\alpha_\infty)-tg\vartheta_\infty\right\}\cdot V_{10}\int_{\hat{\eta}_{Anf}}^{\hat{\eta}\to\infty}\left(\hat{\vartheta}^{(1)}-\vartheta^{(1)}\right)^3 d\hat{\eta}\,.$$

where the upper integration limit $\hat{\eta}$ must be extended to ∞. The above equation is also valid for cascade exit shocks if the incident flow (index 1) is substituted by the exit state (index 2). For the right-handed integral we then have in the entrance region taking the relationships (5.18) and (5.9) derived in Chapter 5 into account:

(6.10)

$$\int_{(\hat{\eta}-\hat{\eta}_0)_{Anf}}^{\hat{\eta}-\hat{\eta}_0 \to \infty} \left(\hat{\theta}^{(1)}-\theta^{(1)}\right)^3 d(\hat{\eta}-\hat{\eta}_0) = \int_0^1 \frac{\bar{A}^3 \cdot z}{\left\{\bar{C}+z\cdot\left[\bar{D}+\bar{C}\left((\hat{\eta}-\hat{\eta}_0)_{Anf}-1\right)\right]\right\}^3} dz \,.$$

The integration here must take place along the shock $\xi_{St} = \xi_{St}(\hat{\eta}) = \xi_{St}(z)$. The functions $\bar{A}$, $\bar{C}$ and $\bar{D}$ are given by

(6.11)

$$\bar{A} = A^{**}\left(\hat{\theta}^{(1)}-\theta_S^{(1)}\right) + \left(\frac{\partial\theta^{(1)}}{\partial(\xi-\xi_0)}\right)_S \cdot \{A^{**}\left[(\xi_S-\xi_0)-(\hat{\xi}-\hat{\xi}_0)\right] +$$

$$+A^*\tilde{N}_1\hat{\theta}^{(1)}\left[(\hat{\eta}_K-\hat{\eta}_0)-(\eta_K-\eta_0)_S+(\hat{\eta}_0-\eta_0)\right]\} +$$

$$+1\Big/\left[tg(\theta_\infty+\alpha_\infty)-tg(\theta_\infty-\alpha_\infty)\right]\cdot\left(\frac{\partial\theta^{(1)}}{\partial(\xi-\xi_0)}\right)_S\{tg(\theta_\infty+\alpha_\infty)\times$$

$$\times\left[(x_K^{(1)}-x_0^{(1)})_S-(\hat{x}_K^{(1)}-\hat{x}_0^{(1)})\right] + \left[\hat{y}_0-y_0\right] - tg(\theta_\infty+\alpha_\infty)\left[\hat{x}_0-x_0\right]\}$$

$$\bar{C} = A^*\tilde{N}_1\left(\frac{\partial\theta^{(1)}}{\partial(\xi-\xi_0)}\right)_S$$

$$\bar{D} = A^{**}+A^*\tilde{N}_1\left(\frac{\partial\theta^{(1)}}{\partial(\xi-\xi_0)}\right)_S\left[(\hat{\eta}_0-\eta_0) - (\eta_K-\eta_0)_S\right]$$

depending only on $\hat{\xi} - \hat{\xi}_0$.

The coefficients, which contain only the entropy changes caused by the

cascade entrance shocks, are plotted in Figs. 38 and 39 for a cascade having convex aerofoil suction sides. In the first graph, the stagger angle is kept constant varying the pitch ratio whilst the second graph shows the loss coefficent for a constant pitch ratio with different stagger angles. The decrease in loss as the incident Mach Number increases is remarkable. However, this is readily explained when it is remembered that for the highest Mach Number considered here, the incident flow takes place exactly as the axial approach flow component reaches the speed of sound. In this case, the cascade entry shock passes over into a Mach line which lies in the cascade face, and the losses become zero as the shock vanishes. The diagrams also show that the assumption of irrotation is justified, at least in the entrance region since the loss coefficients assume extremely low values ($\leq$ 1%) for the cascades of aerofoils with a small camber considered here.

7. Conclusion

In this paper, the method of analytical characteristics by Oswatitsch for the plane irrotational supersonic flow, is developed and applied to the calculation of the flow through straight blade cascades. The characteristic coordinates serve as independent variables. The known closed solution of the compatibility conditions is expanded for perturbation quantities of the variables of state, for simplification. For the solution of the non-linear slope conditions, a perturbation formula in the position coordinates is additionally selected which transforms the slope conditions to a sequence of linear differential equations, which are then successively solved.

Weak compression shocks are subsequently fitted to regions of convolution in such a way that the state on both sides of the shock is compatible with the flow field already known. The resulting envelopes of characteristics which limit the region of convolution, and the cusps which are the deciding factors for the initial points of the shocks, are also calculated.

Using these general solutions, the plane supersonic flow through straight blade cascades is then calculated, namely for semi-infinite as well as for double infinite cascades. For an approach flow with an axial component which is smaller than the speed of sound, the neutral cascade entrance characteristic is obtained as the limiting position of the entrance shocks. The associated coupling between the incident flow direction and the Mach Number, can be stated both for aerofoils having convex and concave suction sides. The flow with an axial supersonic incident flow component, can also be calculated for angles of incidence which are not too large, and the limits arising can be specifically stated. The flow between the blades can be calculated as a flow through a channel. In the case of an axial supersonic outlet flow component, the channel area extends to infinity downstream of the cascade, and the back pressure is uniquely established. If, on the other hand, the axial outlet flow component is smaller than the speed of sound, the back pressure emerges as a freely selectable parameter. In this case, a simple wave flow exist once again behind the cascade.

Specifically, a flow through a cascade is considered where a reaction of the outlet flow on the approach flow occurs in spite of the prevailing flow being supersonic.

Finally, equations are given for entropy changes as a result of weak compression shocks. Using these equations, the shock losses arising in front of the cascade are calculated for a cascade with an approach flow having a subsonic axial component.

Hanns-Jürgen Lichtfuss,
505 Porz-Wahn, Linder Höhe.

8. References

[1] Oswatitsch, K. — Die Wellenausbreitung in der Ebene bei kleinen Störungen. (Wave propagation in a plane with small perturbations) Fluid Dynamics Transactions Vol.1 Symposium, Jablonna, (Sept. 1961), p. 315-329.

[2] Oswatitsch, K. — Das Ausbreiten von Wellen endlicher Amplitude. (The propagation of waves of finite amplitude). ZFW 10 (1962), p. 130-138.

[3] Lin, C.C. — On a Perturbation Theory Based on the Method of Characteristics. Journal of Mathematics and Physics 33 (1954), p. 117-134.

[4] Fox, P.A. — On the Use of Coordinate Perturbations in the Solution of Physical Problems. Doctor Thesis, MIT. 1953.

[5] Fox, P.A. — Perturbation Theory of Wave Propagation Based on the Method of Characteristics. Journal of Mathematics and Physics 34 (1955), p. 133-151.

[6] Van Dyke, M. — Perturbation Methods in Fluid Mechanics. Applied Mathematics and Mechanics, Vol. 8, New York: Academic Press, 1964.

[7] Oswatitsch, K. — Ausbreitungsprobleme (Problems of propagation) Zamm 45 (1965), p. 485-498.

[8] Poincaré, H. — Les méthodes nouvelles de la méchanique céleste. (New methods of celestial mechanics). Vol. 1, Ch. III. Paris: Gauthier-Villars et Fils, 1892.

[9] Lighthill, M.J. — A Technique for Rendering Approximate Solutions to Physical Problems Uniformly Valid. The Philosophical Magazine Vol. XL (1949), seventh series, p. 1179-1201.

[10] Lighthill, M.J. — A Technique for Rendering Approximate Solutions to Physical Problems Uniformly Valid. ZFW 9 (1961), p. 267-275.

[11] Kuo, Y.H. — On the Flow of an Incompressible Viscous Fluid Past a Flat Plate at Moderate Reynolds Numbers. Journal of Mathematics and Physics 32 (1953), p. 83-101.

[12] Kuo, Y.H. — Viscous Flow Along a Flat Plate Moving at High Supersonic Speeds. Journal of the Aeronautical Sciences 23 (1956), p. 125-136 and p. 977-978.

[13] Whitham, G.B. — The Flow Pattern of Supersonic Projectiles. Communications on Pure and Applied Mathematics V (1952), p. 301-348.

[14] Whitham, G.B. — On the Propagation of Weak Shock Waves. Journal of Fluid Dynamics 1 (1956), p. 290-318.

[15] Kantrowitz, A. — The Supersonic Axial-Flow Compressor. NACA Report 974 (1946).

[16] Schwaar, P. — Determination of the Stationary Flow Field in Front of a Supersonic Cascade. Journal of Aeronaut. Sc. 23 (1956), p. 888-889.

[17] Levine, P. — The Two-Dimensional Inflow Conditions for a Supersonic Compressor with Curved Blades. WADC Technical Report 55-387 (1956).

[18] Levine, P. — Two-Dimensional Inflow Conditions for a Supersonic Cascade with Curved Blades. Journal of Applied Mechanics 24 (1957), No. 2, p. 165-169.

[19] Yamaguchi, S. — On the Inlet-Flow Field for a Two-Dimensional Supersonic Cascade with Curved Entrance Regions. Bulletin of JSME 7 (1964), No. 25, p. 91-95.

[20] Novàk, O. — Flow in the Entrance Region of a Supersonic Cascade. Strojnicky Casopis XIX, c. 2-3, p. 138-150.

[21] Starken, H.
Untersuchung der Strömung in ebenen Überschallverzögerungsgittern.
(Investigation into the Flow in Plane Supersonic Deceleration Cascades).
DLR FB 71-99 (1971).

[22] Oswatitsch, K.
Der Stosswellenknall beim Überschallflug.
Vortrag zum 4. Kongress des International Council of the Aeronautical Sciences, Paris 1964.
(The Shock Wave Bang in Supersonic Flight).
(A lecture given at the 4th Congress of the International Council of the Aeronautical Sciences, Paris 1964).
Washington: Spartan Books, 1965.

[23] Oswatitsch K.
Analytische Berechnung von Charakteristikenflächen bei Strömungsvorgängen.
(Analytical calculation of characteristic surfaces for flow processes).
DLR FB 65-62 (1965).

[24] Schneider, W.
Analytische Berechnung achsensymmetrischer Überschallströmungen mit Stössen.
(Analytical calculation of axisymmetric supersonic flows with shocks)
DVL report 275 (1963).

[25] Schneider, W.
Über die Ausbreitung des Mündungsknalles.
(On the propagation of the muzzle blast)
DLR FB 67-50 (1967).

[26] Rothmann, H.
Analytische Untersuchung der Ausbreitung von Kugel- und Zylinderwellen.
(Analytical investigation into spherical and cylindrical waves).
DVL report 280 (1963).

[27] Rothmann, H.
Das asymptotische Verhalten von Kugel- und Zylinderwellen.
(The asymptotic behaviour of spherical and cylindrical waves).
DLR FB 66-38 (1966).

[28] Sun, E.Y.C.
Nicht angestellte Deltaflügel mit Unterschall- und Schallvorderkanten.
(Non-incidence delta weings with subsonic and sonic leading edges)
Journal de Mécanique 3 (1964), p. 141-163.

[29] Sun, E.Y.C.
Die Kopfwelle an einem nichtangestellten Deltaflügel in stationärer Überschallströmung beim Ubergang von Unterschall- zu Überschallvorderkanten.
(The bow wave on a non-incident delta wing in steady state supersonic flow on changing from subsonic to supersonic leading edges)
Journal de Mécanique 7 (1968), p. 521-573.

[30] Leiter, E.
Ein Beitrag zur Charakteristikentheorie der instationären ebenen und achsensymmetrischen Strömungen.
(A contribution to the theory of characteristics of the steady state plane and axisymmetric flows)
Part I, Zamm 47 (1967), Vol. 3, p. 175-190.
Part II, Zamm 47 (1967), Vol. 4, p. 229-237.

[31] Leiter, E.
Zur instationären Umströmung von Rotationskörpern nach der akustischen Theorie und dem plötzlichen Auftreten von Quellen bei Schallanströmung.
(On the non-steady flow around rotating bodies according to the theory of acoustics and the sudden occurrence of sources for sonic incident flow).
ZFW 15 (1967), p. 161-171.

[32] Leiter, E.
Oswatitsch, K.
Ermittlung stationärer schallnaher Strömungen im Absteigeverfahren aus dem Instationären.
(Determination of steady state flows with near sonic speeds by the reduction method from the non-steady state).
Zamm 47 (1967) GAMM-Sonderheft, p. T183.

[33] Stuff, R.
Analytische Berechnung von Verdichtungsstössen beschleunigter oder verzögerter Rotationskörper.
(Analytical calculation of compression shocks of accelerated or decelerated bodies of rotation).
DLR FB 68-62 (1968).

[34] Stuff, R.
Die Theorie der Knallausbreitung in einer geschichteten Atmosphäre.
(Theory of propagation of a bang in a stratified atmosphere).
ZFW 17 (1969), p. 156-164.

[35] Pokorny, W.
Analytische Berechnung von ebenen Überschallfreistrahlen.
(Analytical calculation of plane supersonic free jets)
DLR FB 68-63 (1968).

[36] Sonn, H.
Nachbarlösungen von stossfreien ebenen Überschallströmungen
(Neighbourhood solutions of shock-free plane supersonic flows).
DLR FB 69-27 (1969).

[37] Oswatitsch, K.
Gasdynamik.
(Gas dynamics)
Vienna: Springer, 1952.

[38] Zierep, J.
Vorlesungen über theoretische Gasdynamik.
(Lectures on theoretical gas dynamics)
Karlsruhe: G. Braun, 1963.

[39] Rothe, R.
Szabo, I.
Höhere Mathematik.
Teil VI, 2. Auflage.
(Higher mathematics, Part VI, 2nd edition).
Stuttgart: B.G. Teubner, 1958.

[40] Rothe, R.
Höhere Mathematik.
Teil I, 17. Auflage.
(Higher mathematics, Part I, 17th edition).
Leipzig: B.G. Teubner, 1958.

[41] Sauer, R.
Anfangswertprobleme bei partiellen Differentialgleichungen.
(Initial value problems in partical differential equations)
2nd edition.
Berlin: Springer, 1958.

[42] Courant, R.
Friedrichs, K.O.
Supersonic Flow and Shock Waves.
Pure and Applied Mathematics, Vol. 1,
New York: Interscience Publishers, 1948.

[43] Ostrowski, A.
Aufgabensammlung zur Infinitesimalrechnung.
(Collection of exercises in the infinitesimal calculus)
Vol. II A,
Basel: Birkhäuser, 1972.

[44] Willers, F.A.
Methoden der praktischen Analysis.
(Methods of practical analysis)
Göschens Lehrbücherei, Vol. 12, 3rd edition,
Berlin: Walter de Gruyter & Co., 1957.

[45] Kuipers, L.
Timman, R.
Handbuch der Mathematik.
(Handbook of mathematics)
Berlin: Walter de Gruyter & Co., 1968.

[46] Ferri, A.
Aerodynamic properties of supersonic compressors.
In: High Speed Aerodynamics and Jet Propulsion, Volume X, Aerodynamics of Turbines and Compressors.
Editor: Hawthorne, W.R.
Princeton University Press, 1964.

[47] Scholz, N. Über die Durchführung systematischer Messungen an ebenen Schaufelgittern. (On carrying out systematic measurements on plane blade cascades). ZFW 4 (1956), p. 313-333.

[48] Amecke, J. Anwendungen der transsonischen Ähnlichkeitsregel auf die Strömung durch ebene Schaufelgitter. (Applications of the transonic rule of similarity to the flow through plane blade cascades) VDI-Forschungsheft 540 (1970) (VDI Research Magazine 540 (1970))

[49] Sauer, R. Einführung in die theoretische Gasdynamik. (Introduction to theoretical gas dynamics) 3rd revised edition Berlin: Springer, 1960.

[50] Klapproth, J. F. Approximate Relative-Total-Pressure Losses of an Infinite Cascade of Supersonic Blades with Finite Leading-Edge Thickness. NACA RM E9L21 (1950).

9. Tables

$$c^{*2} = 2 \cdot \frac{\varkappa}{\varkappa+1} R T_{ges} = 2 \cdot \frac{\varkappa}{\varkappa+1} R T_{ges_\infty}$$

$$\sin \alpha = \frac{1}{M}$$

$$M^2 = \frac{(w+1)^2}{1 + \frac{\varkappa-1}{2} M_\infty^2 \left[1-(w+1)^2\right]} M_\infty^2$$

$$M^* = (w+1)\, M_\infty^*$$

$$M^{*2} = \frac{\frac{\varkappa+1}{2}}{1 + \frac{\varkappa-1}{2} M^2} M^2$$

$$M^2 = \frac{\frac{2}{\varkappa-1}}{\left[\frac{\varkappa+1}{\varkappa-1} - M^{*2}\right]} M^{*2}$$

$$\frac{T}{T_\infty} = \left\{1 + \frac{\varkappa-1}{2} M_\infty^2 \left[1-(w+1)^2\right]\right\}$$

$$\frac{p}{p_\infty} = \frac{p_{ges}}{p_{ges_\infty}} \left\{1 + \frac{\varkappa-1}{2} M_\infty^2 \left[1-(w+1)^2\right]\right\}^{\frac{\varkappa}{\varkappa-1}}$$

$$\frac{\rho}{\rho_\infty} = \frac{p_{ges}}{p_{ges_\infty}} \left\{1 + \frac{\varkappa-1}{2} M_\infty^2 \left[1-(w+1)^2\right]\right\}^{\frac{1}{\varkappa-1}}$$

$$\frac{p_{ges}}{p_{ges_\infty}} = e^{-\left(\frac{s-s_\infty}{R}\right)} = \left\{1 - \left(\frac{s-s_\infty}{R}\right) + \frac{1}{2}\left(\frac{s-s_\infty}{R}\right)^2 \mp \cdots\right\}$$

w corresponds to $\tilde{w}$ in Equation (2.3).

Table 1

Initial values along ξ_A

$$\vartheta^{(i)}(\xi,\eta) = \vartheta_K^{(i)}(\xi,\eta_K(\xi)) + \frac{1}{2}\left\{ A^{(i)}(\eta) - A^{(i)}(\eta_K(\xi)) \right\}$$

$$\operatorname{ctg}\alpha_\infty w^{(i)}(\xi,\eta) = -\vartheta_K^{(i)}(\xi,\eta_K(\xi)) + \sum_{j=1}^{i-1}(L_j)_{\xi,\eta} + \frac{1}{2}\left\{ A^{(i)}(\eta) + A^{(i)}(\eta_K(\xi)) \right\}$$

$$x^{(i)}(\xi,\eta) = \frac{y_K^{(i)}(\xi_A,\eta_K(\xi_A))}{\operatorname{tg}(\vartheta_\infty-\alpha_\infty)} + \frac{1}{\operatorname{tg}(\vartheta_\infty+\alpha_\infty)-\operatorname{tg}(\vartheta_\infty-\alpha_\infty)}\left\{ \sum_{j=1}^{i}\int_{\xi_A}^{\xi} C_j \frac{\partial x^{(i-j)}}{\partial\xi}\,d\xi - \frac{\operatorname{tg}(\vartheta_\infty+\alpha_\infty)}{\operatorname{tg}(\vartheta_\infty-\alpha_\infty)}\sum_{j=1}^{i}\left(\int_{\xi_A}^{\xi} C_j \frac{\partial x^{(i-j)}}{\partial\xi}\,d\xi\right)_{\eta_K(\xi)} - \right.$$

$$\left. - \sum_{j=1}^{i}\int_{\eta_K(\xi)}^{\eta} D_j \frac{\partial x^{(i-j)}}{\partial\eta}\,d\eta + E^{(i)}(\eta) - \frac{\operatorname{tg}(\vartheta_\infty+\alpha_\infty)}{\operatorname{tg}(\vartheta_\infty-\alpha_\infty)}\,E^{(i)}(\eta_K(\xi)) \right\}$$

$$y^{(i)}(\xi,\eta) = y_K^{(i)}\left(\xi_A,\eta_K(\xi_A)\right) + \frac{1}{\operatorname{tg}(\vartheta_\infty+\alpha_\infty)-\operatorname{tg}(\vartheta_\infty-\alpha_\infty)}\left\{ \operatorname{tg}(\vartheta_\infty+\alpha_\infty)\left[\sum_{j=1}^{i}\int_{\xi_A}^{\xi} C_j \frac{\partial x^{(i-j)}}{\partial\xi}\,d\xi - \sum_{j=1}^{i}\left(\int_{\xi_A}^{\xi} C_j \frac{\partial x^{(i-j)}}{\partial\xi}\,d\xi\right)_{\eta_K(\xi)} \right] - \right.$$

$$\left. - \operatorname{tg}(\vartheta_\infty-\alpha_\infty)\sum_{j=1}^{i}\int_{\eta_K(\xi)}^{\eta} D_j \frac{\partial x^{(i-j)}}{\partial\eta}\,d\eta + \operatorname{tg}(\vartheta_\infty+\alpha_\infty)\left[E^{(i)}(\eta) - E^{(i)}(\eta_K(\xi)) \right] \right\}$$

Table 2 a

Initial values along η_A

$$\vartheta^{(i)}(\xi,\eta) = \vartheta_K^{(i)}(\xi_K(\eta),\eta) + \frac{1}{2}\left\{ B^{(i)}(\xi) - B^{(i)}(\xi_K(\eta)) \right\}$$

$$\operatorname{ctg}\alpha_\infty w^{(i)}(\xi,\eta) = \vartheta_K^{(i)}(\xi_K(\eta),\eta) + \sum_{j=1}^{i-1}(L_j)_{\xi,\eta} - \frac{1}{2}\left\{ B^{(i)}(\xi) + B^{(i)}(\xi_K(\eta)) \right\}$$

$$x^{(i)}(\xi,\eta) = \frac{y_K^{(i)}\left(\xi_K(\eta_A),\eta_A\right)}{\operatorname{tg}(\vartheta_\infty+\alpha_\infty)} - \frac{1}{\operatorname{tg}(\vartheta_\infty+\alpha_\infty)-\operatorname{tg}(\vartheta_\infty-\alpha_\infty)}\left\{ \sum_{j=1}^{i}\int_{\eta_A}^{\eta} D_j \frac{\partial x^{(i-j)}}{\partial\eta}\,d\eta - \frac{\operatorname{tg}(\vartheta_\infty-\alpha_\infty)}{\operatorname{tg}(\vartheta_\infty+\alpha_\infty)}\sum_{j=1}^{i}\left(\int_{\eta_A}^{\eta} D_j \frac{\partial x^{(i-j)}}{\partial\eta}\,d\eta\right)_{\xi_K(\eta)} - \right.$$

$$\left. - \sum_{j=1}^{i}\int_{\xi_K(\eta)}^{\xi} C_j \frac{\partial x^{(i-j)}}{\partial\xi}\,d\xi + F^{(i)}(\xi) - \frac{\operatorname{tg}(\vartheta_\infty-\alpha_\infty)}{\operatorname{tg}(\vartheta_\infty+\alpha_\infty)} F^{(i)}(\xi_K(\eta)) \right\}$$

$$y^{(i)}(\xi,\eta) = y_K^{(i)}\left(\xi_K(\eta_A),\eta_A\right) - \frac{1}{\operatorname{tg}(\vartheta_\infty+\alpha_\infty)-\operatorname{tg}(\vartheta_\infty-\alpha_\infty)}\left\{ \operatorname{tg}(\vartheta_\infty-\alpha_\infty)\left[\sum_{j=1}^{i}\int_{\eta_A}^{\eta} D_j \frac{\partial x^{(i-j)}}{\partial\eta}\,d\eta - \sum_{j=1}^{i}\left(\int_{\eta_A}^{\eta} D_j \frac{\partial x^{(i-j)}}{\partial\eta}\,d\eta\right)_{\xi_K(\eta)}\right]\right.$$

$$\left. - \operatorname{tg}(\vartheta_\infty+\alpha_\infty)\sum_{j=1}^{i}\int_{\xi_K(\eta)}^{\xi} C_j \frac{\partial x^{(i-j)}}{\partial\xi}\,d\xi + \operatorname{tg}(\vartheta_\infty-\alpha_\infty)\left[F^{(i)}(\xi) - F^{(i)}(\xi_K(\eta))\right] \right\}$$

Table 2 b

Initial values along ξ_A and η_A

$$\vartheta^{(i)}(\xi,\eta) = \frac{1}{2}\left\{ A^{(i)}(\eta) + B^{(i)}(\xi) \right\}$$

$$\operatorname{ctg} \alpha_\infty w^{(i)}(\xi,\eta) = \sum_{j=1}^{i-1} (L_j)_{\xi,\eta} + \frac{1}{2}\left\{ A^{(i)}(\eta) - B^{(i)}(\xi) \right\}$$

$$x^{(i)}(\xi,\eta) = \frac{1}{\operatorname{tg}(\vartheta_\infty+\alpha_\infty) - \operatorname{tg}(\vartheta_\infty-\alpha_\infty)} \left\{ \sum_{j=1}^{i} \int_{\xi_A}^{\xi} C_j \frac{\partial x^{(i-j)}}{\partial \xi}\, d\xi - \sum_{j=1}^{i} \int_{\eta_A}^{\eta} D_j \frac{\partial x^{(i-j)}}{\partial \eta}\, d\eta + E^{(i)}(\eta) - F^{(i)}(\xi) \right\}$$

$$y^{(i)}(\xi,\eta) = \frac{1}{\operatorname{tg}(\vartheta_\infty+\alpha_\infty) - \operatorname{tg}(\vartheta_\infty-\alpha_\infty)} \left\{ \operatorname{tg}(\vartheta_\infty+\alpha_\infty) \sum_{j=1}^{i} \int_{\xi_A}^{\xi} C_j \frac{\partial x^{(i-j)}}{\partial \xi}\, d\xi - \operatorname{tg}(\vartheta_\infty-\alpha_\infty) \sum_{j=1}^{i} \int_{\eta_A}^{\eta} D_j \frac{\partial x^{(i-j)}}{\partial \eta}\, d\eta + \operatorname{tg}(\vartheta_\infty+\alpha_\infty) E^{(i)}(\eta) - \operatorname{tg}(\vartheta_\infty-\alpha_\infty) F^{(i)}(\xi) \right\}$$

Table 2 c

Initial values along ξ_A

$$\vartheta^{(1)}(\xi,\eta) = \vartheta_K^{(1)}(\xi,\eta_K(\xi)) + \frac{1}{2}\left[A^{(1)}(\eta) - A^{(1)}(\eta_K(\xi))\right]$$

$$\operatorname{ctg}\alpha_\infty\, w^{(1)}(\xi,\eta) = -\vartheta_K^{(1)}(\xi,\eta_K(\xi)) + \frac{1}{2}\left[A^{(1)}(\eta) + A^{(1)}(\eta_K(\xi))\right]$$

$$x_K^{(1)}(\xi,\eta_K(\xi)) = \frac{1}{\operatorname{tg}(\vartheta_\infty-\alpha_\infty)}\left\{ y_K^{(1)}(\xi_A,\eta_K(\xi_A)) - A^{**}P_1Q_1\int_{\xi_A}^{\xi}\left[\vartheta_K^{(1)}(\xi,\eta_K(\xi)) - \frac{1}{2}A^{(1)}(\eta_K(\xi))\right]d\xi - A^{**}P_1Q_2\left[\xi-\xi_A\right]\frac{1}{2}A^{(1)}(\eta_K(\xi)) - E^{(1)}(\eta_K(\xi))\right\}$$

$$x^{(1)}(\xi,\eta) - x_K^{(1)}(\xi,\eta_K(\xi)) = \frac{1}{\operatorname{tg}(\vartheta_\infty+\alpha_\infty)-\operatorname{tg}(\vartheta_\infty-\alpha_\infty)}\left\{ -\left[A^{*}P_2Q_2\left[\vartheta_K^{(1)}(\xi,\eta_K(\xi)) - \frac{1}{2}A^{(1)}(\eta_K(\xi))\right]\left[\eta-\eta_K(\xi)\right] + A^{*}P_2Q_1\frac{1}{2}\int_{\eta_K(\xi)}^{\eta} A^{(1)}(\eta)\,d\eta\right] + \right.$$

$$\left. + \left[A^{**}P_1Q_2\left[\xi-\xi_A\right]\frac{1}{2}\left[A^{(1)}(\eta)-A^{(1)}(\eta_K(\xi))\right] + E^{(1)}(\eta) - E^{(1)}(\eta_K(\xi))\right]\right\}$$

$$y^{(1)}(\xi,\eta) = y_K^{(1)}(\xi_A,\eta_K(\xi_A)) + \frac{1}{\operatorname{tg}(\vartheta_\infty+\alpha_\infty)-\operatorname{tg}(\vartheta_\infty-\alpha_\infty)}\left\{ -\operatorname{tg}(\vartheta_\infty-\alpha_\infty)\left[A^{*}P_2Q_2\left[\vartheta_K^{(1)}(\xi,\eta_K(\xi)) - \frac{1}{2}A^{(1)}(\eta_K(\xi))\right]\left[\eta-\eta_K(\xi)\right] + A^{*}P_2Q_1\frac{1}{2}\int_{\eta_K(\xi)}^{\eta} A^{(1)}(\eta)d\eta\right] + \right.$$

$$\left. + \operatorname{tg}(\vartheta_\infty+\alpha_\infty)\left[A^{**}P_1Q_2\left[\xi-\xi_A\right]\frac{1}{2}\left[A^{(1)}(\eta)-A^{(1)}(\eta_K(\xi))\right] + E^{(1)}(\eta) - E^{(1)}(\eta_K(\xi))\right]\right\}$$

Table 3 a

Initial values along η_A

$$\vartheta^{(1)}(\xi,\eta) = \vartheta_K^{(1)}(\xi,\eta) + \frac{1}{2}\left[B^{(1)}(\xi) - B^{(1)}(\xi_K(\eta)) \right]$$

$$\operatorname{ctg} \alpha_\infty \, w^{(1)}(\xi,\eta) = \vartheta_K^{(1)}(\xi,\eta) - \frac{1}{2}\left[B^{(1)}(\xi) + B^{(1)}(\xi_K(\eta)) \right]$$

$$x_K^{(1)}(\xi_K(\eta),\eta) = \frac{1}{\operatorname{tg}(\vartheta_\infty+\alpha_\infty)} \left\{ y_K^{(1)}(\xi_K(\eta_A),\eta_A) - A^* P_2 Q_1 \int_{\eta_A}^{\eta} \left[\vartheta_K^{(1)}(\xi_K(\eta),\eta) - \frac{1}{2} B^{(1)}(\xi_K(\eta)) \right] d\eta - A^* P_2 Q_2 \left[\eta-\eta_A \right] \frac{1}{2} B^{(1)}(\xi_K(\eta)) - F^{(1)}(\xi_K(\eta)) \right\}$$

$$x^{(1)}(\xi,\eta) - x_K^{(1)}(\xi_K(\eta),\eta) = \frac{1}{\operatorname{tg}(\vartheta_\infty-\alpha_\infty) - \operatorname{tg}(\vartheta_\infty+\alpha_\infty)} \left\{ - \left[A^{**} P_1 Q_2 \left[\vartheta_K^{(1)}(\xi_K(\eta),\eta) - \frac{1}{2} B^{(1)}(\xi_K(\eta)) \right] \left[\xi - \xi_K(\eta) \right] + A^{**} P_1 Q_1 \frac{1}{2} \int_{\xi_K(\eta)}^{\xi} B^{(1)}(\xi)\, d\xi \right] + \right.$$

$$\left. + \left[A^* P_2 Q_2 \left[\eta-\eta_A \right] \frac{1}{2} \left[B^{(1)}(\xi) - B^{(1)}(\xi_K(\eta)) \right] + F^{(1)}(\xi) - F^{(1)}(\xi_K(\eta)) \right] \right\}$$

$$y^{(1)}(\xi,\eta) = y_K^{(1)}(\xi_K(\eta_A),\eta_A) + \frac{1}{\operatorname{tg}(\vartheta_\infty-\alpha_\infty) - \operatorname{tg}(\vartheta_\infty+\alpha_\infty)} \left\{ - \operatorname{tg}(\vartheta_\infty+\alpha_\infty) \left[A^{**} P_1 Q_2 \left[\vartheta_K^{(1)}(\xi_K(\eta),\eta) - \frac{1}{2} B^{(1)}(\xi_K(\eta)) \right] \left[\xi - \xi_K(\eta) \right] + A^{**} P_1 Q_1 \frac{1}{2} \int_{\xi_K(\eta)}^{\xi} B^{(1)}(\xi)\, d\xi \right. \right.$$

$$\left. \left. + \operatorname{tg}(\vartheta_\infty-\alpha_\infty) \left[A^* P_2 Q_2 \left[\eta-\eta_A \right] \frac{1}{2} \left[B^{(1)}(\xi) - B^{(1)}(\xi_K(\eta)) \right] + F^{(1)}(\xi) - F^{(1)}(\xi_K(\eta)) \right] \right\}$$

Table 3 b

Initial values along $\bar{g}$ ξ_A and η_A

$$\vartheta^{(1)}(\xi,\eta) = \frac{1}{2}\left[A^{(1)}(\eta) + B^{(1)}(\xi)\right]$$

$$\operatorname{ctg}\alpha_\infty \cdot w^{(1)}(\xi,\eta) = \frac{1}{2}\left[A^{(1)}(\eta) - B^{(1)}(\xi)\right]$$

$$x^{(1)}(\xi,\eta) = \frac{1}{\operatorname{tg}(\vartheta_\infty+\alpha_\infty) - \operatorname{tg}(\vartheta_\infty-\alpha_\infty)} \left\{ A^{**}P_1 \frac{1}{2}\left[Q_2 A^{(1)}(\eta)\left[\xi-\xi_A\right] + Q_1 \int_{\xi_A}^{\xi} B^{(1)}(\xi)d\xi \right] - \right.$$

$$\left. - A^{*}P_2 \frac{1}{2}\left[Q_2 B^{(1)}(\xi)\left[\eta-\eta_A\right] + Q_1 \int_{\eta_A}^{\eta} A^{(1)}(\eta)d\eta \right] + E^{(1)}(\eta) - F^{(1)}(\xi) \right\}$$

$$y^{(1)}(\xi,\eta) = \frac{1}{\operatorname{tg}(\vartheta_\infty+\alpha_\infty) - \operatorname{tg}(\vartheta_\infty-\alpha_\infty)} \left\{ \operatorname{tg}(\vartheta_\infty+\alpha_\infty) A^{**}P_1 \frac{1}{2}\left[Q_2 A^{(1)}(\eta)\left[\xi-\xi_A\right] + Q_1 \int_{\xi_A}^{\xi} B^{(1)}(\xi)d\xi \right] - \right.$$

$$\left. - \operatorname{tg}(\vartheta_\infty-\alpha_\infty) A^{*}P_2 \frac{1}{2}\left[Q_2 B^{(1)}(\xi)\left[\eta-\eta_A\right] + Q_1 \int_{\eta_A}^{\eta} A^{(1)}(\eta)d\eta \right] + \operatorname{tg}(\vartheta_\infty+\alpha_\infty) E^{(1)}(\eta) - \operatorname{tg}(\vartheta_\infty-\alpha_\infty) F^{(1)}(\xi) \right\}$$

Table 3 c

10. Figures

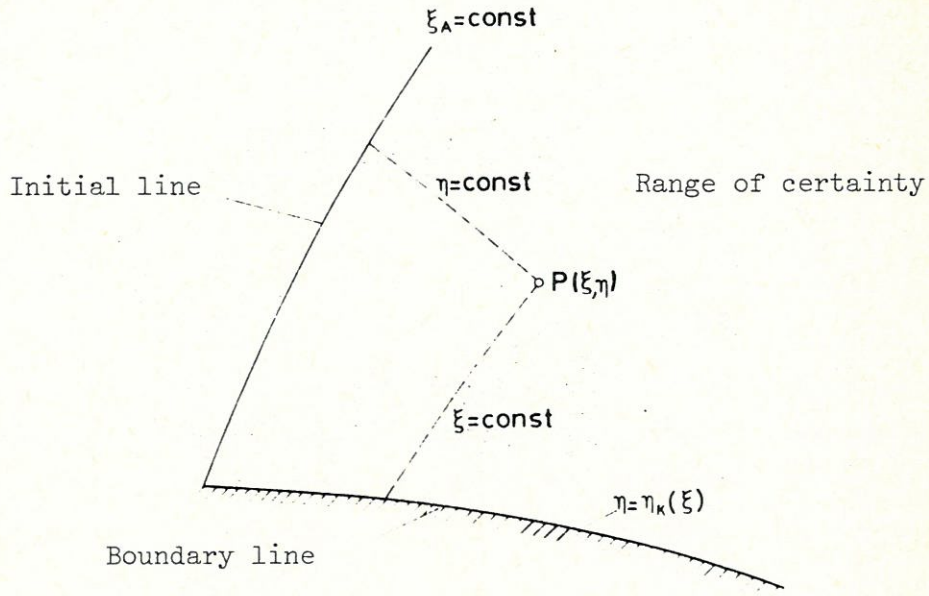

Figure 1: Range of certainty for the mixed, characteristic boundary/ initial value problem.
Initial values given along ξ_A.

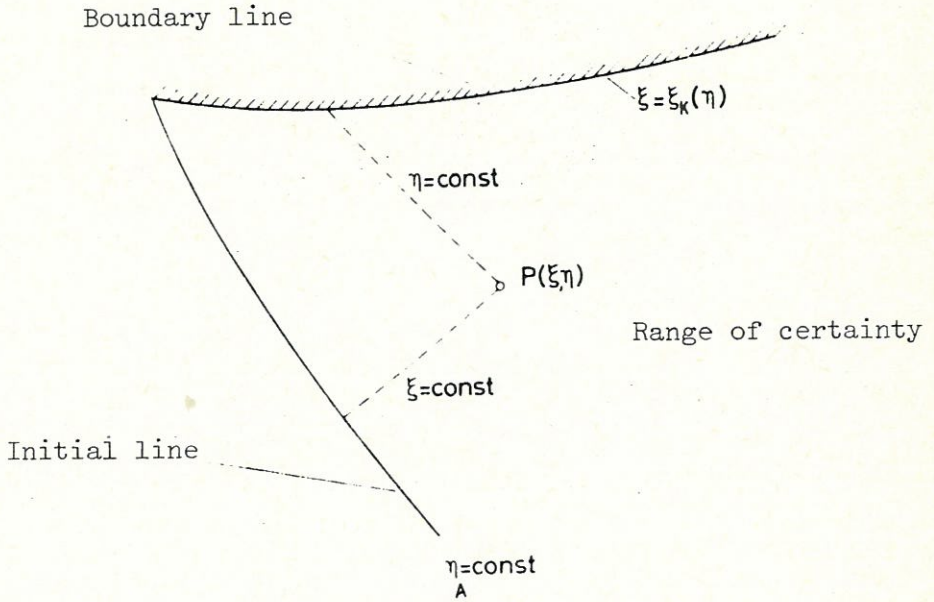

Figure 2: Range of certainty for the mixed, characteristic boundary/ initial value problem.
Initial values given along η_A.

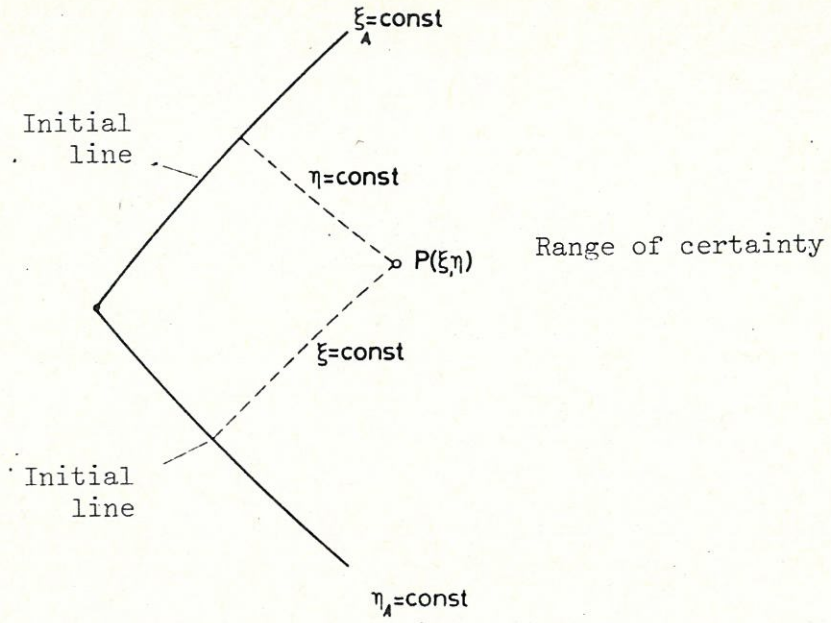

Fig. 3: Range of certainty for the characteristic initial value problem.
Initial values given along ξ_A and η_A.

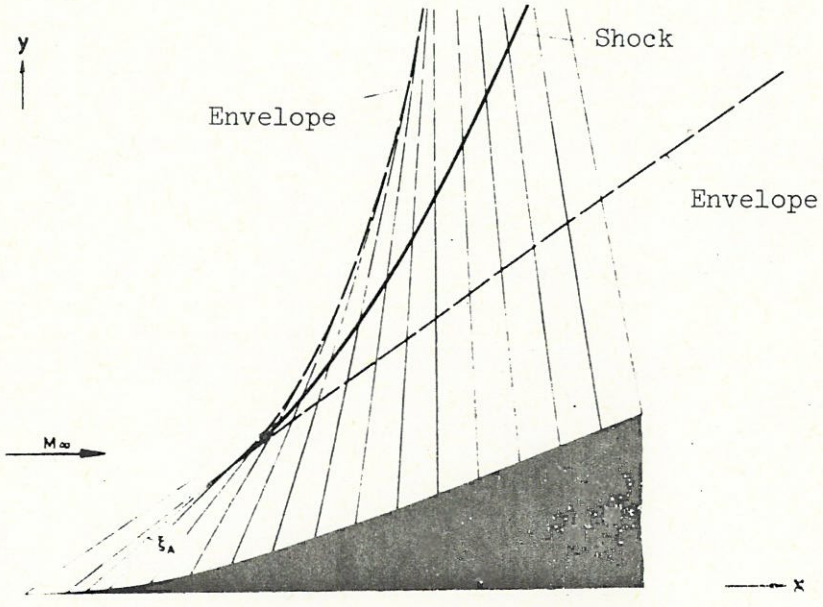

Fig. 4: Generation of a convolution on a concave curved wall.

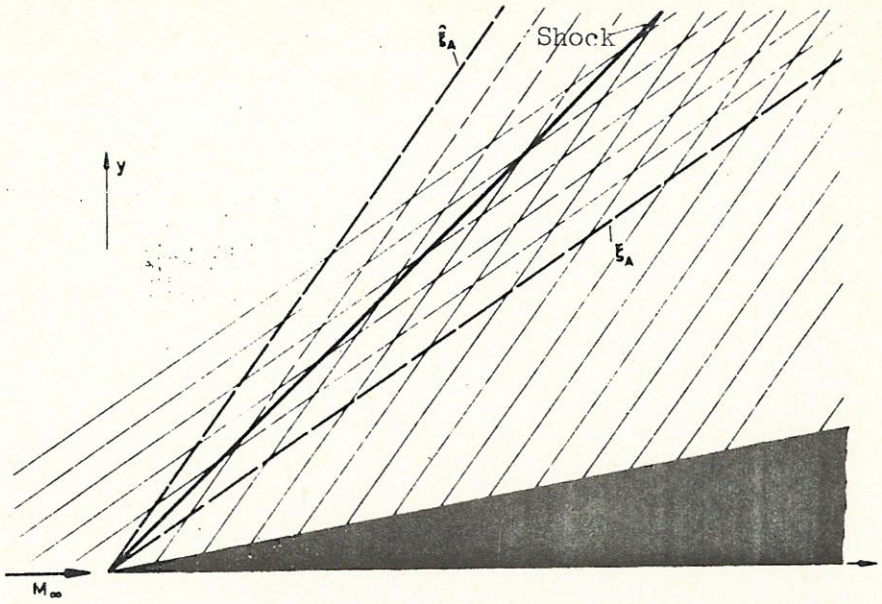

Fig. 5: Generation of a convolution on a wall having a concave break.

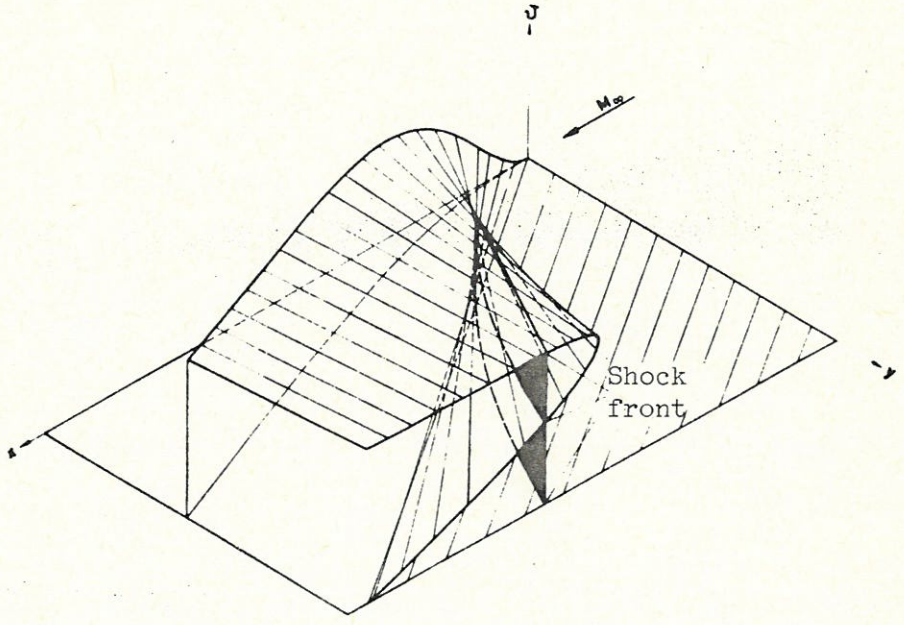

Fig. 6: Surface of state in the area of a convolution occurring on a concave contour.

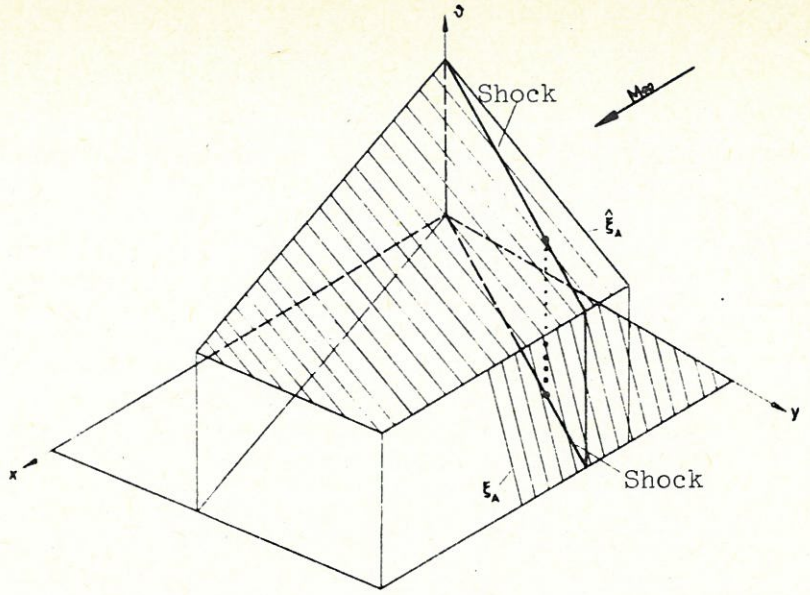

Fig. 7: Surface of state in the area of a convolution occurring on a contour having a concave break.

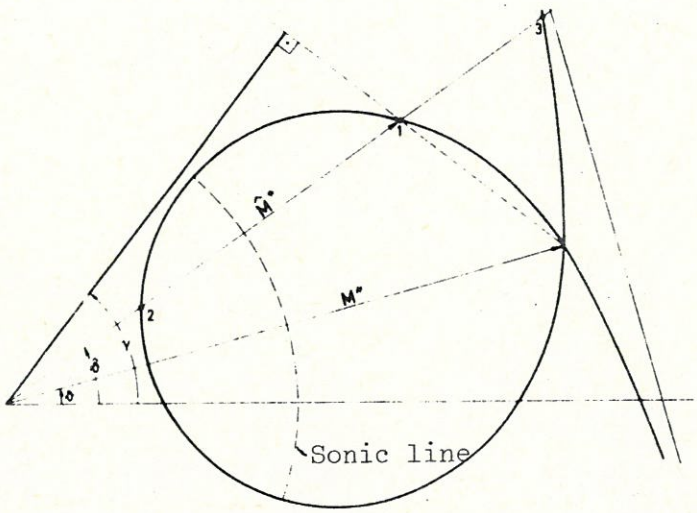

θ	=	Direction of flow ahead of the shock
$\hat{\theta}$	=	Direction of flow after the shock
γ	=	Shock angle
M^*	=	Critical Mach Number ahead of the shock
$\hat{M}^*$	=	Critical Mach Number after the shock
1	$\hat{=}$	Weak shock
2	$\hat{=}$	Severe shock
3	$\hat{=}$	No physical significance

Fig. 8: Shock Polars

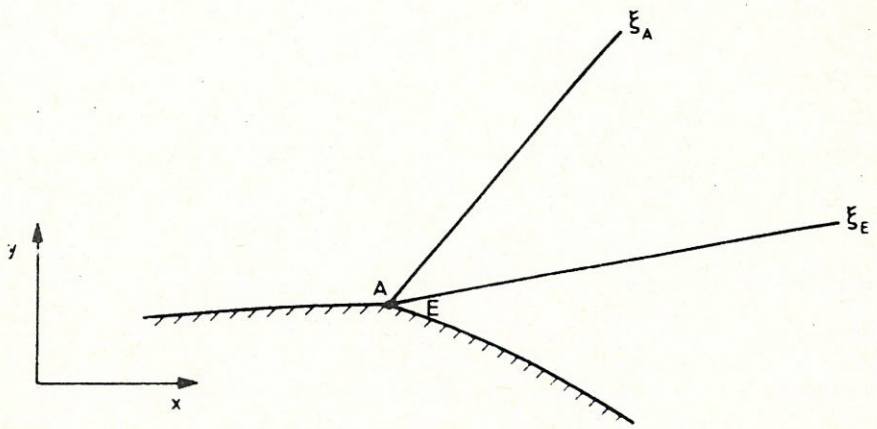

Fig. 9: Centered Prandtl-Meyer expansion in the physical plane.

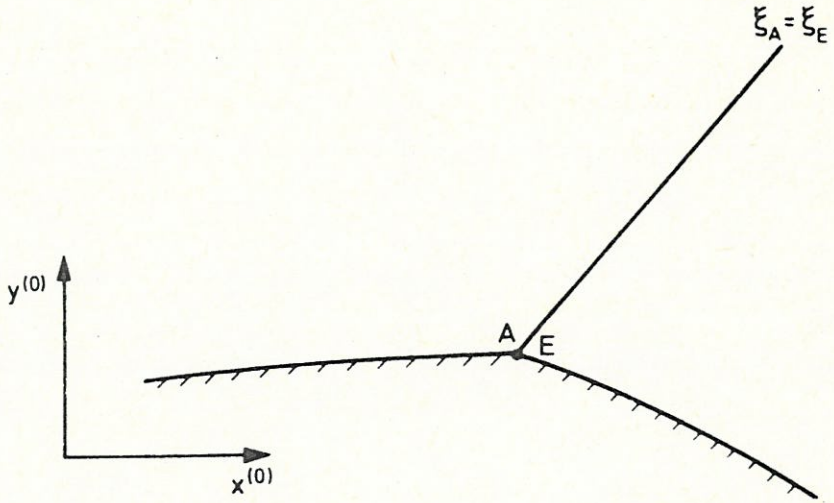

Fig. 10: Centered Prandtl-Meyer expansion in the physical plane (Acoustics Theory).

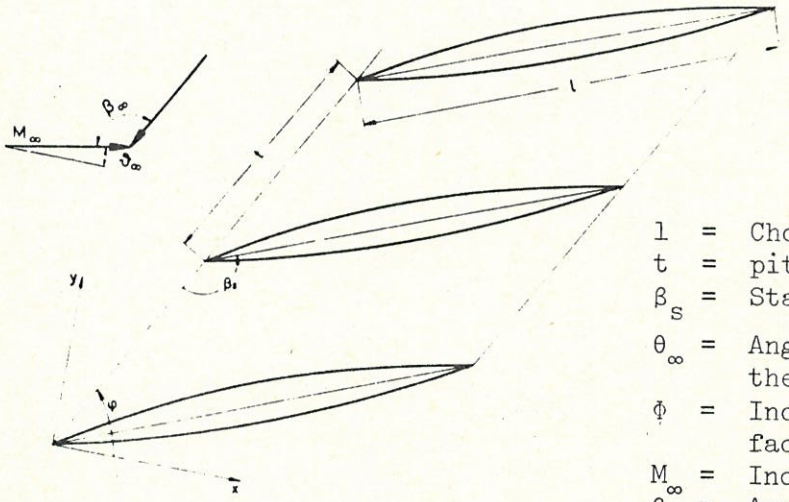

l = Chord length
t = pitch
β_s = Stagger angle
θ_∞ = Angle of incident flow to the x-axis
Φ = Inclination of the cascade face to the x-axis
M_∞ = Incident flow Mach Number
β_∞ = Angle of incident flow to the cascade face

Fig. 11: Geometry and notation for a blade cascade.

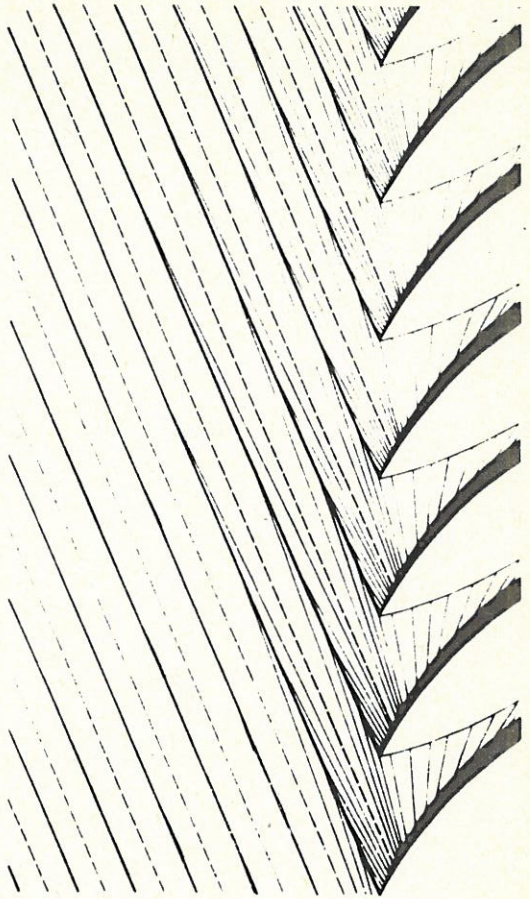

Fig. 12: Double infinite cascade.

$(M_{ax})_1 < 1$ $\beta_s = 140^\circ$

$M_1 = 1,31$ $\beta_1 = 153,95^\circ$

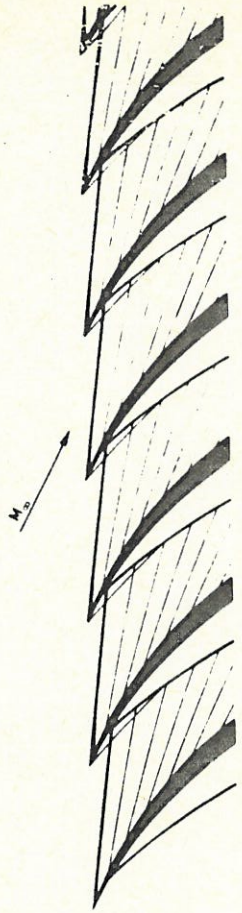

Fig. 13: Semi- or double infinite cascade.

$(M_{ax})_\infty = (M_{ax})_1 > 1$
$\beta_s = 140^\circ$
$M_\infty = M_1 = 3,3$
$\beta_\infty = \beta_1 = 154^\circ$

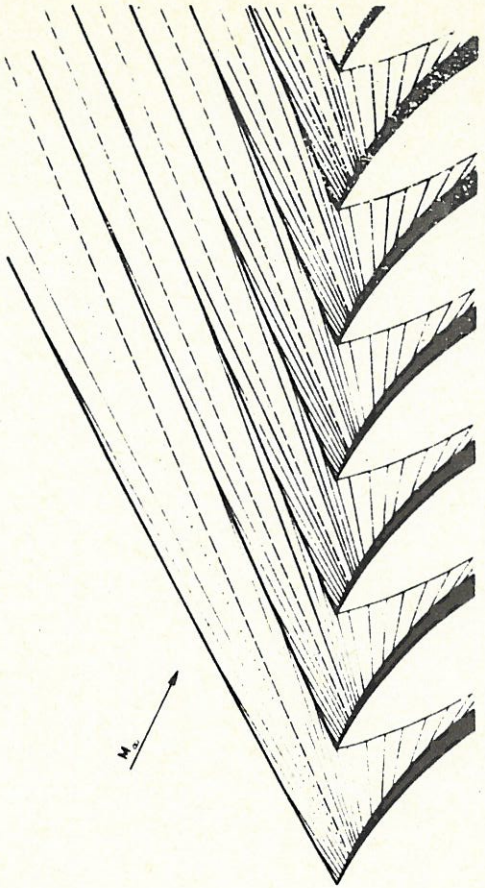

Fig. 14: Semi-infinite cascade.

$(M_{ax})_\infty < 1 \quad (M_{ax})_1 < 1 \quad \beta_s = 140^\circ$
$M_\infty = 1,3 \quad \beta_\infty = 154^\circ$
$M_1 = 1,31 \quad \beta_1 = 153,95^\circ$

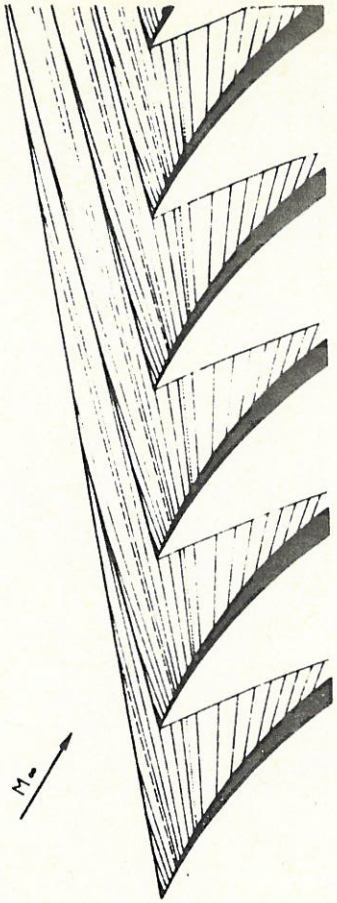

Fig. 15: Semi-infinite cascade.

$(M_{ax})_\infty < 1$ $(M_{ax})_1 < 1$ $\beta_s = 140^\circ$

$M_\infty = 1{,}7$ $\beta_\infty = 149^\circ$

$M_1 = 1{,}54$ $\beta_1 = 153.9^\circ$

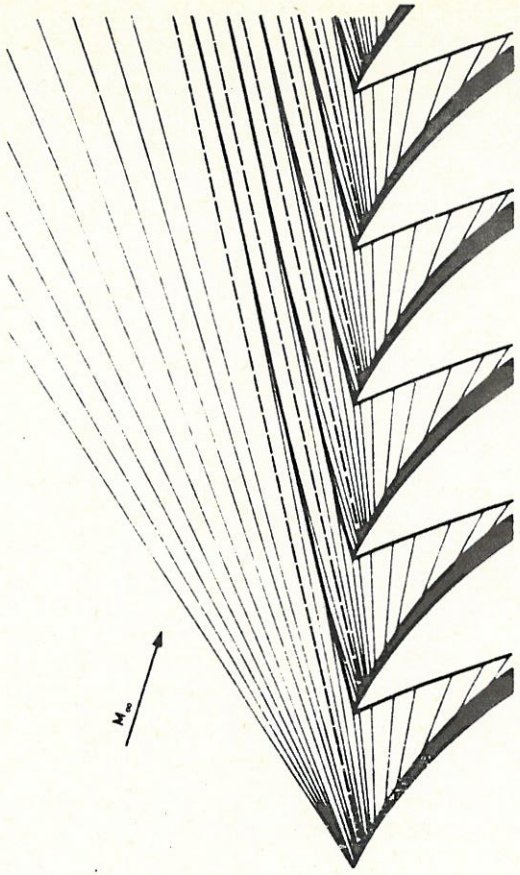

Fig. 16: Semi-infinite cascade.

$(M_{ax})_\infty < 1$ $(M_{ax})_1 < 1$ $\beta_s = 140^\circ$

$M_\infty = 1{,}3$ $\beta_\infty = 162^\circ$

$M_1 = 1.56$ $\beta_1 = 155{,}44^\circ$

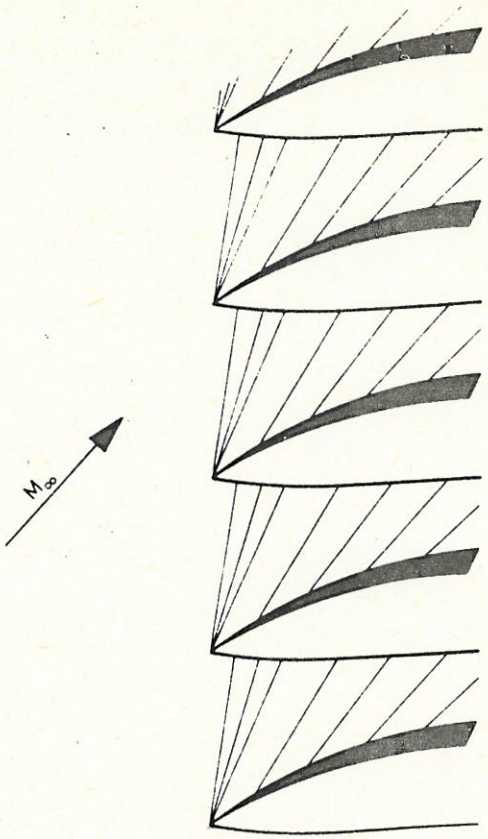

Fig. 17: Semi- or double infinite cascades.

$(M_{ax})_\infty = (M_{ax})_1 > 1 \quad \beta_s = 110^\circ$

$M_\infty = M_1 = 1{,}80$

$\beta_\infty = \beta_1 = 138^\circ$

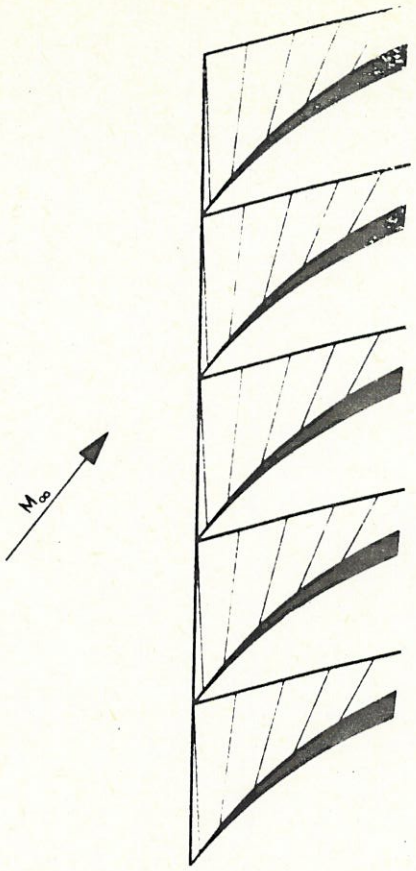

Fig. 18: Semi- or double infinite cascades

$(M_{ax})_\infty = (M_{ax})_1 > 1 \quad \beta_s = 130^\circ$

$M_\infty = M_1 = 1{,}79$

$\beta_\infty = \beta_1 = 143^\circ$

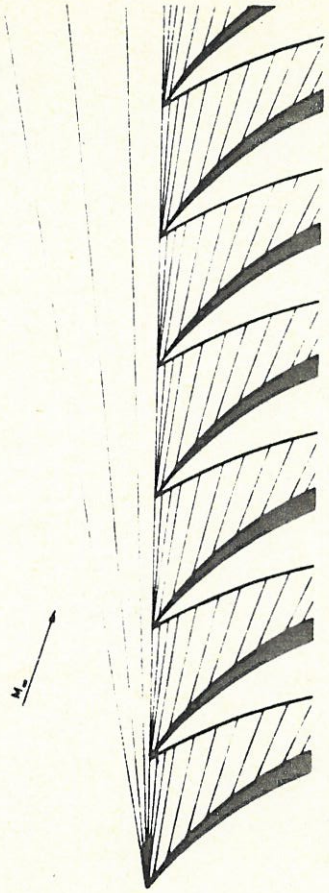

Fig. 19: Semi-infinite cascade.
$(M_{ax})_\infty < 1$ $(M_{ax})_1 = 1$ $\beta_s = 130^\circ$
$M_\infty = 2.1$ $\beta_\infty = 162^\circ$
$M_1 = 2.42$ $\beta_1 = 154.27^\circ$

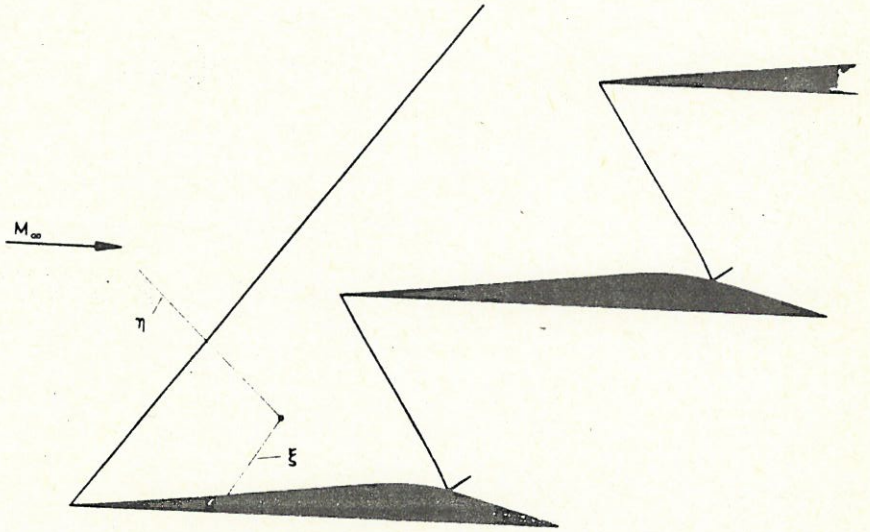

Fig. 20: Entrance region of a blade cascade with upstream effect

——— Compression shocks
——— Mach lines

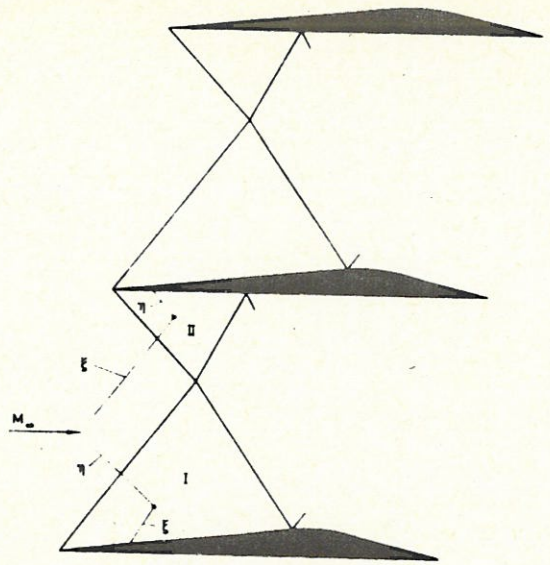

Fig. 21: Entrance regions of a cascade with no upstream effect.

——— Compression shocks

– – – – Mach lines

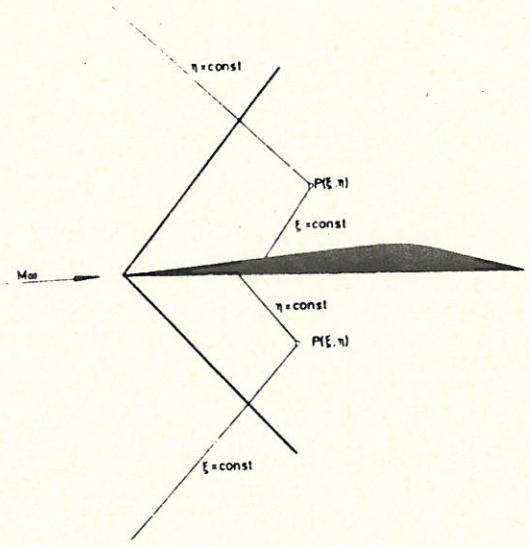

Fig. 22: Flow regions on a single aerofoil.

——— Compression shocks

– – – – Mach lines

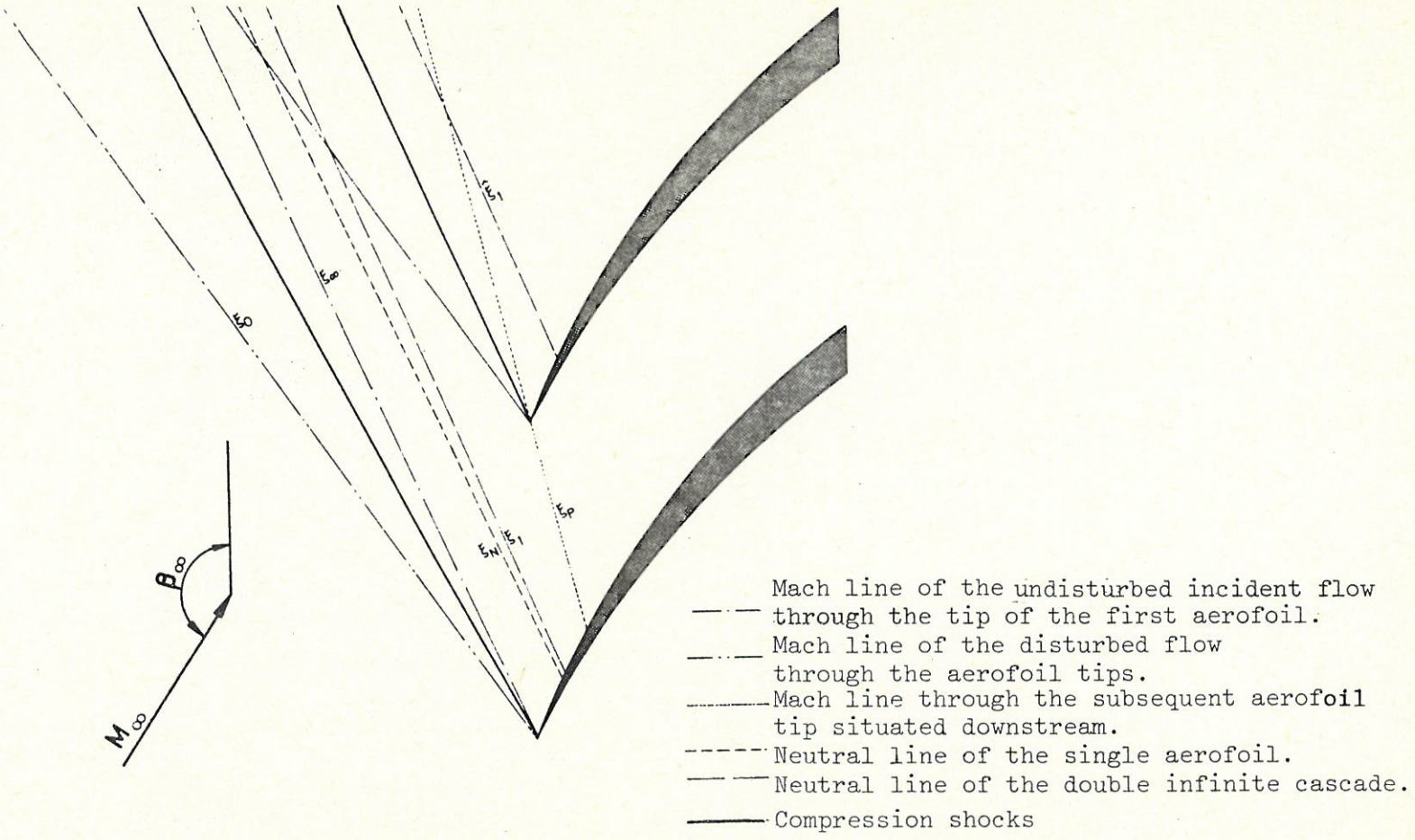

Fig. 23: Notation of the left-handed Mach lines of a semi-infinite cascade (convex shaped aerofoil suction side)

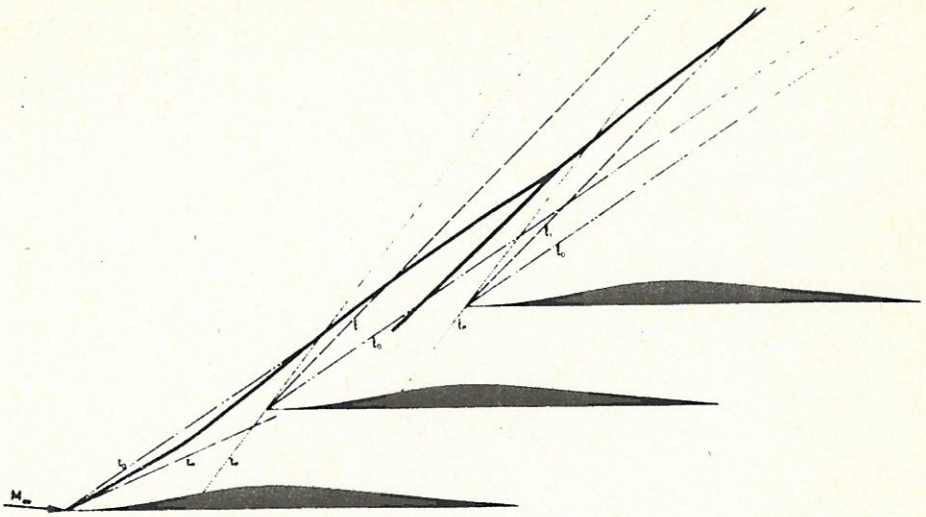

Fig. 24: Notation for the left-handed Mach lines of a semi-infinite cascade (concave shaped aerofoil suction side)

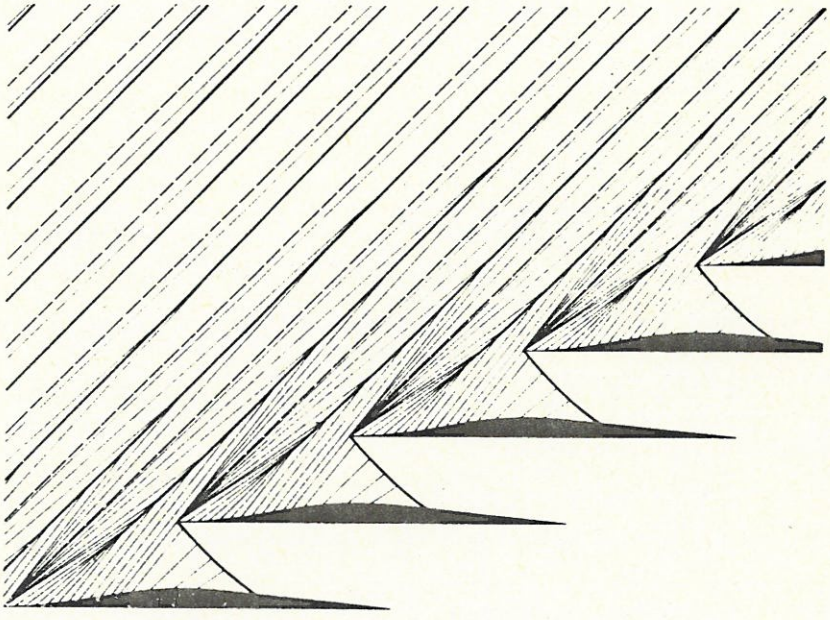

Fig. 25: Double infinite cascade (concave shaped aerofoil suction side)

$(M_{ax})_1 < 1$ $\qquad \beta_s = 153{,}5^\circ$

$M_1 = 1{,}59$ $\qquad \beta_1 = 159{,}6^\circ$

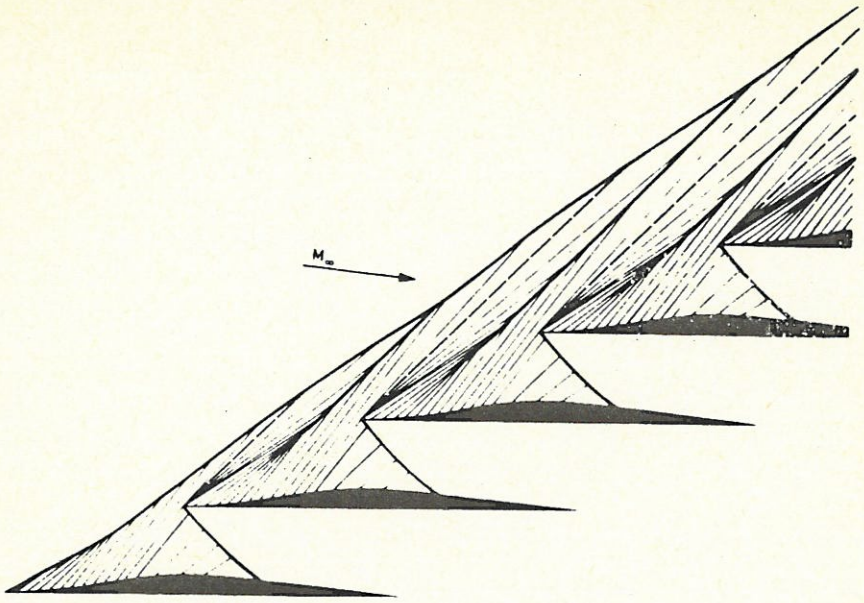

Fig. 26: Semi-infinite cascade (concave shaped aerofoil suction side)

$(M_{ax})_\infty > 1$ $(M_{ax})_1 < 1$ $\beta_s = 153{,}5^\circ$

$M_\infty = 2{,}01$ $\beta_\infty = 147{,}6^\circ$ $M_1 = 1{,}59$ $\beta_1 = 159{,}6^\circ$

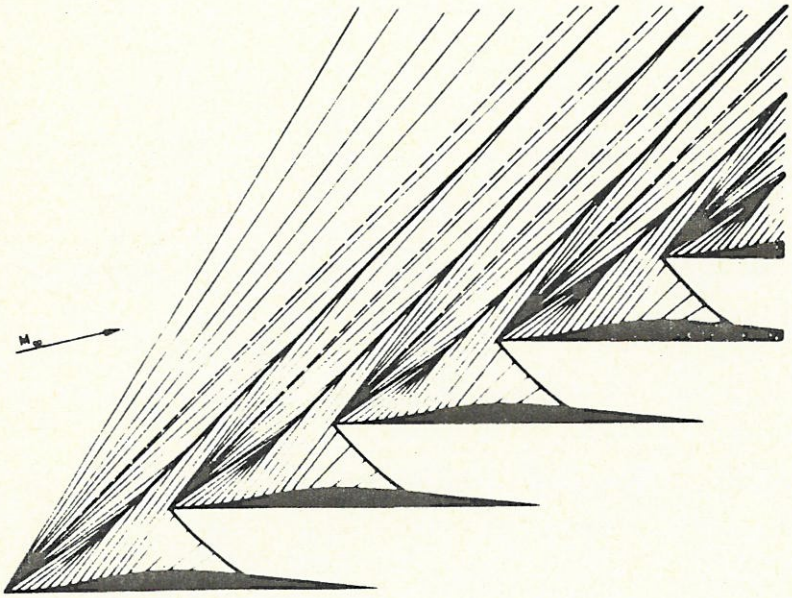

Fig. 27: Semi-infinite cascade (concave shaped aerofoil suction side)

$(M_{ax})_\infty < 1$ $(M_{ax})_1 < 1$ $\beta_s = 153{,}5^\circ$

$M_\infty = 1{,}39$ $\beta_\infty = 165{,}5^\circ$ $M_1 = 1{,}59$ $\beta_1 = 159{,}6^\circ$

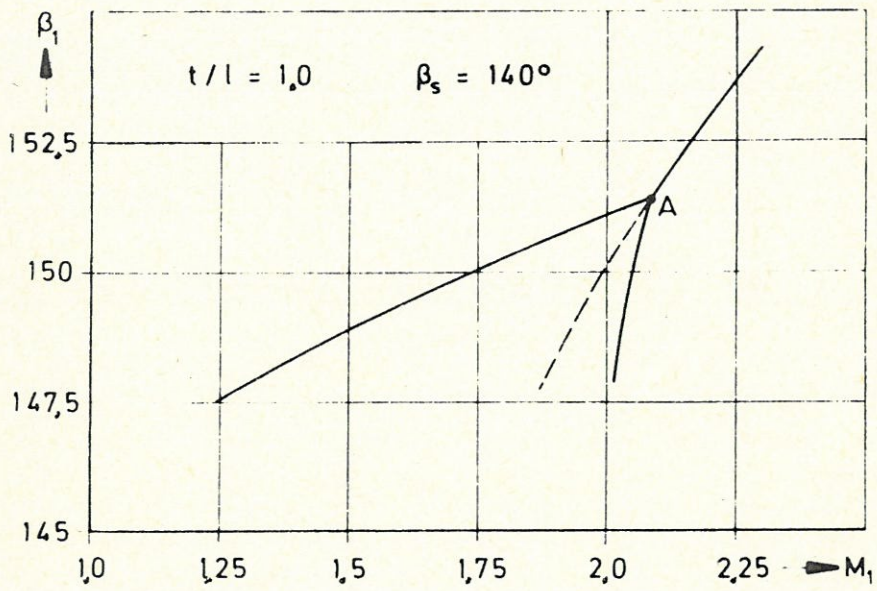

Fig. 28: Interrelationship between the incident flow Mach No. M_1 and the incident flow direction β_1.

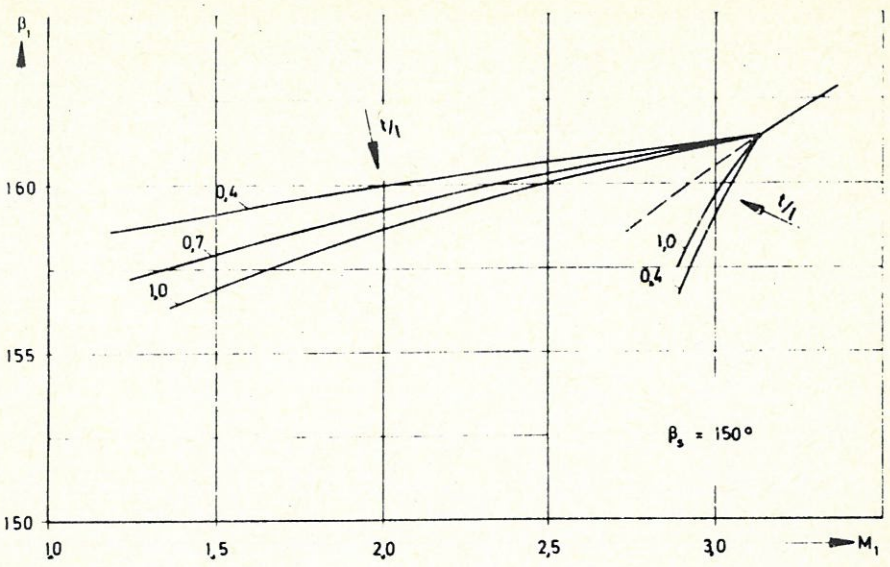

Fig. 29: Effect of the pitch ratio on the interrelationship between the incident flow Mach Number and the incident flow direction.

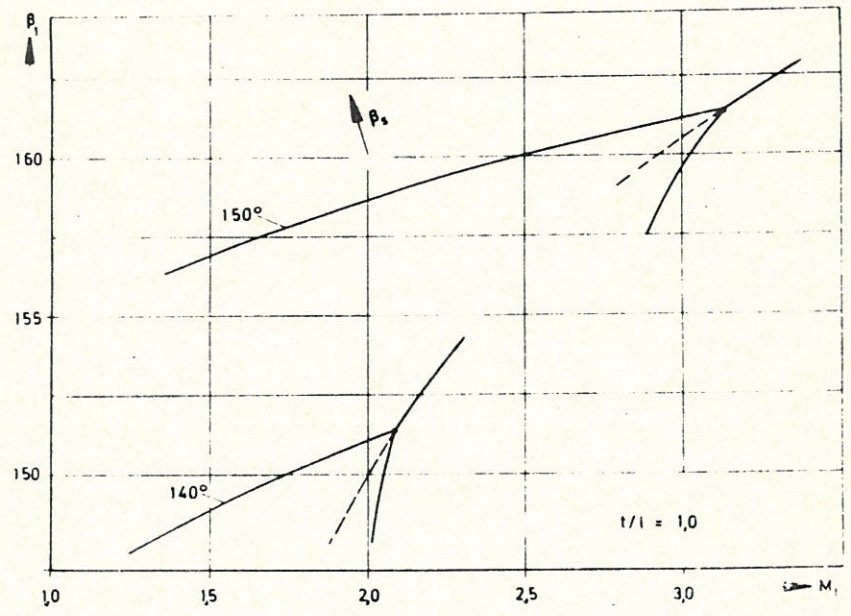

Fig. 30: Effect of the stagger angle on the interrelationship between the incident flow Mach Number and the incident flow direction.

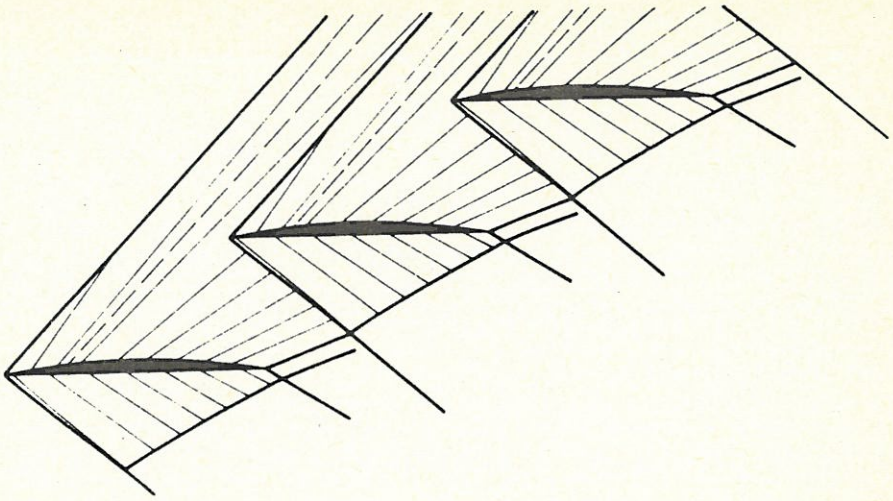

Fig. 31: Illustration of a cascade with a supersonic flow passing through it

$(M_{ax})_1<1$ $(M_{ax})_2>1$ $\beta_s=150^\circ$

$M_1=1,47$ $\beta_1=156,6^\circ$ $M_2=2,07$ $\beta_2=141,5^\circ$

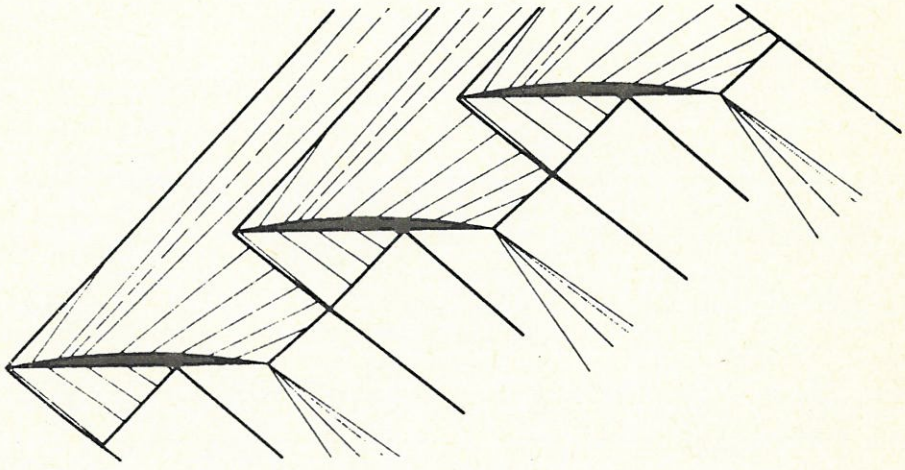

Fig. 32: Flow field of a cascade with a supersonic flow through it.

$(M_{ax})_1<1$ $(M_{ax})_2<1$ $\beta_s=150^\circ$

$M_1=1,47$ $\beta_1=156,6^\circ$ $M_2=1,40$ $\beta_2=157,6^\circ$

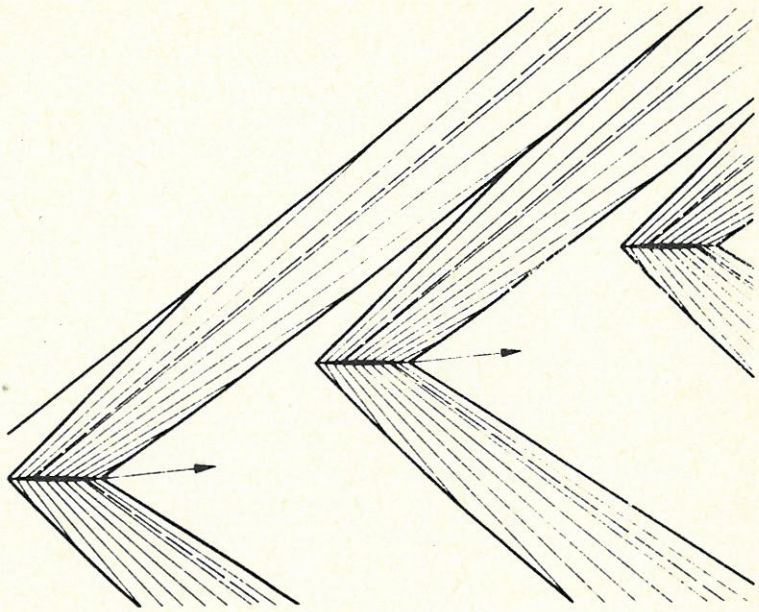

Fig. 33: Reaction of the outlet flow on the inlet flow for a cascade with a supersonic flow through it

$(M_{ax})_1 < 1$ $(M_{ax})_2 < 1$ $\beta_s = 160^\circ$

$M_1 = 1,69$ $\beta_1 = 162,5^\circ$ $M_2 = 1,57$ $\beta_2 = 163,9^\circ$

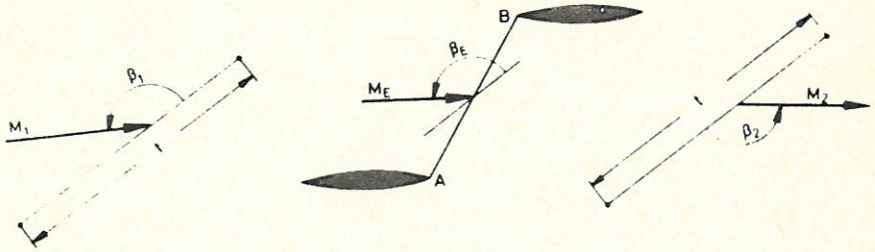

Fig. 34: Notation for the reaction cascade

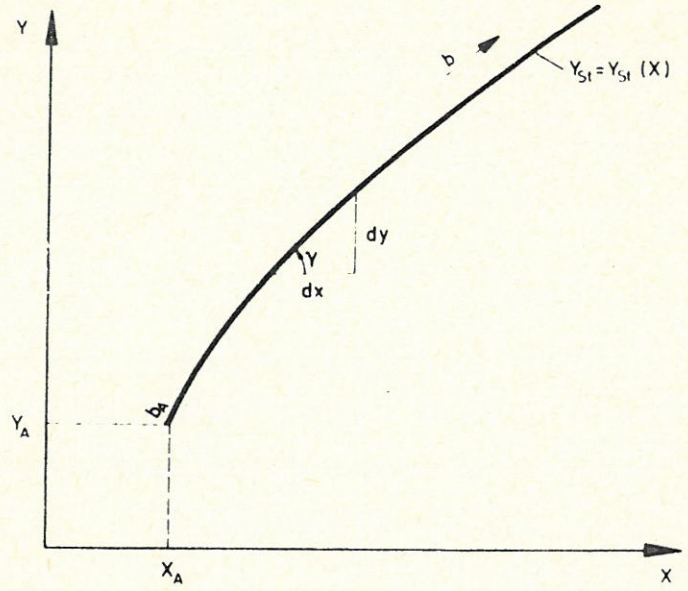

Fig. 35: Notation for the compression shock in the physical plane

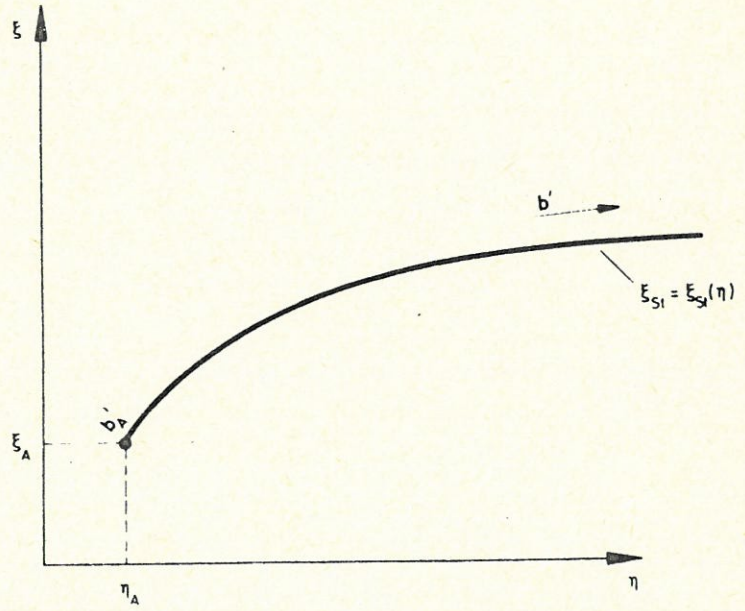

Fig. 36: Notation for the compression shock in the characteristic plane

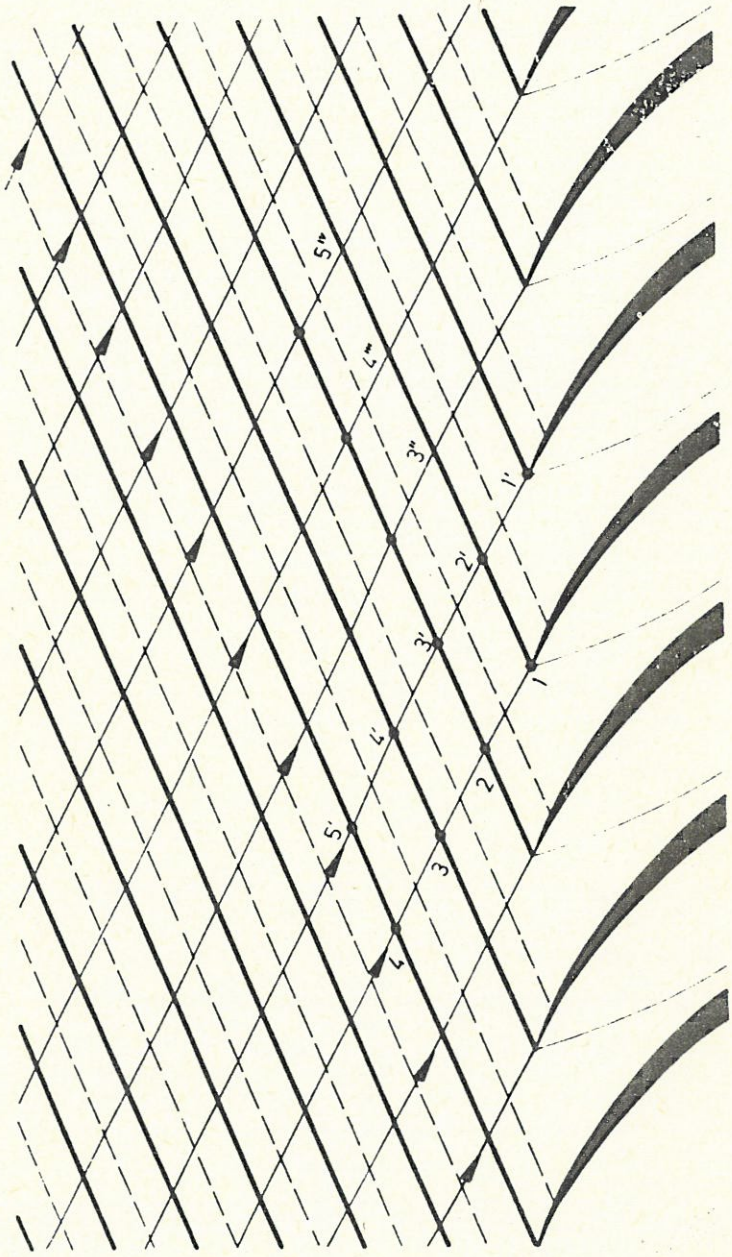

Fig. 37: Flow diagram of a double infinite cascade with upstream effect

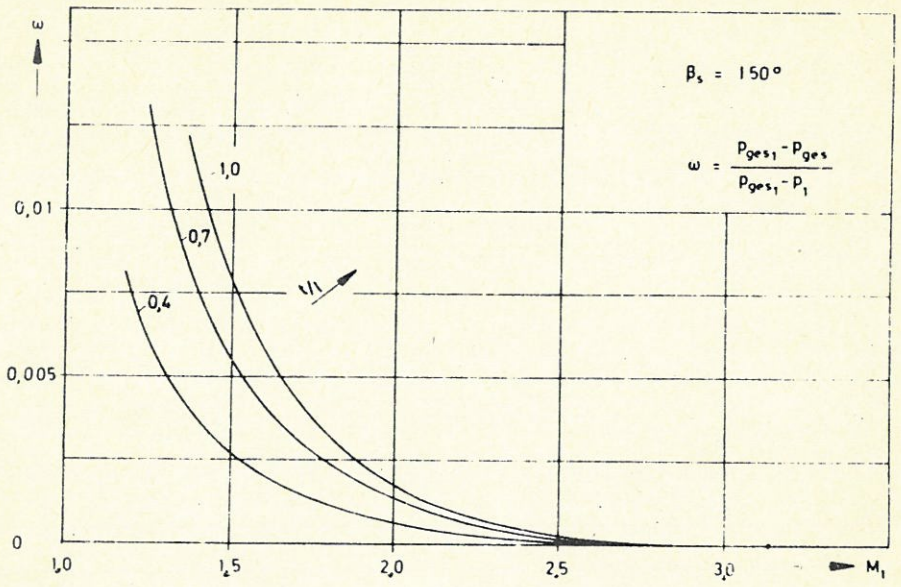

Fig. 38: Effect of the pitch ratio on the loss coefficient of the cascade entrance shocks

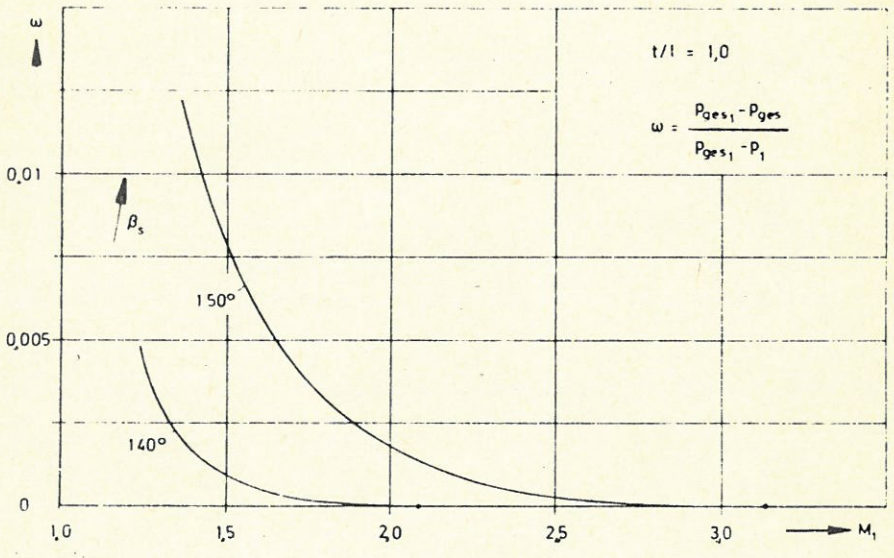

Fig. 39: Effect of the stagger angle on the loss coefficient of the cascade entrance shocks